Nytt Flymåleutstyr (NFU)
Evaluation of the MXU-648A/A Cargo/Travel Pod internal environment as installed on the F-16A aircraft

Steve Potter and Eirik Blix Madsen

Forsvarets forskningsinstitutt / Norwegian Defence Research Establishment (FFI)

30 April 2010

FFI-rapport 2010/01184

1115

P: ISBN 978-82-464-1796-7
E: ISBN 978-82-464-1797-4

Keywords

Nytt Flymåleutstyr

NFU

MXU-648A/A

NSM

F-16 jagerfly

Flymåling

Approved by

Lars Trygve Heen	Project Manager
Stein Grinaker	Director of Research
Johnny Bardal	Director

Summary

There have been performed tests to evaluate the internal environment and to determine the effects of increasing the moment of inertia of a MXU-648A/A Travel Pod as installed on the F-16A aircraft for the Norwegian Captive Carry (NFU) program. Three flight events with typical research flight profiles totaling 3.6 hours were conducted under daylight visual meteorological conditions. All test objectives were met.

The test aircraft and instrumented MXU-648A/A were representative of production models. The external configuration was selected to mimic future research missions and to maximize the aeroelastic stability (flutter) margins. External fuel tanks were incorporated on stations 4 and 6 and captive air-to-air training missiles (CATM-120) were mounted on each wing tip. The instrumented MXU-648A/A was installed on station 3 and all other stations were empty. The MXU-648A/A yawing moment of inertia (I_{zz}) varied from 27.1 kg·m^2 (20.0 slug·ft^2) during the first flight, to 40.4 kg·m^2 (29.8 slug·ft^2) on the second flight, and finally to 66.4 kg·m^2 (49.0 slug·ft^2) on the third flight.

Substantial data was gathered to describe the behavior of the MXU-648A/A internal thermal environment during typical low altitude, high speed flight conditions. Six temperature sensors were continuously recorded to provide local skin temperature at three locations, internal air temperature in the cargo bay and in the nose cavity, and external air temperature. The maximum skin temperature recorded was 26.2 °C at the aft section of the pod. The data at this specific location appears to correlate with the preliminary results from the computational fluid dynamics (CFD) wall temperature contour models which indicate that warmer skin temperatures can be present at the aft section of the pod when compared to the forward section of the pod. Additional data was gathered at high altitude conditions to document typical ferry conditions. The coldest temperature recorded was -37.6 °C at the forward skin location.

Nine accelerometers were installed to characterize the MXU-648A/A vibration environment while varying the pod moment of inertia over three flights. While the vibration magnitude appeared to grow by as much as 63.5% with an increase in moment of inertia during certain events (low altitudes, > 500 KCAS), this trend did not occur during most other test points. In fact, the change in g_{rms} vibration level from the first flight to third flight was less than 10% during 68% of the test events. The data indicates that the most significant vibration occurred in the lateral axis (y-axis) over a frequency range of 60-85 Hz. While these observed vibration levels exceed the guidance specified in MIL-STD-810F, DOD Test Method Standards for Environmental Engineering Considerations and Laboratory Tests, they are being described as “frequencies of interest” since the final NFU designs will differ in terms of aerodynamic shape and mass properties.

It is recommended that this data be reviewed by the NFU design teams. Consideration should be given to incorporating this information into the development and design process.

Sammendrag

Det er gjennomført tester for å evaluere internt miljø og for å undersøke virkningen av å øke treghetsmoment i en MXU-648A/A Cargo/Travel Pod montert på et F-16A jagerfly for prosjekt Nytt Flymåleutstyr (NFU). Tre flyvninger med typiske baneprofiler på til sammen 3,6 timer ble gjennomført, og alle testmål ble møtt.

Luftforsvarets standardutgaver av F-16 jagerfly og MXU-648A/A Cargo/Travel Pod ble benyttet. Under testene ble F-16 konfigurert for å etterligne forventet last under framtidige flyvninger med NFU. Eksterne drivstofftanker ble montert på stasjon 4 og 6 og luft-til-luft treningsmissiler (CATM-120) ble montert på hver vingespiss (stasjon 1 og 9). Instrumentert MXU-648A/A ble installert på stasjon 3, mens resten av stasjonene var uten last. Treghetsmomentet om vertikal akse til instrumentert MXU-648A/A varierte fra 27,1 $kg \cdot m^2$ (20.0 $slug \cdot ft^2$) under første flyvning, 40,4 $kg \cdot m^2$ (29.8 $slug \cdot ft^2$) under andre flyvning, og 66,4 $kg \cdot m^2$ (49.0 $slug \cdot ft^2$) under tredje flyvning.

Data ble innsamlet for å beskrive termisk miljø i MXU-648A/A under lav høyde/høy hastighet flyforhold – typisk for hvordan NFU vil operere. Seks temperatursensorer ble fortløpende avlest for å måle hudtemperatur på tre steder, intern lufttemperatur i lasterom og i nesen, og utvendig lufttemperatur. Maksimal registrert hudtemperatur var 26,2 °C, målt på siden av haleseksjonen. Data ser ut til å korrelere med foreløpige resultater fra strømningsanalyser, som indikerer varmere hudtemperaturer ved haleseksjonen i forhold til neseseksjonen og senterseksjonen. Temperaturdata ble også innsamlet i stor høyde for å dokumentere forhold under transitt. Kaldeste temperatur målt under transitt var -37,6 °C på siden av neseseksjonen.

Ni akselerometre ble montert for å karakterisere vibrasjonsmiljøet i MXU-648A/A. Mens vibrasjonene så ut til å øke med hele 63,5 % ved en økning i treghetsmoment under visse tester (lav høyde, høy hastighet), var økningen liten for de fleste andre testene. Faktisk endring i g_{rms} vibrasjonsnivå fra første flyvning til tredje flyvning var mindre enn 10 % i 68 % av testene. Dataene indikerer at mest signifikante vibrasjoner skjedde om vertikal akse over frekvensområdet 60-85 Hz. Selv om observerte vibrasjonsnivåer overstiger anbefalingene spesifisert i MIL-STD-810F, blir de beskrevet som ”frekvenser av interesse” siden endelig aerodynamisk form og massefordeling for NFU vil variere i forhold til MXU-648A/A med benyttet nyttelast.

Det anbefales at resultater og erfaringer fra disse målingene benyttes under design av NFU, og for å gi føringer til underleverandører og til produsent av modifisert MXU-648A/A.

Contents

1 Background

The Norwegian Defence Research Establishment (FFI) and Kongsberg Defense and Aerospace (KDA) are manufacturing independent airborne research pods under contract from the Norwegian Defence Logistics Organization (FLO/I) for project 6450, “Nytt Flymåleutstyr” (NFU). The purpose of the NFU program is to provide an airborne test facility for several imaging infrared seekers and associated software algorithms. Both NFU configurations will be based on the existing MXU-648A/A Cargo/Travel Pod (part number 402136), manufactured by Cobham plc (formerly Sargent Fletcher, Inc.), as shown in figure 1.1.

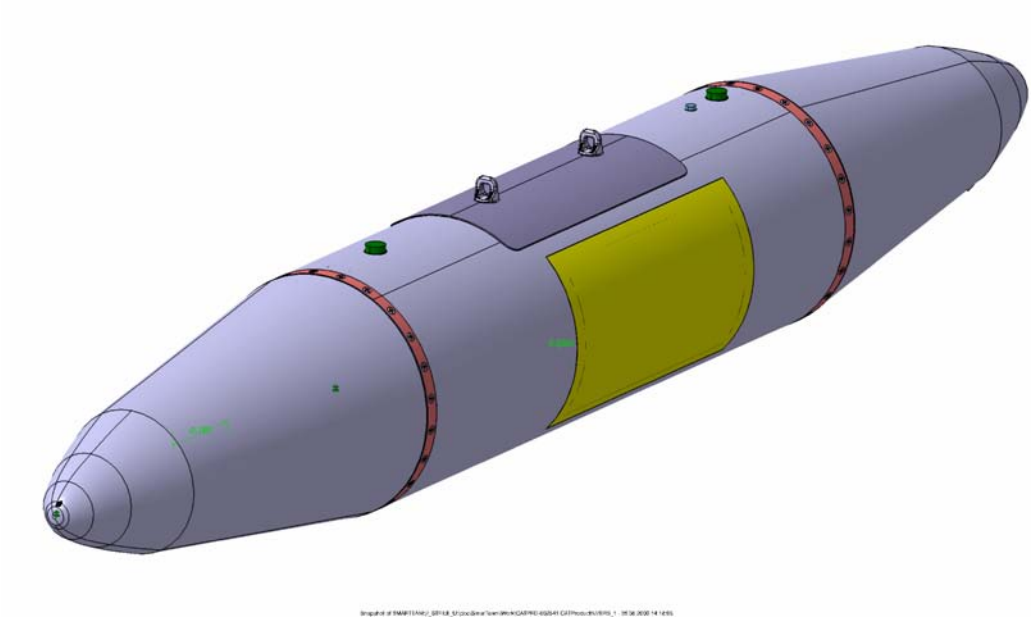

Figure 1.1 Unmodified MXU-648A/A Cargo/Travel Pod.

The MXU-648A/A Cargo/Travel Pod was selected as the host platform for the NFU project based on its circular cross-section, payload capability, and compatibility with many existing aircraft, including the F-16 aircraft. In order to accommodate the unique experimental sensors, electronics, and cooling systems of each NFU configuration, Cobham plc will produce a new design with structural modifications to satisfy the special payload and mass distribution requirements. The NFU design teams are planning to keep the gross weight and center of gravity (CG) position within the limits of the cleared MXU-648A/A Cargo/Travel Pod, however, the moment of inertia about the lateral and vertical axes will differ significantly when compared to the baseline MXU-648A/A due to the installation of infrared seeker and camera components in the forward section of each NFU and thermal control equipment in the aft section. Other design features will include two large access panels and provisions for aircraft/pod electrical connections and externally mounted antennas. Cobham plc will deliver a total of six structurally modified pods to FLO/I consisting of two prototype pods and four pods that will be certified for flight. FFI will receive one prototype and one flight-worthy unit. KDA will receive one prototype and two flight-worthy units. FLO/I will retain one flight-worthy unit as a spare.

1.1 Next Generation Nytt Flymåleutstyr (NG NFU)

The Next Generation Nytt Flymåleutstyr (NG NFU) will be built by FFI. The design will consist of both infrared and visual cameras and the necessary supporting electronics, stabilization systems, cooling equipment, and communication systems. The shape of the forward conical section will be designed to accommodate multiple cameras and specialized optical windows. A preliminary design is shown in figure 1.2 and the NG NFU internal components are shown in figure 1.3.

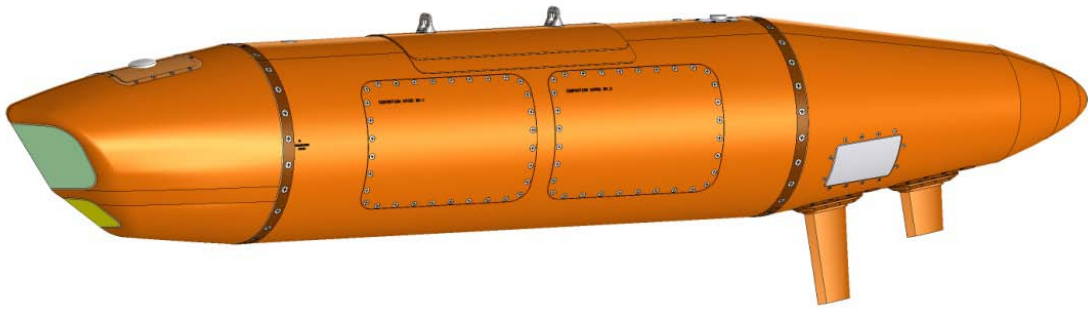

Figure 1.2 Preliminary Design of the Next Generation Nytt Flymåleutstyr (NG NFU).

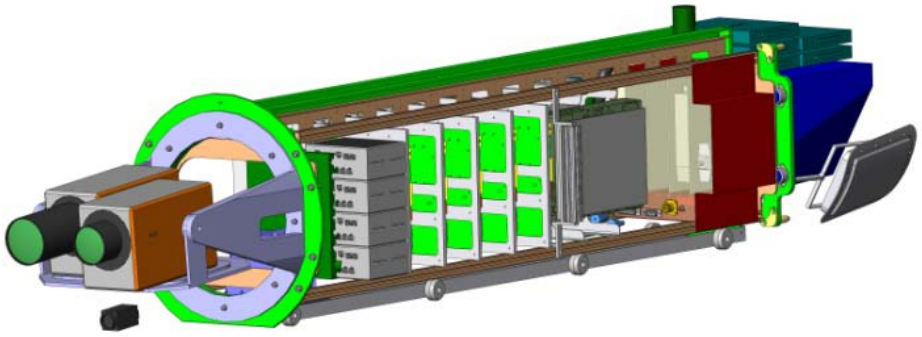

Figure 1.3 NG NFU Internal Components (Preliminary).

1.2 Naval Strike Missile Nytt Flymåleutstyr (NSM NFU)

The Naval Strike Missile Nytt Flymåleutstyr (NSM NFU) will be built by KDA to serve as a test facility for the components of the NSM. The design will consist of the production NSM seeker and avionics section mounted to the forward strong ring, electronics and recording equipment in the center section, and cooling systems in the aft section. A preliminary design is shown in figure 1.4 and the NSM NFU internal components are shown in figure 1.5.

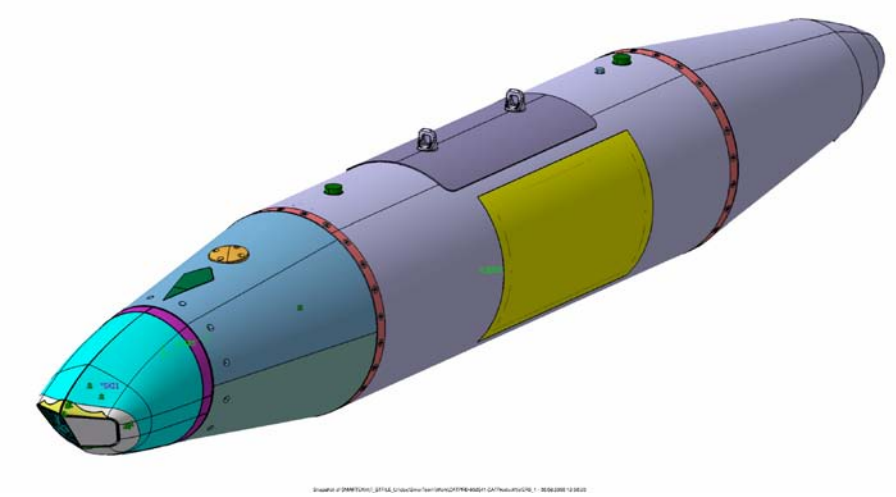

Figure 1.4 Preliminary Design of the Naval Strike Missile Nytt Flymåleutstyr (NSM NFU).

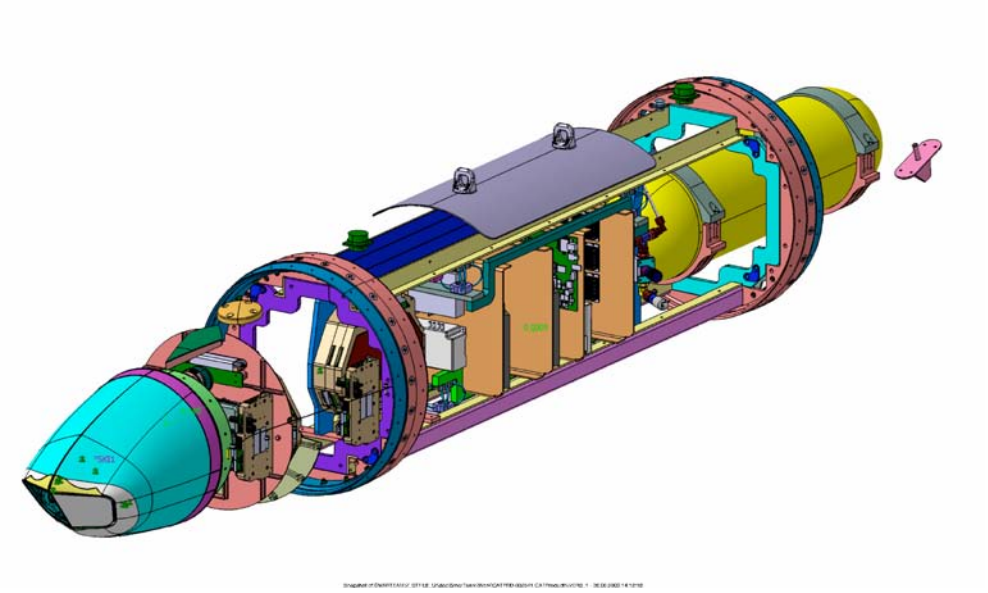

Figure 1.5 NSM NFU Internal Components (Preliminary).

Flight clearance of each NFU pod will be performed by the Norwegian Defence Logistics Organization (FLO/S/LU) in conjunction with the Royal Norwegian Air Force. In preparation for the certification program, Project 6450 appointed a working group to develop and clarify the scope of the flight certification process. This team highlighted the increased moment of inertia as a major uncertainty in the design effort and planned a series of flight tests with a variable mass distribution to determine how changes to the moment of inertia affect the dynamic properties of the baseline MXU-648A/A Cargo/Travel Pod.

2 Purpose

A test program was conducted to evaluate the MXU-648A/A Cargo/Travel Pod internal environment as installed on the F-16A aircraft for the NFU Program. Another primary objective was to determine the effects of increasing the MXU-648A/A moment of inertia during typical research flight profiles.

3 Description of Test Aircraft

The F-16 used for these flight tests was a single engine, multirole tactical fighter and is depicted in figure 3.1. The fuselage was characterized by a large bubble canopy, fore body strakes, and an under fuselage engine air inlet. The wing and tail surfaces were thin and featured moderate aft sweep. The wing design included eight weapon stations and was capable of carrying a wide variety of external stores and targeting sensors. A more detailed description of the F-16A aircraft can be found in the F-16A/B Flight Manual [1]. The aircraft used for this test (RNoAF F-16A tail number 665, side number 107) was considered representative of production models.

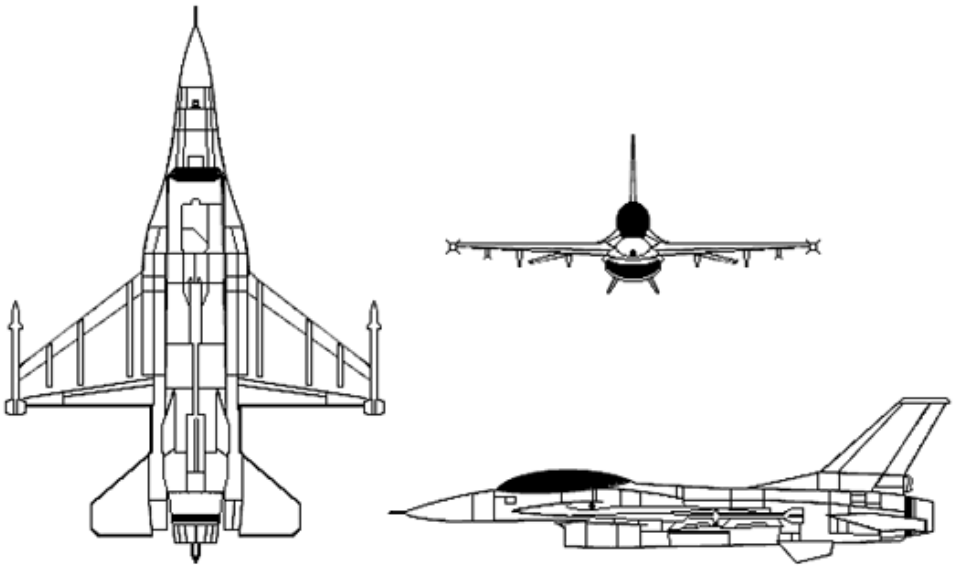

Figure 3.1 F-16 Aircraft.

4 Description of Test Equipment

The baseline MXU-648A/A Cargo/Travel Pod, depicted in figure 1.1, was an all welded, cylindrical storage container designed to transport up to a maximum of 300 pounds of personal equipment or cargo. Key features included a large access door with quick release fasteners, 56 inches of flat cargo space, and adequate provisions for securing the cargo. There were no provisions for external power or communication with the host aircraft. The MXU-648A/A used for this test was representative of production models.

The test equipment consisted of two weights (lead bars) and a frame structure to distribute the weight to the load bearing floor in the MXU-648A/A. Each weight was mounted to a tray that could be easily positioned in order to set the desired center of gravity and mass distribution. This design feature permitted the pod moment of inertia to be adjusted prior to each flight. Figure 4.1 depicts the frame structure isolated from the cargo pod, while figure 4.2 and figure 4.3 depict the MXU-648A/A with the frame and weights installed in two different locations.

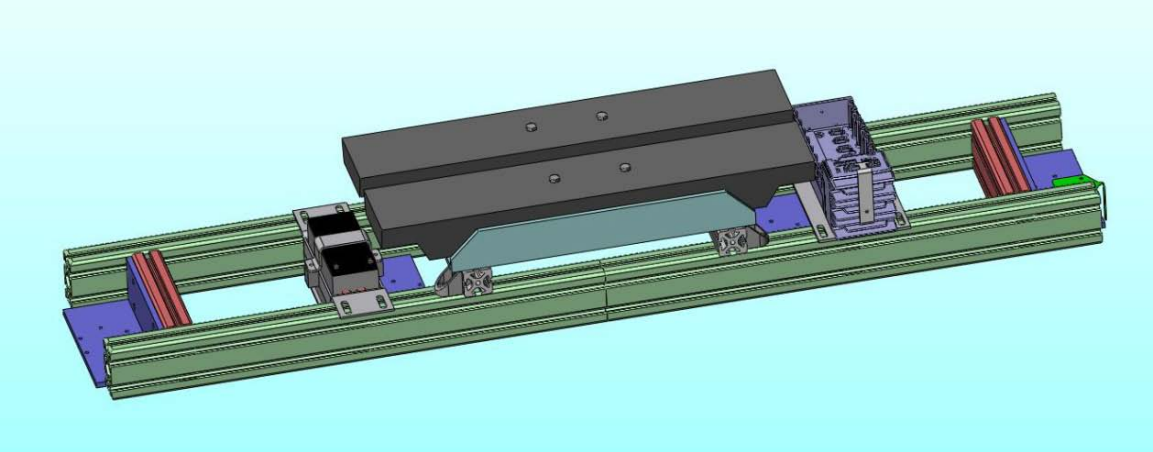

Figure 4.1 Load frame with centered weights. The data recorder is placed to the right of the weights while the power supply is located on the left.

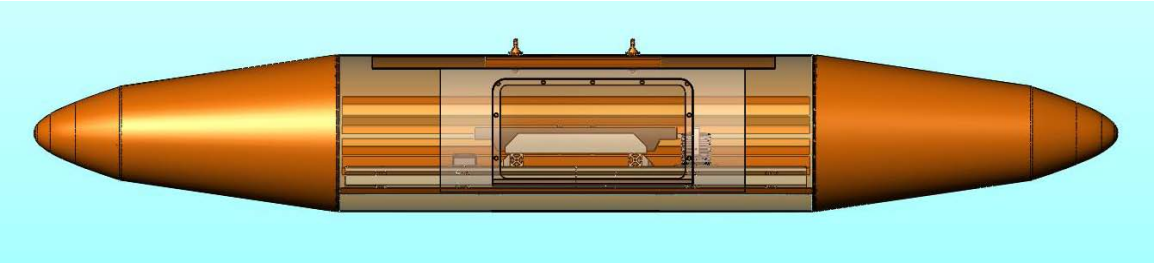

Figure 4.2 MXU-648A/A with the payload installed and the weights centered. The center section is shown with a semi-transparent skin.

Figure 4.3 Cross section of the MXU-648A/A with the lead weights distributed. The distance between the weights can be adjusted incrementally from zero to the outer position as shown in the figure.

The weight of each payload component is presented in table 4.1. The moment of inertia about the vertical axis (z-axis) varied from 27.1 kg·m^2 (20.0 slug·ft^2) on the first flight to 66.4 kg·m^2 (49.0 slug·ft^2) on the third flight. Additional details regarding the moment of inertia are provided in sections 5 and 6.

Table 4.1 MXU-648A/A Payload Weights.

Payload Component	Weight
Lead Weight (2 @ 97 lb)	194 lb
Frame Structure	57 lb
Battery with holder	8 lb
Data Recorder and Sensors	5 lb
Total	**264 lb**

Note: The MXU-648A/A is capable of carrying a maximum of 300 lb.

4.1 Instrumentation

Four types of detectors were used to measure the internal pod environment: Accelerometers, temperature sensors, an acoustic pressure sensor, and an atmospheric pressure sensor. All of the sensors were small and lightweight and were temporarily glued to the inside of the MXU-648A/A or were mounted to the data recorder support structure. Figure 4.4 presents the approximate location of the sensors.

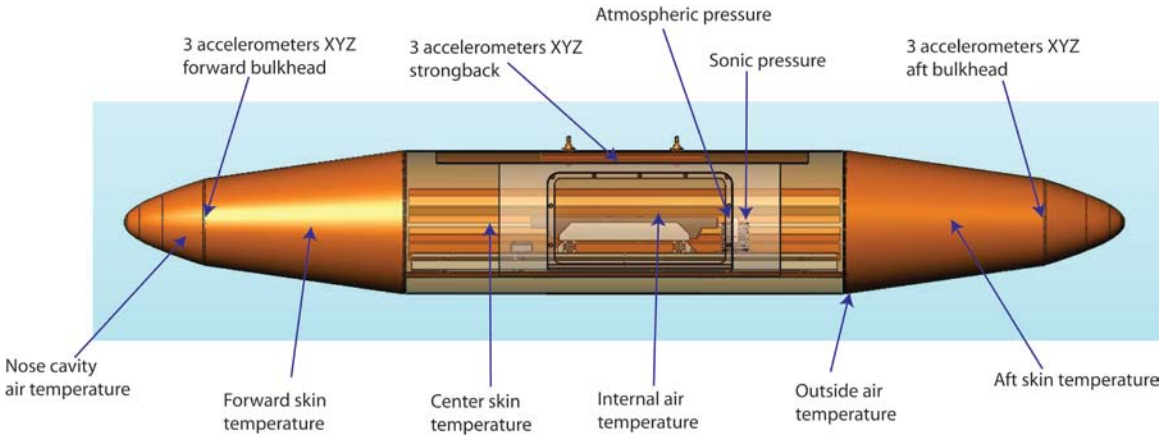

Figure 4.4 MXU-648A/A sensor placement. All sensors were mounted inside. The "Outside air temperature" probe was mounted to protrude from the rear drain hole so that the sensor element was in contact with the outside air flow.

4.1.1 Accelerometers

A total of nine accelerometers were used to measure vibrations in each principal axis (x, y, and z as defined in figure 4.5) at three separate locations (forward, center, and aft). Each set of three accelerometers were mounted to a block of aluminum in an orthogonal configuration as shown in Figure 4.6. Each aluminum block was glued firmly to an internal surface of the MXU-648A/A with cement. Photographs of the installed locations are presented in figures 4.7 – 4.9.

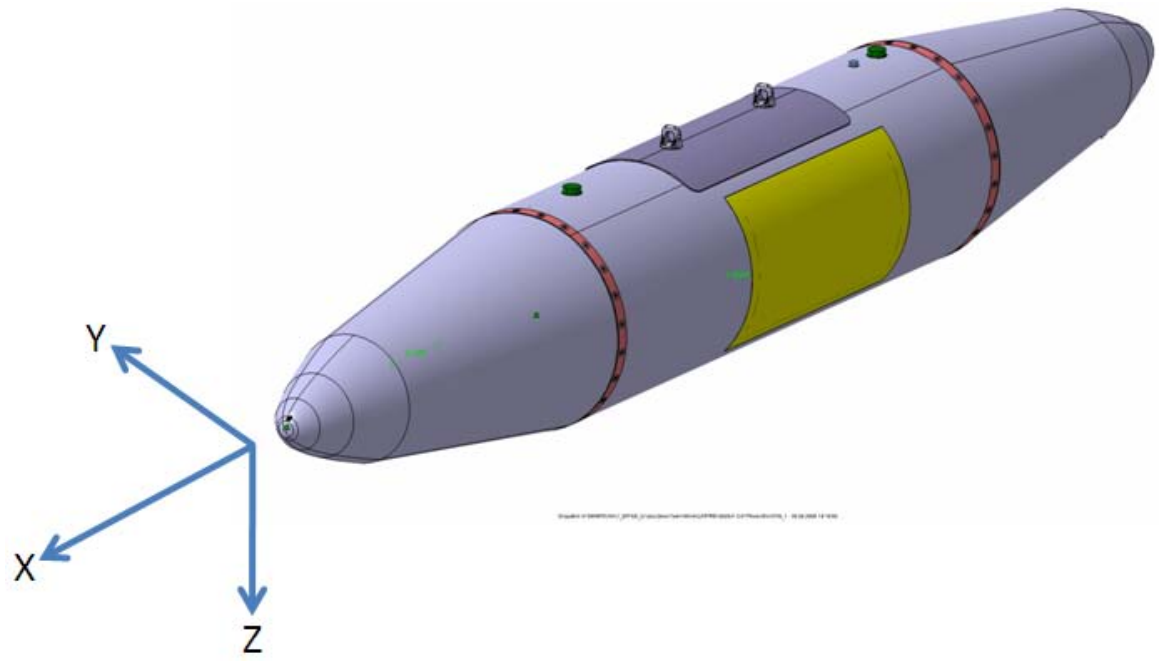

Figure 4.5 MXU-648A/A Coordinate System.

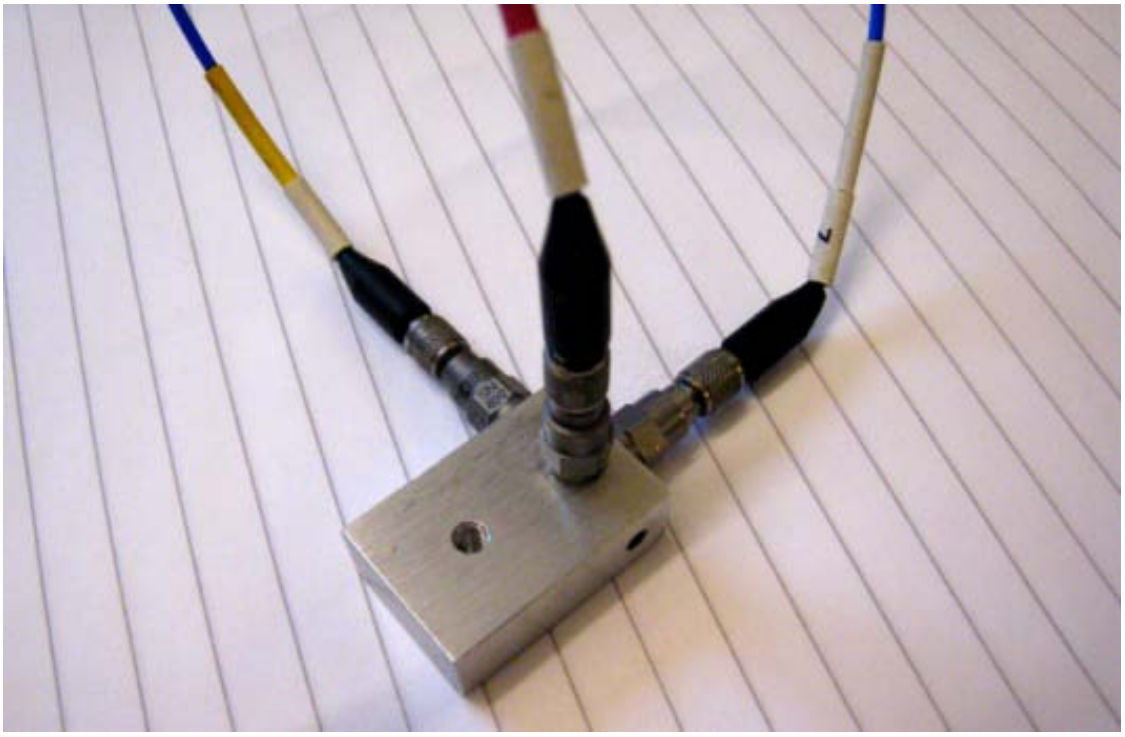

Figure 4.6 Accelerometers attached to the aluminum block.

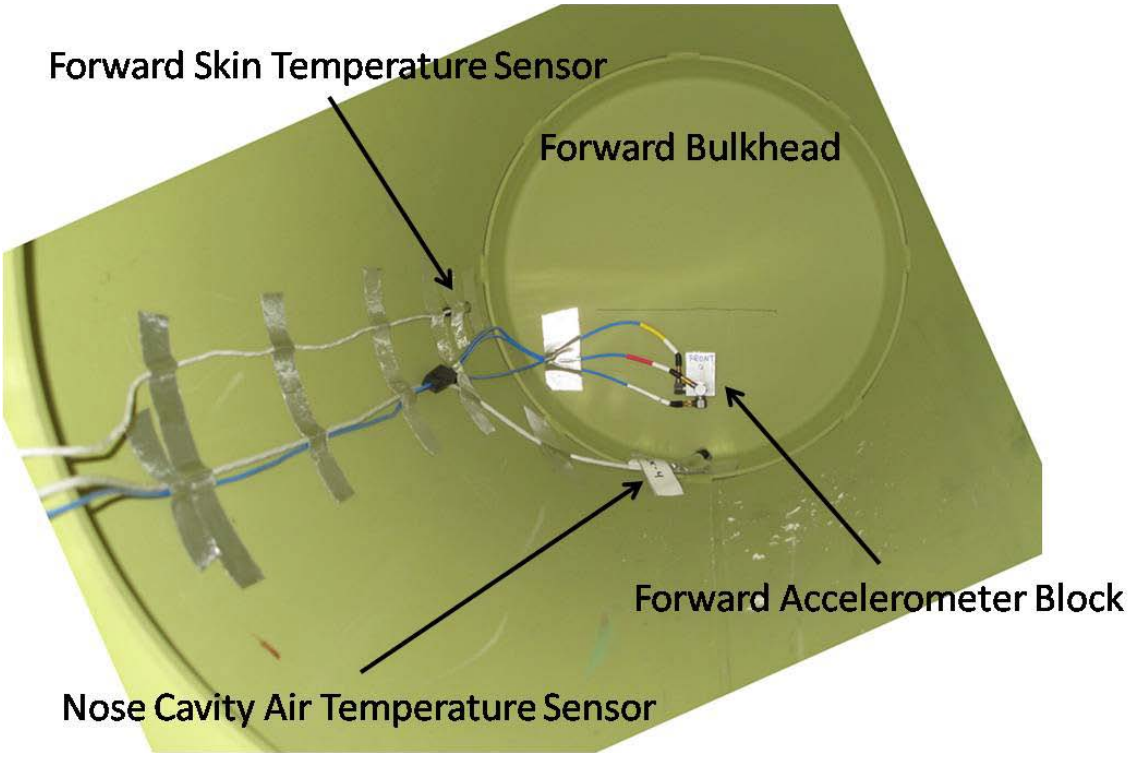

Figure 4.7 Mounting locations of MXU-648A/A instrumentation (forward section).

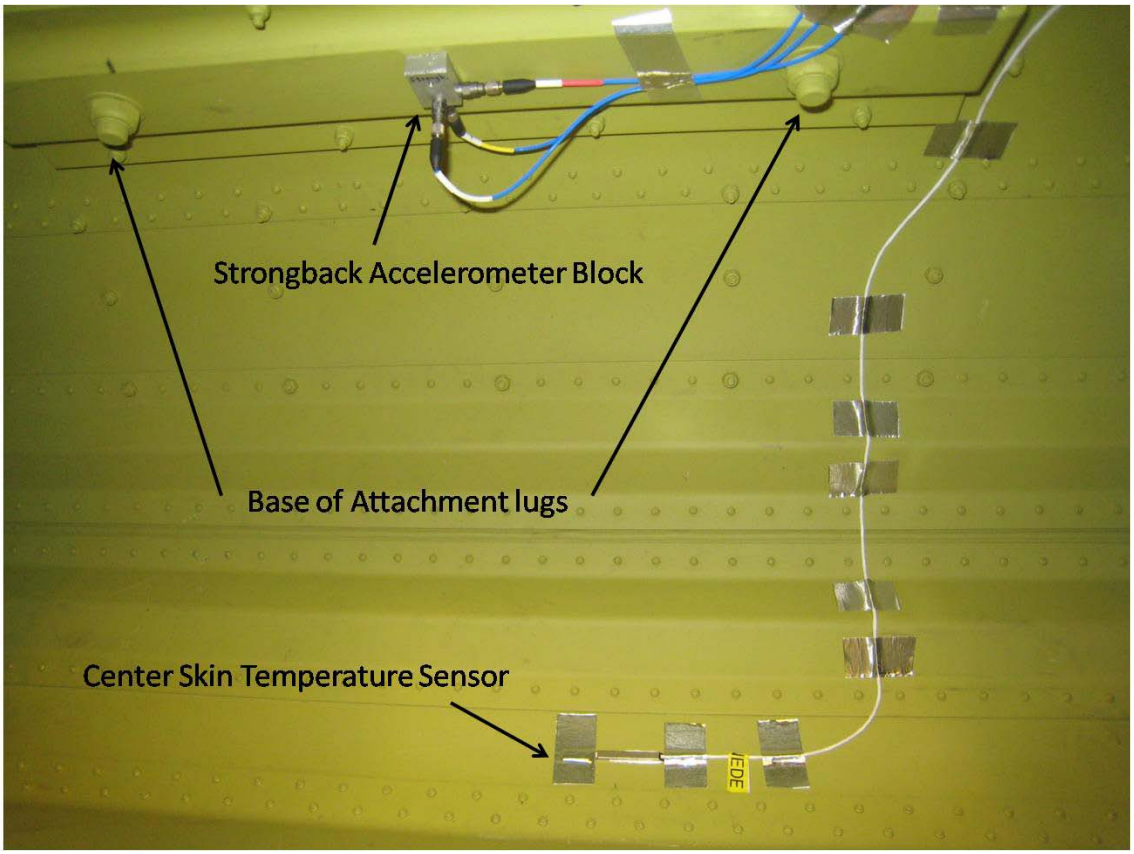

Figure 4.8 Mounting locations of MXU-648A/A instrumentation (center section).

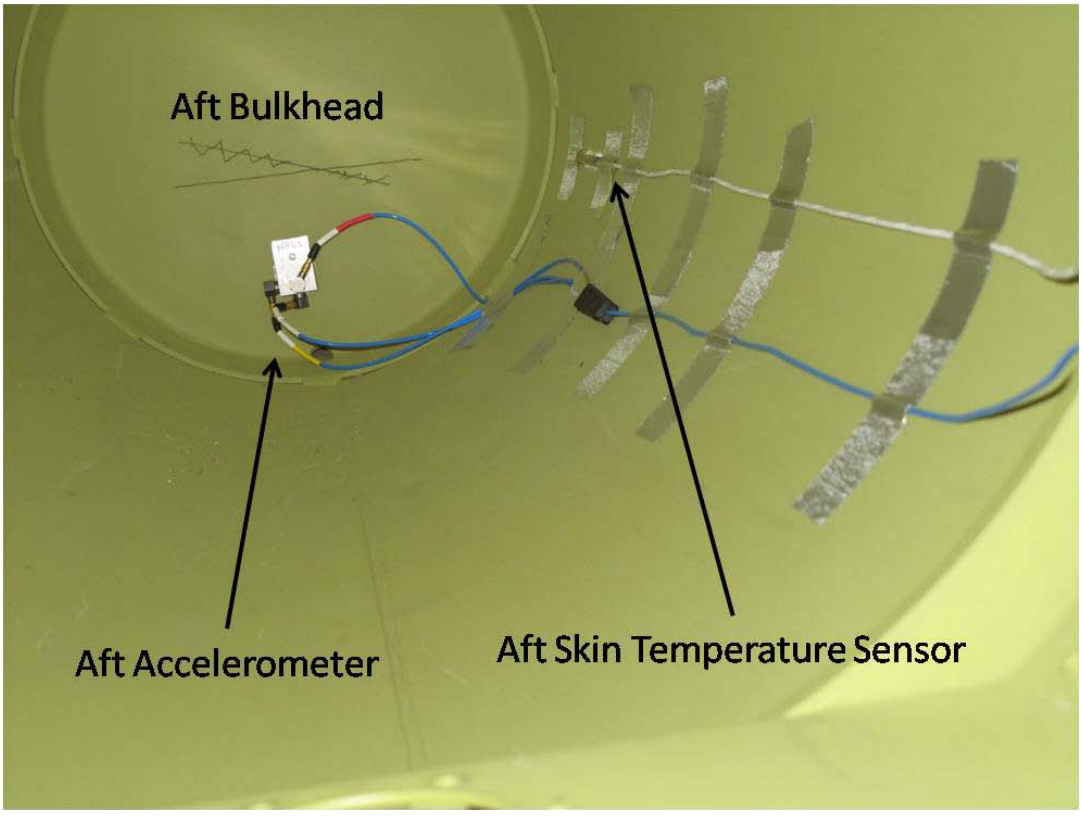

Figure 4.9 Mounting locations of MXU-648A/A instrumentation (aft section).

4.1.2 Temperature Sensors

Six temperature sensors, of the 4-wire Pt100 type, were used to document the thermal environment of the MXU-648A/A. A total of three skin temperature sensors were installed; one in each of the forward, center, and aft sections of the pod. These sensors were attached to the hull with aluminum tape and included a layer of thermally conductive material between the hull and sensor. One air temperature probe was installed in the nose cavity. The wires for this sensor were routed through a pressure equalization hole in the forward plate (bulkhead) and were held in place with insulating material and aluminum tape. The sensor that measured the outside air temperature was attached to a drainage hole with polyurethane and held in place with a cable clamp. The internal air temperature probe was installed in the center section and was attached to the data recorder bracket so that the sensor element was exclusively in contact with air. Photographs of the installed locations are presented in figures 4.7 – 4.10.

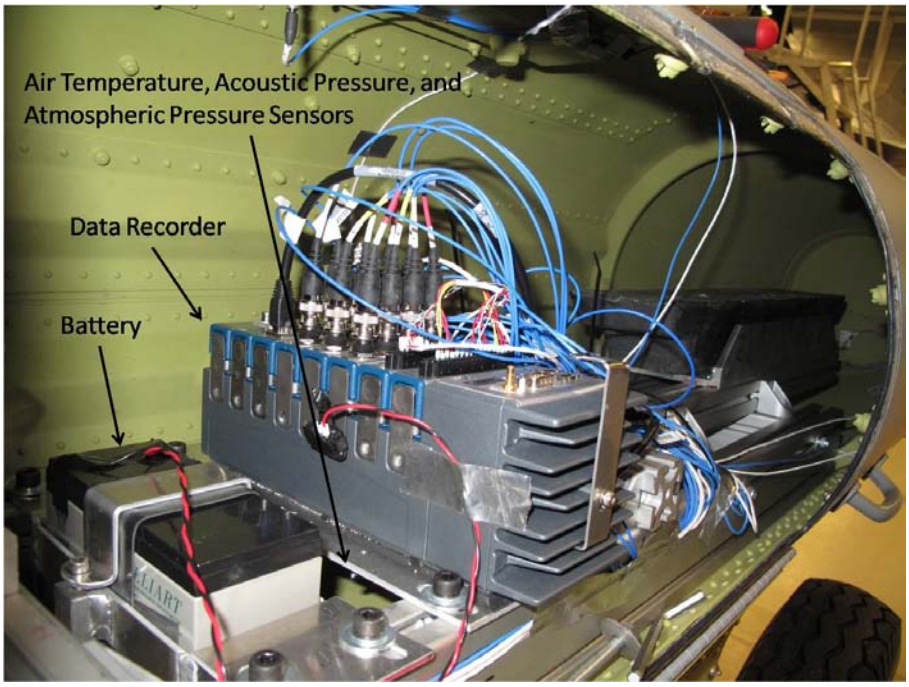

Figure 4.10 Mounting locations of MXU-648A/A instrumentation and power supply.Air temperature, acoustic pressure and atmospheric pressure sensors are mounted underneath the data recorder.

4.1.3 Microphone

The acoustic air pressure sensor was a microphone of the type PCB 103A02 as shown in figure 4.11. The sensor provided acoustic frequency information in addition to the absolute sound pressure. The sensor was attached to the data recorder bracket as shown in figure 4.10.

Figure 4.11 Acoustic Air Pressure Sensor PCB 103A02.

4.1.4 Atmospheric Pressure Sensor

The atmospheric pressure sensor was mounted in a separate aluminum box with electronics for customizing the electrical interface to the data recorder. The assembly was mounted to the data recorder mounting bracket as shown in figure 4.10.

4.1.5 Data Acquisition System

The National Instruments CompactRIO 9012 data recorder was used to control, store, and manage the signals from each of the 19 data channels. The recorder was mounted in the center section of the MXU-648A/A as shown in figure 4.10. The design featured rugged construction, small size, and reconfigurable input/output modules with built-in signal conditioning. The programmable recording rate was set to 5000 samples per second for each channel for these tests. A more detailed description of the data acquisition system can be found in the CompactRIO Operating Manual [2].

4.1.6 Power Supply

The NP7 12L battery, manufactured by Yuasa Batteries Inc., was used to power the data recorder. This gel based, sealed lead battery was designed to not leak with mechanical damage (cracks) or when ambient temperatures exceed 50 °C and was recommended by the International Air Transport Association (IATA). The location of the battery is shown in figure 4.10.

5 Scope of Test

The evaluation consisted of three test flights totaling 3.6 hours. All test flights were conducted from Bodø Main Air Station during visual meteorological conditions (VMC). The external configuration is presented in table 5.1 and a photograph of the aircraft loaded with the stores is shown in figure 5.1. This configuration was based on Ferry Configuration 140.01, Line 21 from the F-16A/B Flight Manual [1], as shown in figure 5.2. This configuration was selected to reduce the risk associated with aeroelastic stability (flutter) as this store arrangement provided the most flutter speed margin primarily due to the wing tip mounted captive air-to-air training missiles (CATM-120).

Table 5.1 External Configuration.

Station	Store
1	CATM-120
2	EMPTY
3	Instrumented MXU-648A/A
4	370 Gallon External Fuel Tank
5	EMPTY
6	370 Gallon External Fuel Tank
7	EMPTY
8	EMPTY
9	CATM-120

Figure 5.1 F-16A External Configuration.

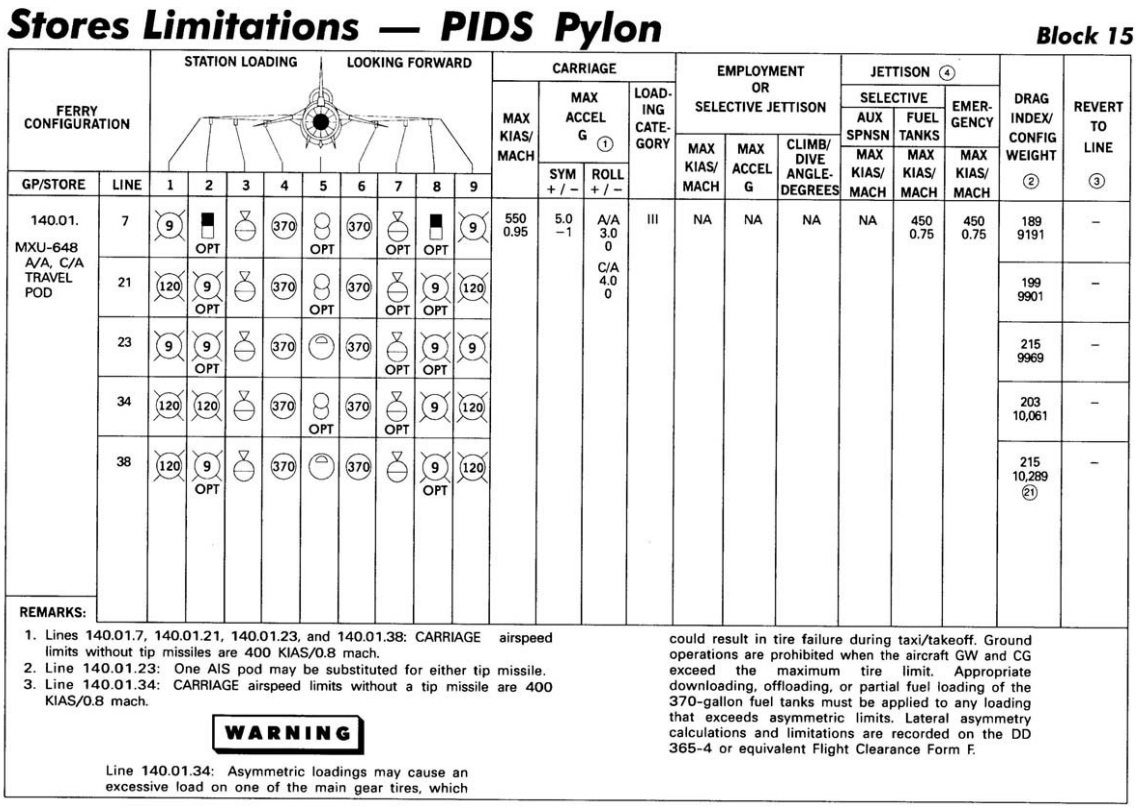

Stores Limitations — PIDS Pylon — Block 15

FERRY CONFIGURATION		STATION LOADING — LOOKING FORWARD									CARRIAGE				EMPLOYMENT OR SELECTIVE JETTISON			JETTISON ④			DRAG INDEX/ CONFIG WEIGHT ②	REVERT TO LINE ③
											MAX KIAS/ MACH	MAX ACCEL G ①		LOAD-ING CATE-GORY	MAX KIAS/ MACH	MAX ACCEL G	CLIMB/ DIVE ANGLE-DEGREES	SELECTIVE		EMER-GENCY		
												SYM + / −	ROLL + / −					AUX SPNSN	FUEL TANKS			
GP/STORE	LINE	1	2	3	4	5	6	7	8	9								MAX KIAS/ MACH	MAX KIAS/ MACH	MAX KIAS/ MACH		
140.01. MXU-648 A/A, C/A TRAVEL POD	7	9	OPT		370	OPT	370	OPT	OPT	9	550 0.95	5.0 −1	A/A 3.0 0 C/A 4.0 0	III	NA	NA	NA	NA	450 0.75	450 0.75	189 9191	–
	21	120	9 OPT		370	OPT	370	OPT	9 OPT	120											199 9901	–
	23	9	9 OPT		370		370	OPT	9 OPT	9											215 9969	–
	34	120	120		370	OPT	370	OPT	9	120											203 10,061	–
	38	120	9 OPT		370		370		9 OPT	120											215 10,289 ㉑	–

REMARKS:

1. Lines 140.01.7, 140.01.21, 140.01.23, and 140.01.38: CARRIAGE airspeed limits without tip missiles are 400 KIAS/0.8 mach.
2. Line 140.01.23: One AIS pod may be substituted for either tip missile.
3. Line 140.01.34: CARRIAGE airspeed limits without a tip missile are 400 KIAS/0.8 mach.

WARNING

Line 140.01.34: Asymmetric loadings may cause an excessive load on one of the main gear tires, which could result in tire failure during taxi/takeoff. Ground operations are prohibited when the aircraft GW and CG exceed the maximum tire limit. Appropriate downloading, offloading, or partial fuel loading of the 370-gallon fuel tanks must be applied to any loading that exceeds asymmetric limits. Lateral asymmetry calculations and limitations are recorded on the DD 365-4 or equivalent Flight Clearance Form F.

Figure 5.2 Approved Ferry Configurations from TO 1F-16AM-1-3 [1].

The test envelope and applicable flight manual limits are presented in table 5.2.

Table 5.2 F-16 Test Envelope.

Parameter	Test Envelope		Flight Manual Limit	
	Min	Max	Min	Max
Altitude (ft)	200 ft AGL	36,000 ft Hp	Surface	50,000 ft MSL
Airspeed (KCAS)	250	540	0	550
Mach Number (IMN)	0	0.92	0	0.95
Symmetric Load Factor (g)	1	4.8	-1	5.0
MXU-648A/A Cargo Weight (lb)	-	264	0	300

A detailed matrix of test conditions and tolerances is presented in Appendix A and graphically in figure 5.3. The individual test points were designed to collect data at the flight conditions that the NG NFU and NSM NFU will encounter during future research missions. Typical NFU research missions will consist of the following maneuvers and flight conditions:

- Normal takeoff and landing
- Climbs and descents
- Transit cruise to and from test airspace at high and low altitudes
- Navigational turns
- Shallow dive profiles (5°-30°), including pull-out
- High speed, low level target runs

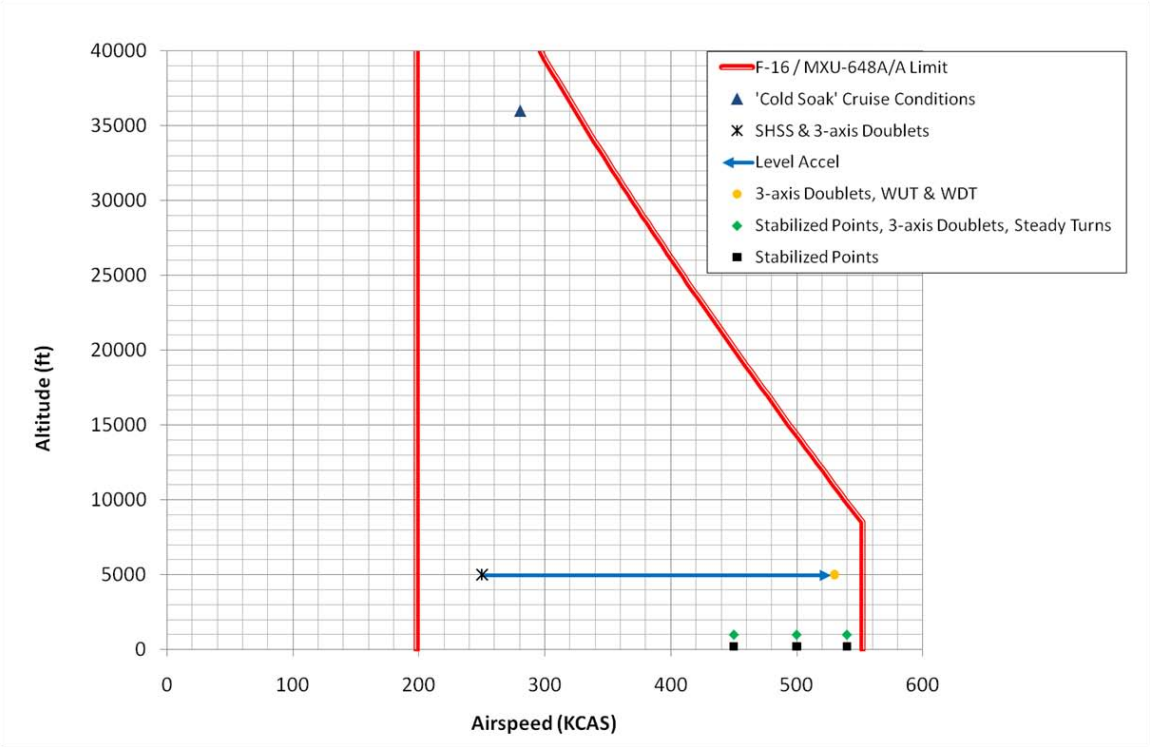

Figure 5.3 Test Points and Test Envelope. Red lines indicate speed limits for F-16 with MXU-648A/A. Maneuvers are described in table 6.1.

The test matrix was planned so that all test points could be completed in a 1.0 hour test flight. This approach permitted the test points to be precisely repeated on successive flights in order to determine the effects of varying the MXU-648A/A moment of inertia. Table 5.3 lists the measured MXU-648A/A moment of inertia about the yaw axis for each of the three test flights. The empty configuration is provided for reference.

Table 5.3 MXU-648A/A Moment of Inertia About the Yaw Axis (I_{zz}).

Configuration	Position of Lead Bars	I_{zz}, Moment of Inertia	
		$kg \cdot m^2$	$slug \cdot ft^2$ (1)
Empty MXU-648A/A	-	16.7	12.3
Flight #1	Centered	27.1	20.0
Flight #2	Intermediate	40.4	29.8
Flight #3	Spread	66.4	49.0

(1) A "slug" of mass will accelerate at 1 ft/sec^2 when subjected to 1 lb_f of unbalanced force.

6 Method of Test

The test aircraft ground and flight procedures were executed in accordance with the F-16A/B Flight Manual [1], and the Royal Norwegian Air Force Standard Operating Procedures. The flight test techniques and procedures were conducted in accordance with the United States Naval Test Pilot School Flight Test Manual 103 – Fixed Wing Stability and Control [3]. A brief description of each test maneuver and its purpose is provided in Table 6.1.

Table 6.1 Test Maneuver Descriptions.

Test Maneuver	Description	Purpose
Stabilized Point	Aircraft is carefully stabilized in wings level, 1g flight at the specified airspeed and altitude for > 2 minutes	Collect data during unaccelerated flight conditions. Remaining on conditions for long durations will permit the internal pod temperature to stabilize.
Level Acceleration	Aircraft accelerates to specified conditions using MIL power (or MAX) while maintaining wings level, 1g flight	Collect vibration and acoustic data over wide range of speed
Wind Up Turn	Aircraft climbs above test altitude and enters a descending turn back towards test altitude. As the turn continues, the normal acceleration is gradually increased while maintaining constant airspeed or Mach. Altitude is sacrificed as needed to maintain airspeed or Mach.	Collect vibration and acoustic data over a wide range of normal acceleration.
Steady Turn	Aircraft enters a turn using any necessary pitch and roll axis inputs to stabilize at the specified airspeed and normal acceleration	Collect vibration and acoustic data at specific values of normal acceleration
Wind Down Turn	Aircraft is decelerated (IDLE power) while increasing angle of attack and maintaining constant altitude	Collect vibration and acoustic data over wide range of angle of attack
Steady Heading Side Slip	From wings level flight at the specified airspeed and altitude, the aircraft sideslip angle is slowly increased using rudder pedal inputs (1/4 pedal increments) while simultaneously applying any necessary roll and pitch axis inputs in order to maintain a steady heading at constant airspeed	Collect vibration and acoustic data over range of sideslip angles.
Pitch Axis Doublet	From wings level flight at the specified airspeed and altitude, the aircraft pitching motion is excited by applying a small nose down input followed by an equivalent nose up input and then returning the control stick to trim position	Excite pitching motion in order to determine frequency and damping of pod motion
Yaw Axis Doublet	From wings level flight at the specified airspeed and altitude, the aircraft yawing motion is excited by applying a small rudder pedal input followed by an equivalent opposite pedal input and then returning the pedals to trim position	Excite yawing motion in order to determine frequency and damping of pod motion
Low Angle Dive Profile	Aircraft follows a precise dive pattern towards a ground based reference point. Dive parameters are outlined in a "Z diagram".	Replicate NFU mission profile. Rate of change of internal pod pressure during typical dive.

Specific test events were executed according to the detailed test matrix presented in Appendix A, as outlined in the FLO/S/LU/PF 06-2009 Test Plan [4]. The test flights were accomplished in a specific sequence in order to gather data at smaller moments of inertia prior to the larger values. During each flight, testing was accomplished at high altitudes before low altitudes, at low speeds prior to high speeds, and at low levels of normal acceleration (n_z) prior to higher values in order to safely progress to the final test conditions.

The MXU-648A/A moment of inertia about the yaw axis was determined during ground tests using the bifilar pendulum method as described in the Sargent Fletcher, Inc. Weight, Center of Gravity, and Moment of Inertia Test Report for the Cargo/Travel (MXU) Pod [5].

The test aircraft was equipped with a production pitot-static system and g-meter. Except for the 200 ft above ground level tests, the test points were executed at the specified pressure altitudes (altimeter set to 1013 mm Hg) so that unique test day data from each of the three flights could be referred to standard day conditions.

7 Data Reduction and Analysis

7.1 Aircraft Data Sources

Time and Space Position Information (TSPI) from the test aircraft was downloaded following each flight. Time history plots were processed using Microsoft Excel software. This data was used to verify that specific tolerances on the test conditions (altitude, airspeed, etc.) were achieved. The aircraft Heads Up Display (HUD) video tapes were acquired after each flight and were used to determine the exact start and stop time of each test event. The HUD tapes also provided documentation of the pilot's qualitative comments of cockpit vibration levels and observed wing and pod (forward section) movement. The start and stop times for each test event are provided in Appendix B, tables B-1 to B-3.

7.2 MXU-648A/A Data Recorder

During each flight, the data recorder inside the MXU-648A/A was activated shortly after engine start and was deactivated following engine shutdown. Nineteen channels were continuously recorded at 5000 samples per second. Due to the high sample rate, individual binary data files were created and saved to memory every 5 minutes. Table 7.1 provides the list of parameters. The raw binary data files from each flight were converted to a matrix format that was compatible with MATLAB software. The complete set of raw data is located on the FFI internal drive in the folder: \\Ffi.no\grupper\Prosjekt-NFU\Tester\Tester_med_F-16\MXU-tests\Bodø-Jan-2010.

Table 7.1 Flight Test Parameters.

Channel #	Parameter
1	Time
2	Acceleration – Front Plate X axis (Longitudinal)
3	Acceleration – Front Plate Y axis (Lateral)
4	Acceleration – Front Plate Z axis (Vertical)
5	Acceleration – Strong Back X axis (Longitudinal)
6	Acceleration – Strong Back Y axis (Lateral)
7	Acceleration – Strong Back Z axis (Vertical)
8	Acceleration – Aft Plate X axis (Longitudinal)
9	Acceleration – Aft Plate Y axis (Lateral)
10	Acceleration – Aft Plate Z axis (Vertical)
11	Sound Pressure - Forward
12	Sound Pressure – Aft
13	Atmospheric Pressure
14	Temperature – Nose
15	Temperature – Skin Forward
16	Temperature – Skin Center
17	Temperature – Skin Aft
18	Temperature – External Probe
19	Temperature – Internal Probe

7.2.1 Temperature Sensor Data Reduction

MATLAB function files were developed to generate time history plots of temperature for each stabilized point test event. The value of each channel was determined once the temperature had stabilized to within +/- 0.5 °C over a period of 30 seconds. The stabilized temperatures were recorded and plotted to display the variation of temperature with airspeed at 1000 ft pressure altitude and 200 ft above ground level. Time history plots were also created for the level acceleration test points for each flight and the climb to 36000 ft and 5 minute cold soak during the first flight.

7.2.2 Acceleration Spectral Density (ASD)

MATLAB function files were developed to analyze the variation of vibration magnitude and frequency with MXU-648A/A moment of inertia. First, spectral density information was generated using the periodogram method as described by Stoica and Moses [6] and Welch [7]. This procedure and subsequent ASD plots displayed the distribution of acceleration ‘power’ per unit frequency and were used to determine the dominant vibration frequencies of each test event. Individual plots were constructed for each accelerometer (9) and test event (25) and included results from all three flights on the same plot in order to illustrate how the vibration characteristics varied with changes to the MXU-648A/A moment of inertia.

7.2.3 Vibration Envelope

Special ‘Vibration Envelope’ plots were created by combining all of the individual ASD plots from one accelerometer during one flight in order to identify which test events created the most severe vibration environment. These plots were also used to determine how the peak vibration

frequencies varied from the first flight to the third flight. Each line in the vibration envelope plot (total of 22) represents the spectral density from a separate test event. The maximum values throughout the flight highlight the dominant vibration frequencies and define the overall envelope. These plots also include the recommended limits for jet aircraft store buffet response and jet aircraft store equipment vibration exposure from guidance provided in MIL-STD-810F, Department of Defense Test Method Standard for Environmental Engineering Considerations and Laboratory Tests [8]. Only the test events that triggered an exceedance of the MIL-STD-810F guidance were identified on the plots. The vibration envelope plots were constructed only for the y- and z-axes as no specific MIL-STD-810F guidance was provided for the x-axis.

7.2.4 Root Mean Square - Acceleration (g_{rms}) Metrics

MATLAB function files were created to calculate the root mean square of the acceleration (g_{rms}) for each test point. This statistical metric was used to compare vibration magnitudes between individual flight events in order to determine the effect of the increased moment of inertia during the second and third flights. Plots were created to present the metric for all 9 accelerometer channels during each flight.

7.2.5 Low Frequency Pod Dynamics

MATLAB function files were developed to filter the raw data and generate time history plots of acceleration for each 3-axis doublet test point during each of the 3 test flights. These plots were used to analyze MXU-648A/A dynamic motion, including estimates of damping ratio, following a low frequency excitation initiated by the pilot in each principal axis (pitch, roll, and yaw doublets).

7.2.6 Pressure Sensor Data Reduction

MATLAB function files were developed to generate time history plots of pressure for each flight. These plots were used to document the internal pod pressure as the test aircraft altitude was varied.

8 Results

8.1 Temperature Measurements

The temperature data were gathered at two different altitudes (1000 ft pressure altitude and 200 ft above ground level) and three separate airspeeds (450, 500, and 540 KCAS) using the stabilized point technique. An additional stabilized point was executed on the first flight at 36000 ft pressure altitude and 0.84 Mach to determine the pod temperatures at typical high altitude ferry conditions. Additional test day meteorological conditions, including static temperature versus altitude, were also collected from the daily weather balloon that was launched from Bodø Main Air Station. Each stabilized point consisted of flying at constant airspeed and altitude for 2 minutes. The stable temperature was determined within the last 30 seconds of the test point when the change in temperature was less than +/- 0.5 °C. Table 8.1 summarizes the stabilized temperatures for each flight condition.

Table 8.1 Stabilized Temperatures.

Flight #	Altitude (ft)	Airspeed (KCAS)	OAT[(1)] (°C)	Forward Skin (°C)	Center Skin (°C)	Aft Skin (°C)	Nose Cavity[(2)] (°C)	Internal[(2)] (°C)	External Probe (°C)
1	1000	450	-9	15.4	15	16	14.2	2.5	12.2
1	1000	500	-9	17.3	18.6	19.6	17.8	4.2	16.6
1	1000	540	-9	22.6	24.1	25.0	22.7	6.8	20.9
1	200	450	-11	16.0	16.3	17.0	16.5	8.8	14.7
1	200	500	-11	20.0	21.0	21.9	19.5	9.5	19.0
1	200	540	-11	23.7	25.3	26.2	23.1	10.2	22.1
1	36000	280	-61	-37.6	-33.0	-34.9	-34.6	6.9	-38.8
2	1000	450	-9	13.3	13.4	14.2	13.4	0.1	11.1
2	1000	500	-9	17.0	18	19.1	15.9	1.9	15.0
2	1000	540	-9	21.5	23.1	23.9	21.1	4.5	18.7
2	200	450	-11	15.2	15.2	15.8	15.7	6.4	13.1
2	200	500	-11	18.0	19.0	20.0	17.1	7.0	16.2
2	200	540	-11	22.5	24.1	25.0	22.5	8.2	20.3
3	1000	450	-7	13.2	13.4	14.1	13.2	4.7	10.8
3	1000	500	-7	16.8	18.0	19.1	15.9	6.3	14.7
3	1000	540	-7	20.8	22.5	23.3	20.0	9.0	18.0
3	200	450	-6	15.5	15.8	16.3	16.7	11	13.5
3	200	500	-6	19.4	20.5	21.4	19.4	11.7	17.9
3	200	540	-6	23.0	24.3	25.1	22.5	12.8	20.2

(1) Outside Air Temperature as reported from the Bodø Main Air Station weather balloon.

(2) The Nose Cavity and Internal temperatures had not reached stable values after 2 minutes.

8.1.1 Skin Temperatures

In all cases, each skin temperature sensor achieved a stable reading within approximately 30 seconds from when the aircraft was established on the test conditions. Plots showing the variation of temperature with airspeed for the first test flight are presented in figures 8.1 and 8.2. Results from the second and third flights are similar and are presented in Appendix C, figures C-1 to C-4.

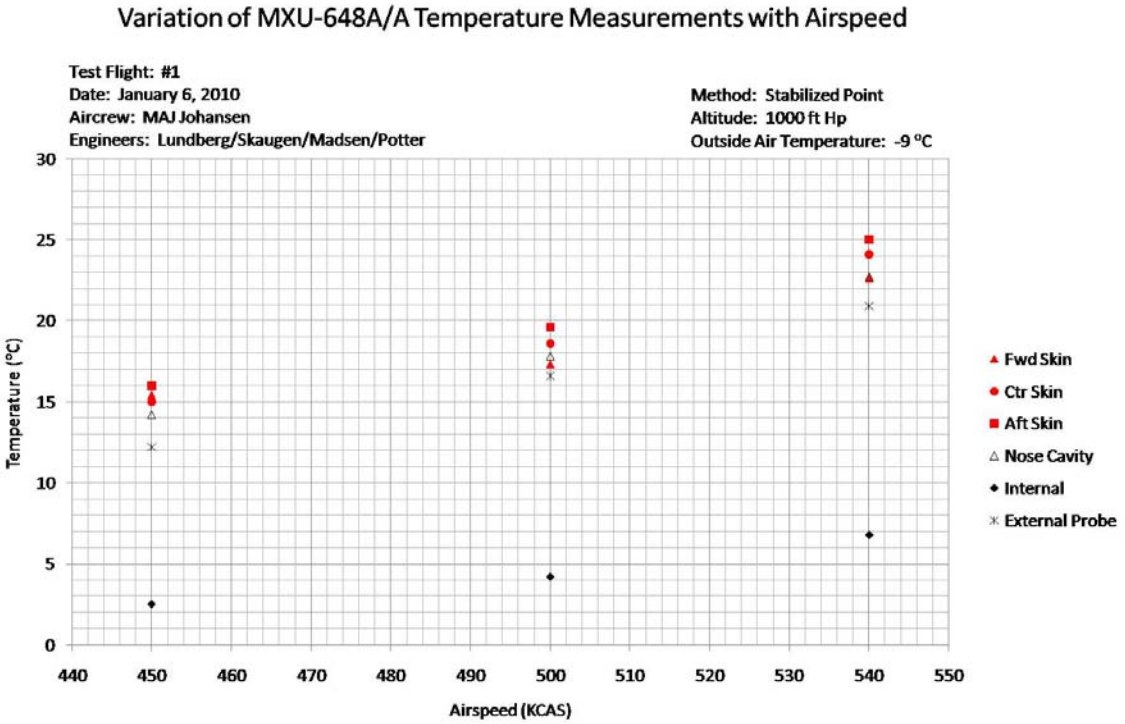

Figure 8.1 Variation of Temperature with Airspeed (1000 ft Pressure Altitude).

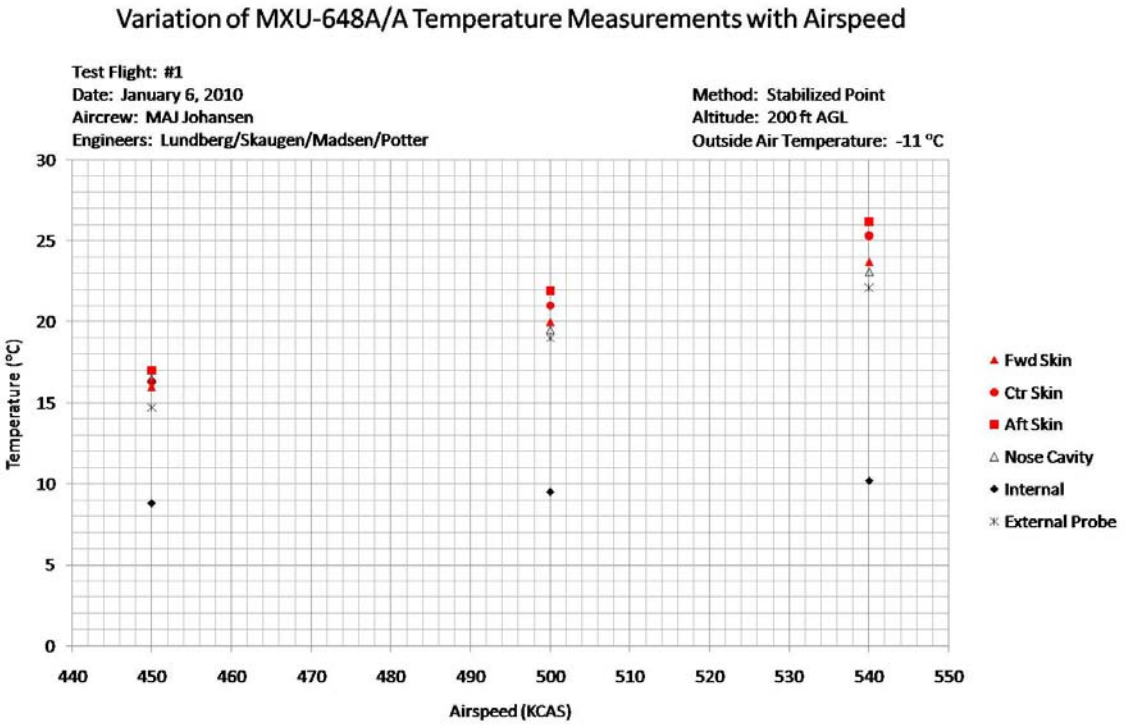

Figure 8.2 Variation of Temperature with Airspeed (200 ft Above Ground Level).

The warmest temperature recorded was the aft skin temperature of 26.2 °C during the first flight at 540 KCAS and 200 ft AGL. The forward skin temperature was only 23.7 °C and the static outside air temperature was -11 °C during this test point. As shown in figure 4.7, the forward

skin temperature sensor was mounted to the side of the MXU-648A/A approximately 30 cm from the stagnation point at the forward tip of the pod. The aft skin temperature sensor was mounted in a similar side mounted location approximately 30 cm from the aft end. Preliminary CFD wall temperature contour modeling appears to back up the flight data which indicates that warmer temperatures can be achieved at the aft end of the MXU-648A/A over a wide range of angles of attack as shown in figures 8.3 – 8.6.

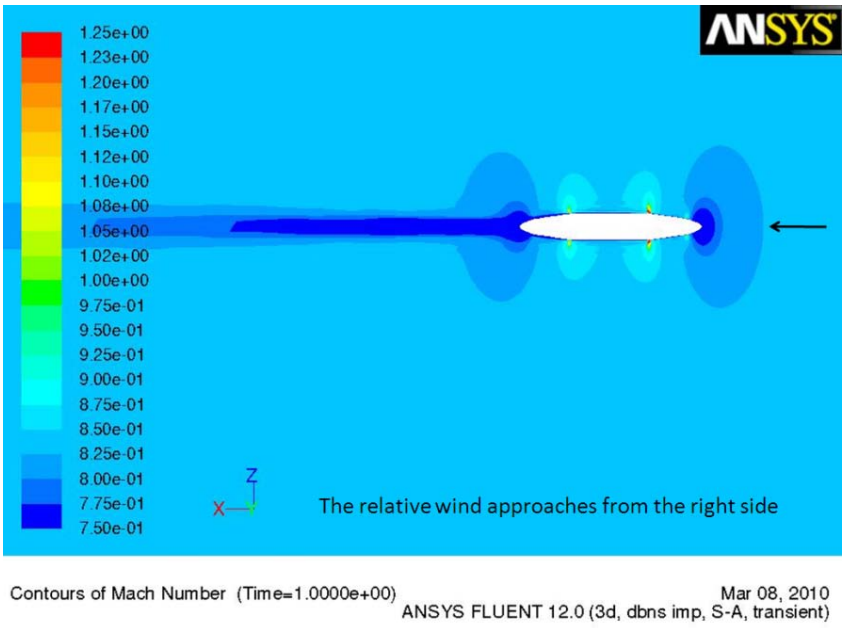

Figure 8.3 MXU-648A/A Mach Contours (0 ° Angle of Attack).

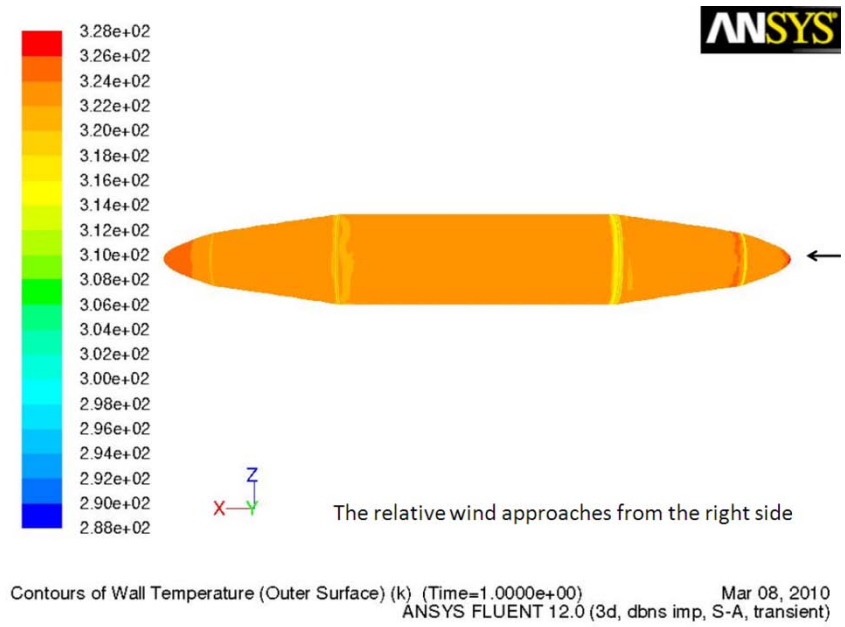

Figure 8.4 MXU-648A/A Wall Temperatures (0 ° Angle of Attack).

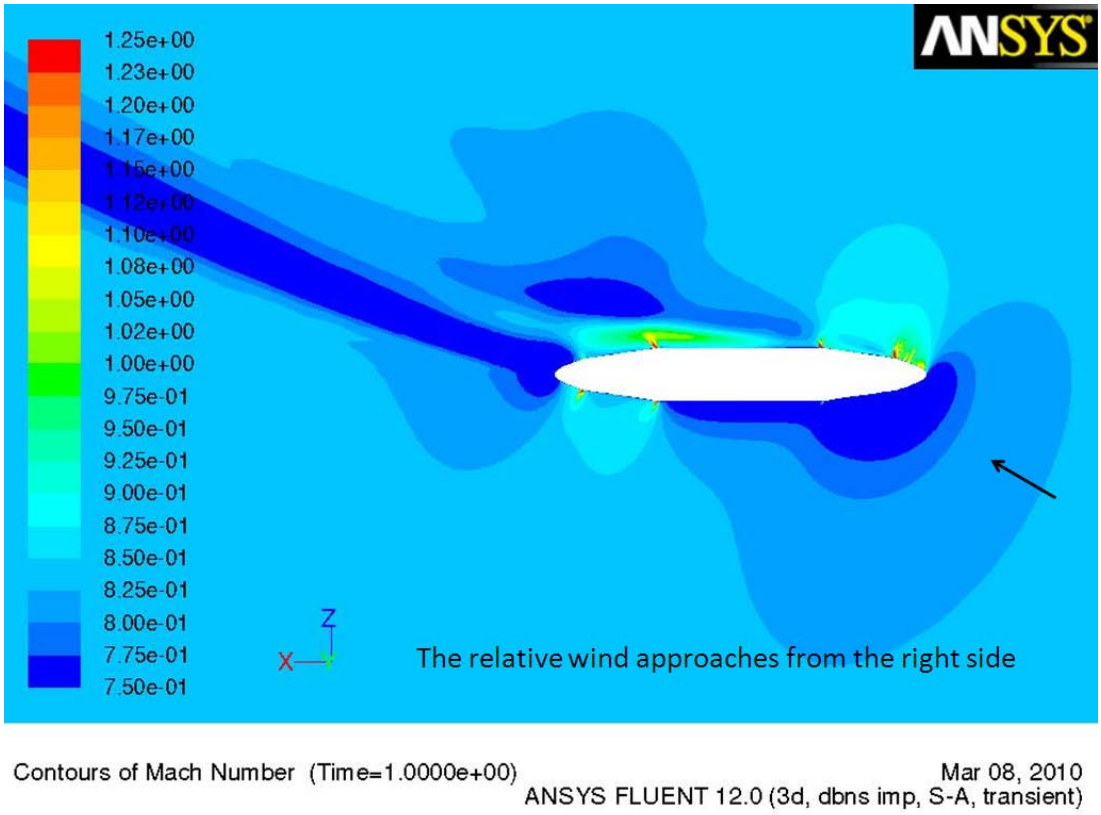

Figure 8.5 MXU-648A/A Mach Contours (30 ° Angle of Attack).

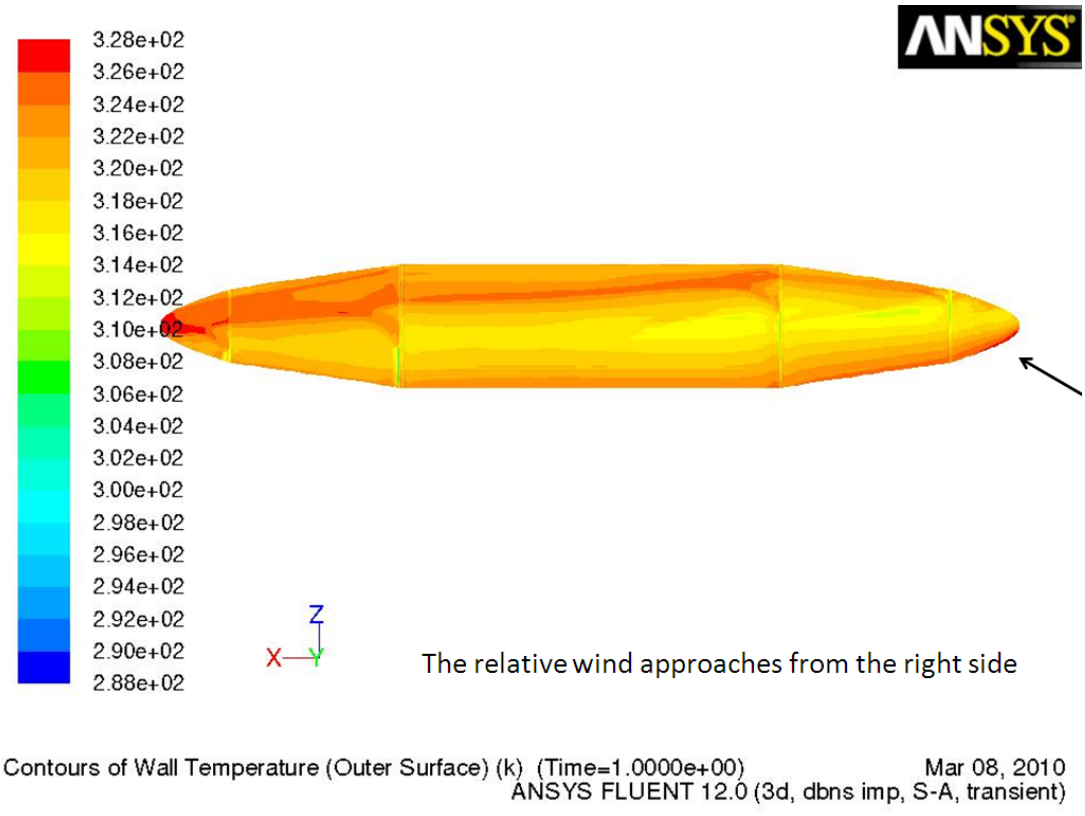

Figure 8.6 MXU-648A/A Wall Temperatures (30 ° Angle of Attack).

Data also indicates that the skin temperatures appeared to be very sensitive to small changes in speed or altitude as shown in figure 8.7. These trends were similar during each of the three flights.

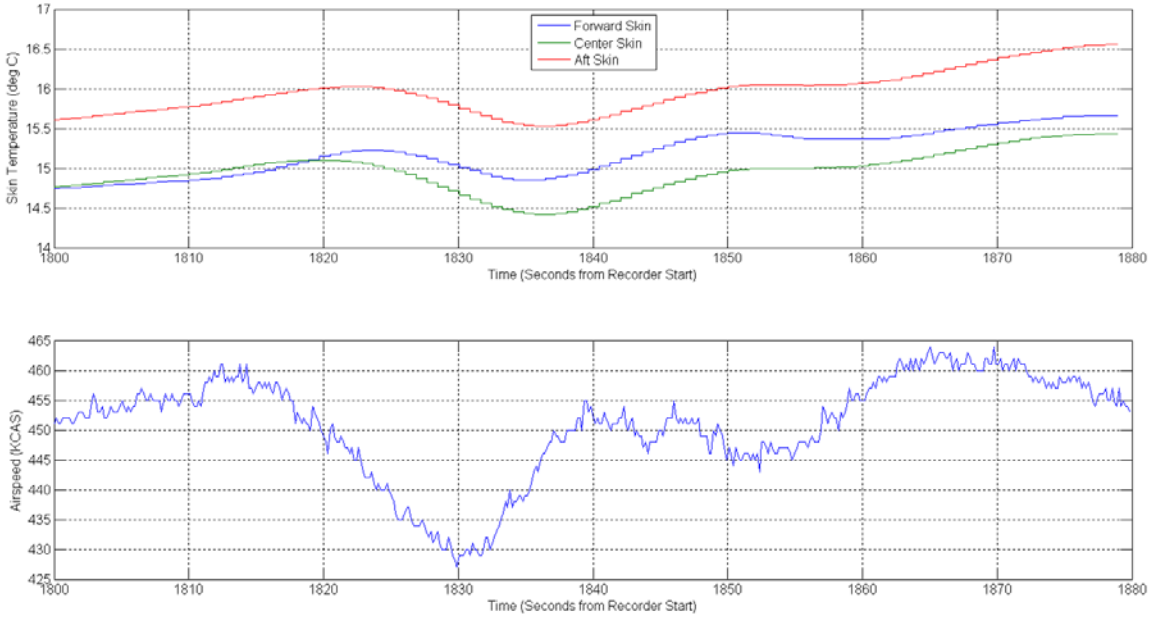

Figure 8.7 Time history plots of MXU-648A/A showing sensitivity of skin temperatures to changes in airspeed (Flight #1, 450 KCAS, 1000 ft Hp).

8.1.2 Internal Air Temperatures

Two air temperature probes were installed to document the internal static temperature of the MXU-648A/A. One probe was mounted under the data recorder support structure (figure 4.10) and the other was inserted into a pressure equalization hole in the nose cavity as shown in figure 4.7. Table 8.1 summarizes the internal temperature readings for each flight condition. It should be noted that in all cases, the internal air and nose cavity temperature probe readings had not stabilized after each two minute test point. Both of these measurements appeared to lag the skin and external temperature readings. This effect occurred during each test point but was most noticeable during the level acceleration maneuver as shown in figure 8.8. This lag may be attributed to the extra time required for the internal air mass to convectively warm (or cool) in response to a change in skin temperature. The apparent time constant for the nose cavity was much less than the internal air temperature as the volume of air in the nose cavity was significantly less than the volume of air in the main center section. These trends were observed during each of the three flights.

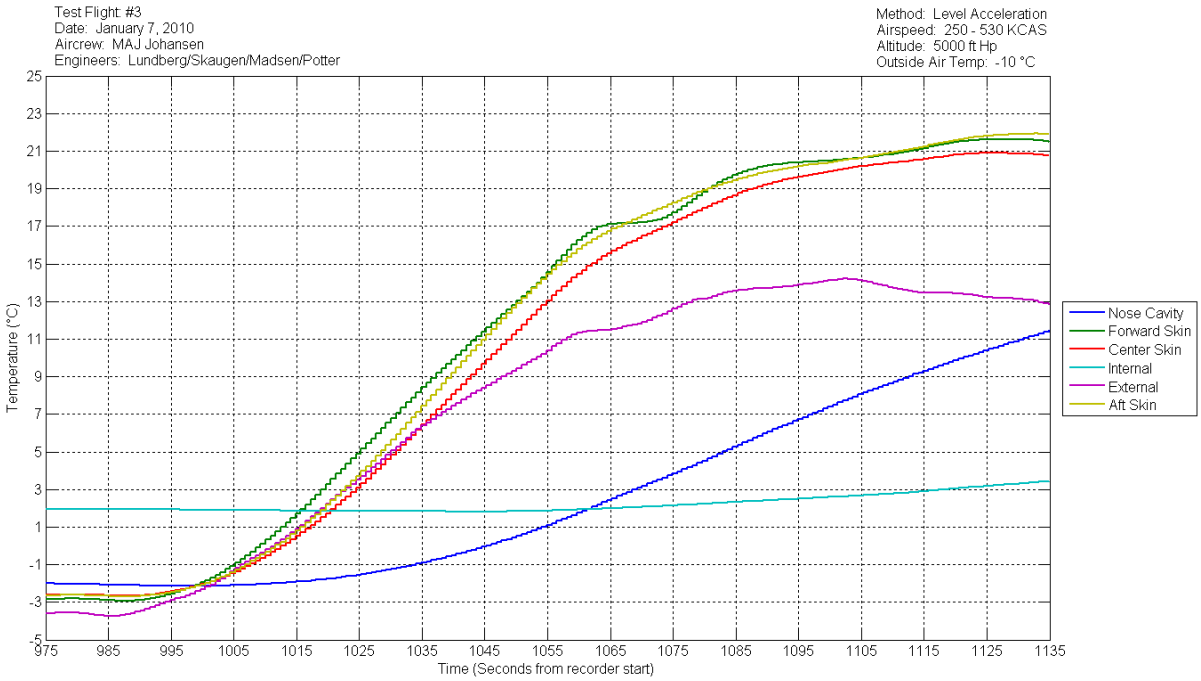

Figure 8.8 Time history plot of MXU-648A/A temperature instrumentation showing apparent lag of the Internal and Nose Cavity readings.

8.1.3 External Air Temperature Probe

One air temperature probe was mounted to protrude from a drain hole located in the aft section of the MXU-648A/A in order to measure the external air temperature. Table 8.1 summarizes the stabilized probe temperature for each flight condition. During each test event, the external probe was approx 1-3 °C colder than the lowest skin temp. The external air temperature readings were also more dynamic than the skin temperature measurements and also appeared to be sensitive to small changes in airspeed or altitude as shown in figure 8.8. It should be noted that this simple external probe was not designed to measure total air temperature. The temperature probe recovery factor was not determined for these specific flight conditions and the effects of conduction and radiation errors were not determined.

8.2 Internal Pressure Measurements

One atmospheric pressure sensor was installed on the battery support bracket to document the internal pressure of the MXU-648A/A throughout each flight. The pressure sensor required re-calibration at the time of this report; however, useful data was obtained for analysis. The pod was not designed to be pressurized and the hull structure incorporated several pressure equalization and drain holes. Time history plots of internal pressure were compared to the time history plots of aircraft altitude for the first flight as shown in figure 8.9. The maximum rate of climb was observed to be approximately 20000 ft/min during the climb to 36000 ft on the first flight. The internal pressure appeared to decrease in proportion to the increase in altitude. The maximum rate of descent occurred during the low angle dive maneuvers and was approximately 7000 ft/min. No over-pressure or under-pressure conditions were noted throughout these maneuvers.

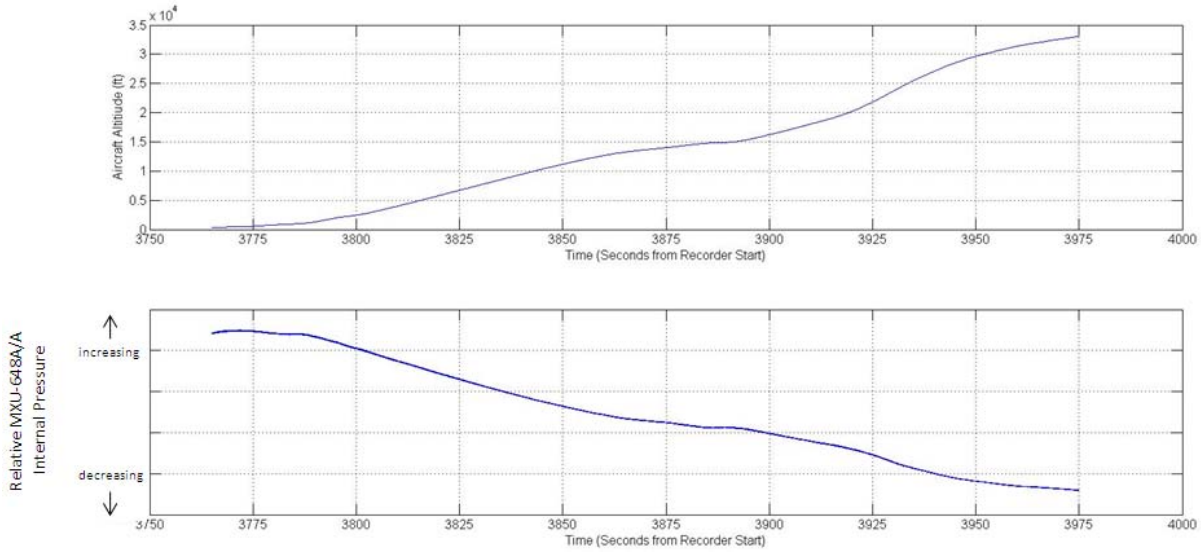

Figure 8.9 Time history plots showing variation of relative MXU-648A/A internal pressure with changes in aircraft altitude. Specific values of the internal pressure were not available due to calibration issues.

8.3 Vibration Measurements

The vibration data were gathered throughout each flight. Specific test points of interest included flight at mission representative stabilized conditions, level acceleration from 250 – 530 KCAS, turns to the normal acceleration limit, 3-axis doublets (pitch, roll, and yaw), and during observation maneuvers and low angle dive profiles. The data reduction methods are described in section 7.2.2.

8.3.1 X-Axis Accelerations

Of all nine accelerometers, the strong back x-axis vibration levels were always the lowest with values < 1.0 g_{rms}. Conversely, the g_{rms} vibration levels of the forward and aft plate x-axis accelerometers were approximately ten to twelve times greater than the associated strong back x-axis accelerometer readings during each event over all three flights as shown in figure 8.10. Detailed plots which compare individual accelerometer vibration levels between flights are presented in Appendix C, figures C-8 to C-10. Also, the ASD plots show that the dominant vibration frequencies of the forward and aft plate x-axis accelerometers were very high (typically > 400 Hz). When compared to the same events, the strong back x-axis dominant vibration frequencies differed significantly from the values measured by the forward and aft plate x-axis accelerometers as shown in figure 8.11. These unique results may have been caused by the mounting location of the accelerometers as shown in figures 4.7 and 4.9. The forward and aft accelerometers appeared to be measuring the flexible, x-axis movement of the bulkhead mounting plate rather than the vibration of the overall MXU-648A/A. The term "drum effect" has been used to describe this phenomenon. It is recommended that only the strong back x-axis measurements be used to represent the MXU-648A/A vibration environment, however, the excessive x-axis vibration levels of the forward and aft bulkhead should be noted by the NFU design teams to ensure that equipment mounting structures are sufficiently stiff and adequately supported in the x-axis.

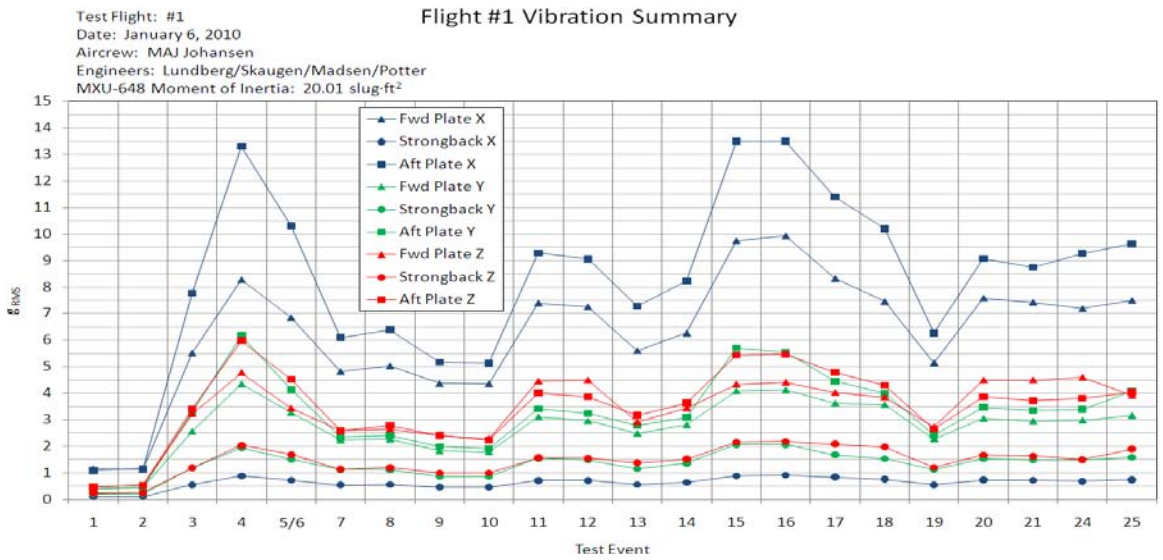

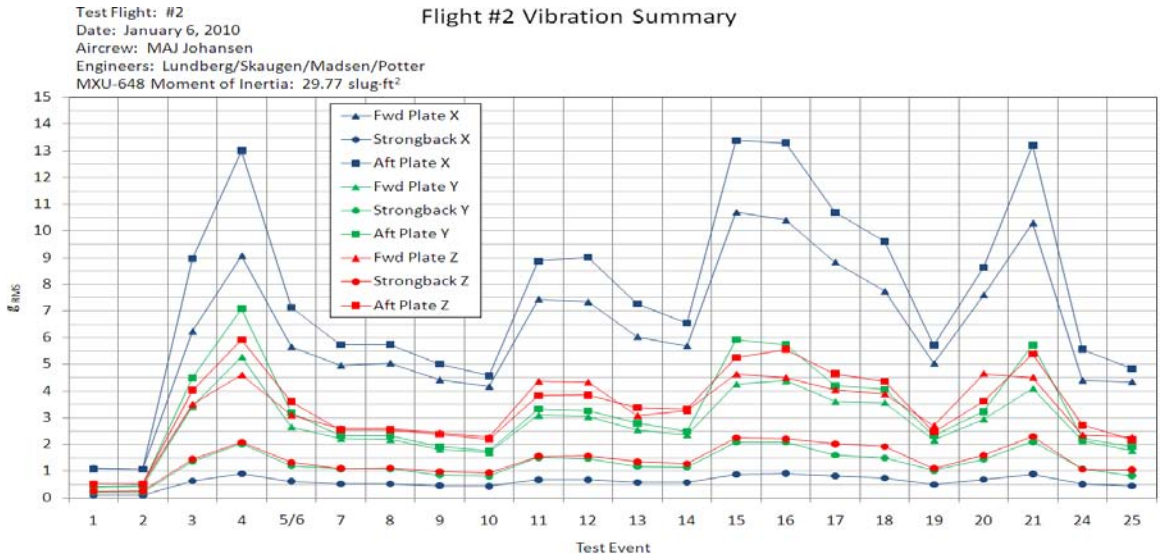

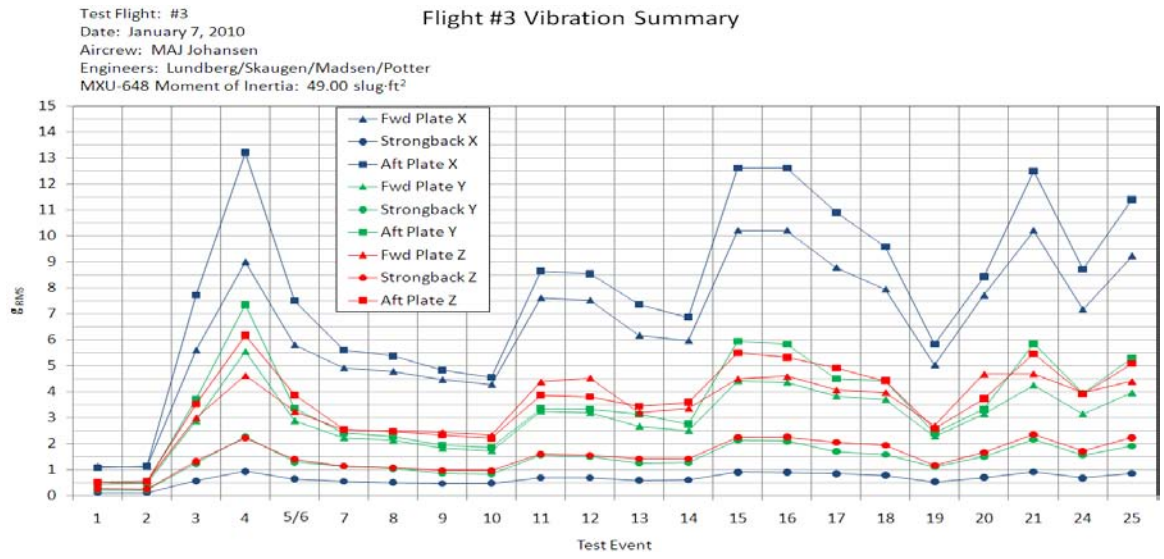

Figure 8.10 Summary of vibration magnitude for each test flight. Note the dramatic difference between the x-axis measurements. See Appendix C, figures C-5 to C-7 for more detail.

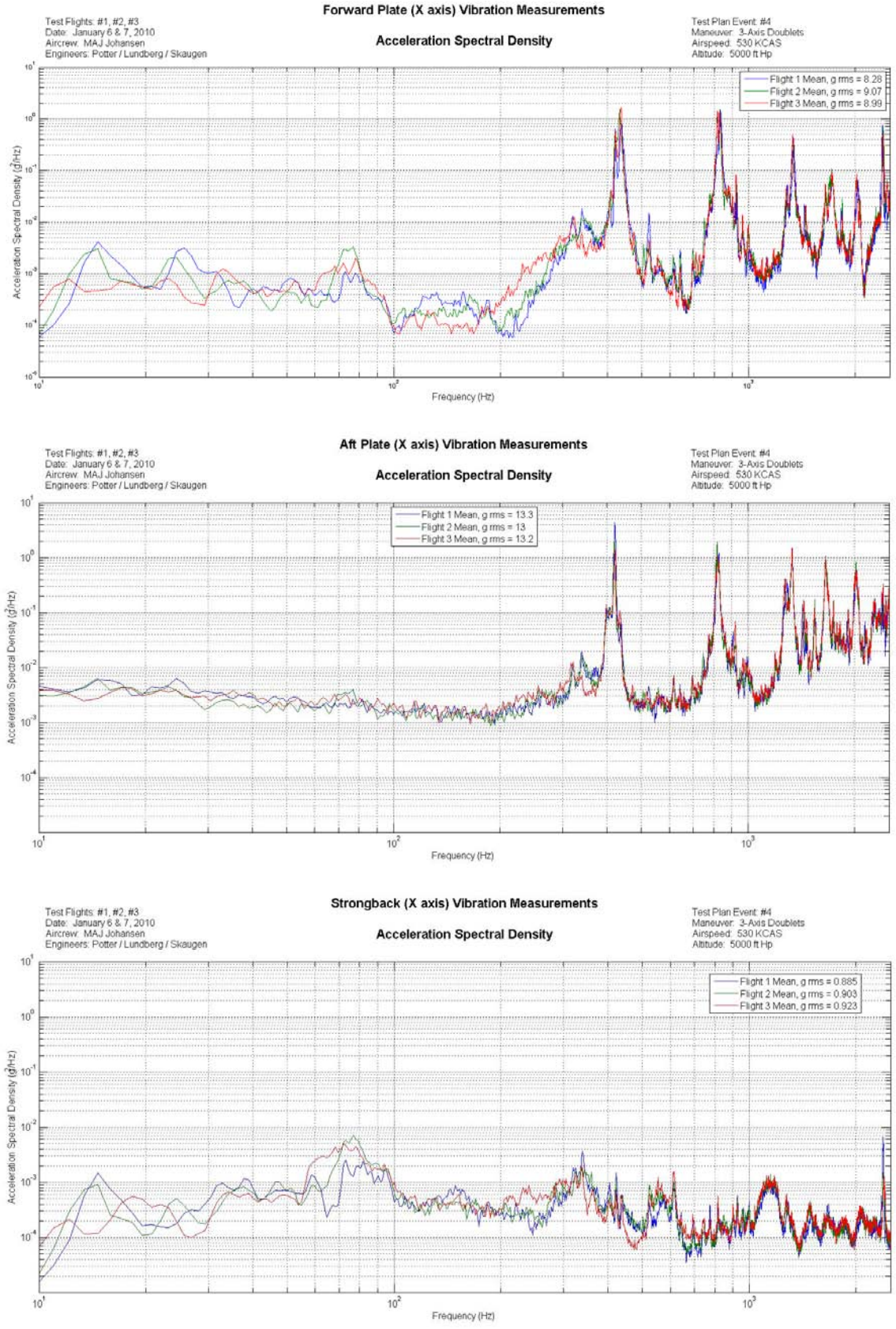

Figure 8.11 ASD plots for the 3-Axis Doublet test event at 530 KCAS and 5000 ft Hp. Note the dramatic differences in vibration frequency and magnitude between the forward and aft plates and the strong back x-axis accelerometer measurements.

8.3.2 Y-Axis Accelerations

The largest vibration magnitude in the y-axis was measured to be 7.34 g_{rms} at the aft plate (aft bulkhead) during flight #3 while executing pitch, roll, and yaw doublets at 5000 ft and 530 KCAS (Event 4). This aft plate accelerometer reading was 3.4% higher than the flight #2 vibration level for this event and 15.8% higher than the flight #1 value as shown in figure 8.10. The largest change in y-axis vibration levels over the three flights occurred during the observation maneuver at 500 ft and 500 KCAS (Event 25). The vibration level of the aft plate accelerometer (5.29 g_{rms}) was 63.5% higher than the value measured on flight #2, but only 22.9% higher than the level measured during flight #1. It should be noted that the highest y-axis vibration levels did not always occur during the third flight (with the largest moment of inertia). In fact, flight #1 (smallest moment of inertia) produced the highest vibration levels during 41% of the evaluated test points. Flight #2 recorded 4.5% of the test points with the highest vibration levels and Flight #3 had the highest readings during 54.5% of the test points. Also, the change in y-axis g_{rms} vibration levels from the first flight to third flight was less than 10% during 14 of the 22 test events (64%). In all cases, the vibration levels of the aft plate accelerometer were always larger than the values measured at the forward plate as can be seen in figure 8.10. Detailed plots which compare individual accelerometer vibration levels between flights are presented in Appendix C, figures C-11 to C-13. Table 8.2 provides a comparison of the y-axis vibration levels for each accelerometer over all three flights. The values in the table represent the percentage change in g_{rms} vibration level compared to the maximum value measured over the three flights.

Table 8.2 Comparison of Y-Axis vibration magnitudes (g_{rms}).

Event #	Maneuver	Airspeed/ Altitude (KCAS/ft)	Forward Plate Y-axis			Strong back Y-axis			Aft Plate Y-axis		
			Flight 1	Flight 2	Flight 3	Flight 1	Flight 2	Flight 3	Flight 1	Flight 2	Flight 3
1	Steady Heading Sideslip	250/5000	-7.2%	-5.4%	Max	-5.2%	-2.8%	Max	-6.2%	-0.5%	Max
2	3-Axis Doublets	250/5000	-4.5%	-9.4%	Max	-2.7%	-4.6%	Max	-4.6%	-3.7%	Max
3	Level Acceleration	250-530/5000	-25.1%	Max	-16.1%	-13.2%	Max	-9.6%	-26.7%	Max	-17.6%
4	3-Axis Doublets	530/5000	-21.5%	-4.7%	Max	-14.1%	-11.0%	Max	-15.8%	-3.4%	Max
5/6	Wind Up/Down Turn	530/5000	Max	-18.7%	-12.2%	Max	-19.9%	-15.2%	Max	-23.0%	-18.9%
7	Stabilized Point	450/1000	Max	-0.9%	-0.9%	Max	-3.6%	Max	-2.5%	-2.5%	Max
8	3-Axis Doublets	450/1000	Max	-3.5%	-6.6%	Max	-3.6%	-8.0%	Max	-2.9%	-5.4%
9	3g Steady Turn	450/1000	Max	Max	-1.1%	Max	-0.5%	-1.0%	Max	-3.5%	-3.0%
10	4g Steady Turn	450/1000	Max	-5.0%	-3.9%	Max	-5.2%	-3.5%	Max	-7.3%	-3.1%
11	Stabilized Point	500/1000	-4.3%	-4.6%	Max	Max	-2.6%	-0.6%	Max	-2.6%	-2.3%
12	3-Axis Doublets	500/1000	-6.9%	-4.1%	Max	Max	-0.7%	Max	-1.8%	-1.2%	Max
13	3g Steady Turn	500/1000	-6.4%	-4.1%	Max	-8.0%	-5.6%	Max	-11.2%	-10.5%	Max
14	4g Steady Turn	500/1000	Max	-16.0%	-11.4%	Max	-15.4%	-7.4%	Max	-19.4%	-11.0%
15	Stabilized Point	540/1000	-7.3%	-3.4%	Max	-2.4%	-1.9%	Max	-3.7%	Max	Max
16	3-Axis Doublets	540/1000	-5.9%	Max	-0.9%	-1.0%	-0.5%	Max	-4.8%	-1.2%	Max
17	3g Steady Turn	540/1000	-5.0%	-5.5%	Max	-0.6%	-5.3%	Max	-0.9%	-6.5%	Max
18	4g Steady Turn	540/1000	-3.3%	-3.3%	Max	-1.9%	-5.1%	Max	-9.3%	-7.7%	Max
19	Stabilized Point	450/200	Max	-5.3%	Max	Max	-8.8%	-2.7%	Max	-4.1%	-0.4%
20	Stabilized Point	500/200	-2.9%	-6.1%	Max	Max	-5.8%	-3.2%	Max	-6.9%	-4.6%
21	Stabilized Point	540/200	-30.4%	-3.3%	Max	-31.0%	-2.8%	Max	-42.6%	-1.9%	Max
24	Low Angle Dive	~470/ ~15000	-5.1%	-31.8%	Max	-3.2%	-29.9%	Max	-14.0%	-43.9%	Max
25	Observation Maneuver	500/500	-20.0%	-55.2%	Max	-16.3%	-56.1%	Max	-22.9%	-63.5%	Max

The MXU-648A/A Vibration Envelope plots for the forward plate y-axis accelerometer recorded during each flight are presented in figure 8.12 and the aft plate y-axis accelerometer are presented

in figure 8.13. Larger plots are provided in Appendix C, figures C-17 to C-22. Each line in the Vibration Envelope plot represents the spectral density from a separate test event during the specified flight. The data shows that the forward plate frequency peak at 32 Hz during the first flight appears to shift to 18 Hz as the moment of inertia increases from the first flight to the third flight (figure 8.12). The other forward plate dominant frequency peaks remain relatively constant over the course of each flight. A similar frequency shift trend occurs at the aft plate, however, an additional peak appears at 35 Hz by the third flight (figure 8.13). This peak can be identified in flight 2 at same frequency and amplitude, and it can possibly be hidden in the data of flight 1.

The Vibration Envelope plots also include the recommended limits for jet aircraft store buffet response and jet aircraft store equipment vibration exposure from guidance provided in MIL-STD-810F [8]. The analysis has shown that the measured vibration levels at the forward and aft plates in the y-axis (lateral) exceed the guidance specified in MIL-STD-810F during the second and third flights. While several events exceeded the recommended limit, this was not regarded as a requirement or specification failure. The points where the spectral density lines exceed the limits are being treated as “frequencies of interest” since the final NG-NFU and NSM-NFU designs (mass properties and external mold line) will be different than the baseline MXU-648A/A used during this test. Table 8.3 summarizes the frequencies of interest and the triggering events.

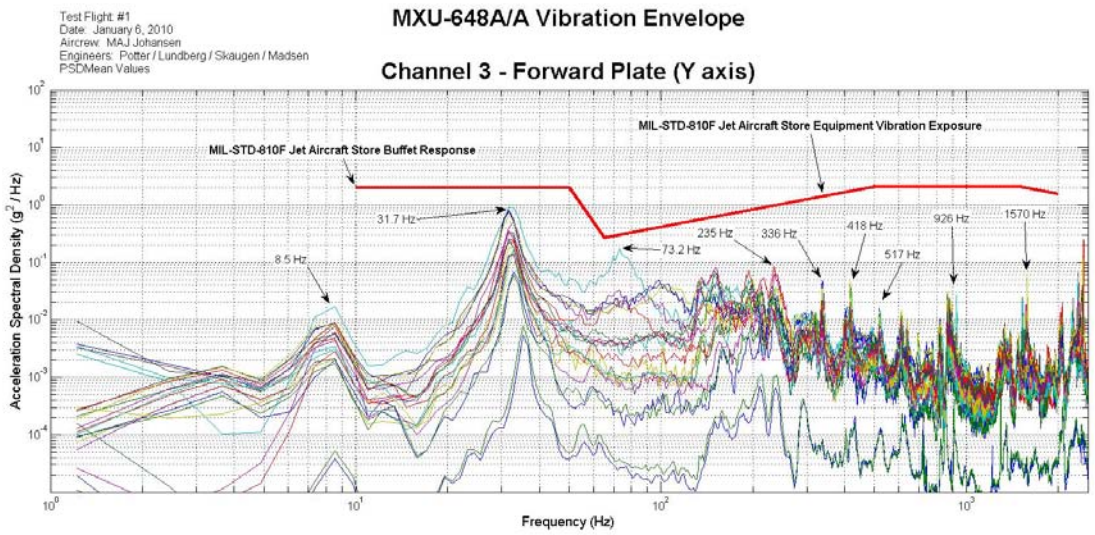

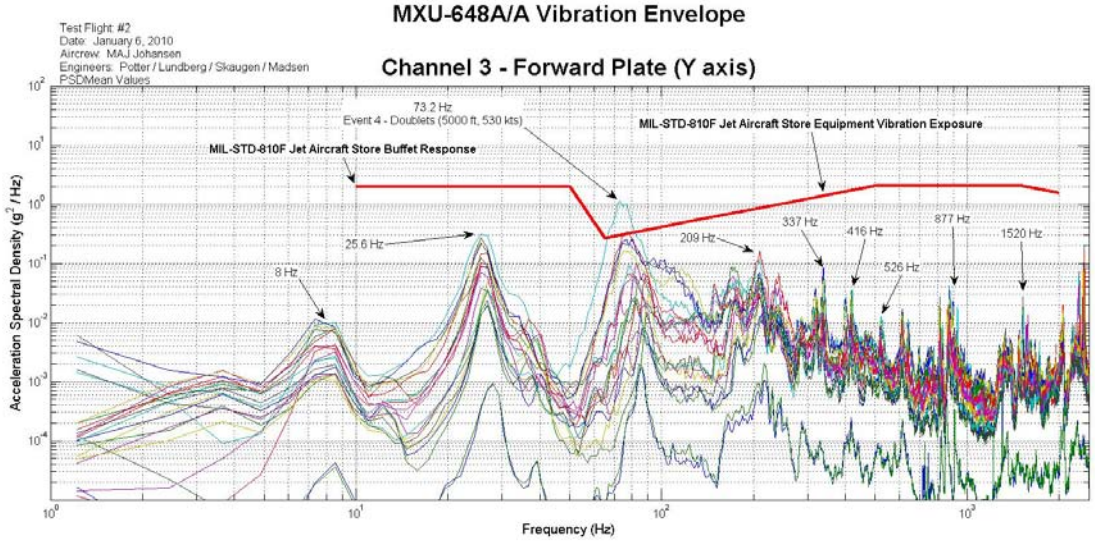

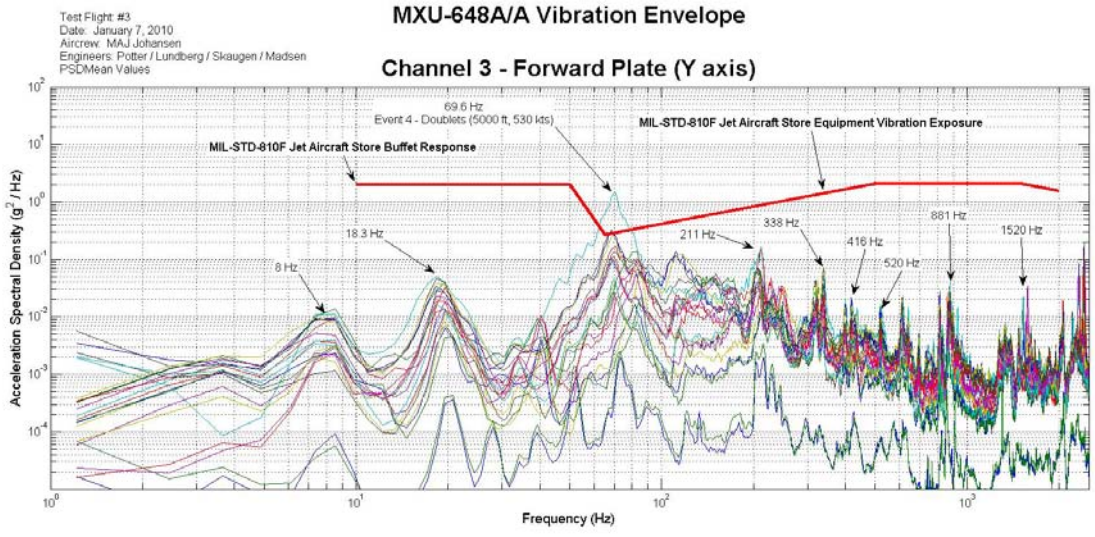

Figure 8.12 Forward Plate Vibration Envelope Plots.

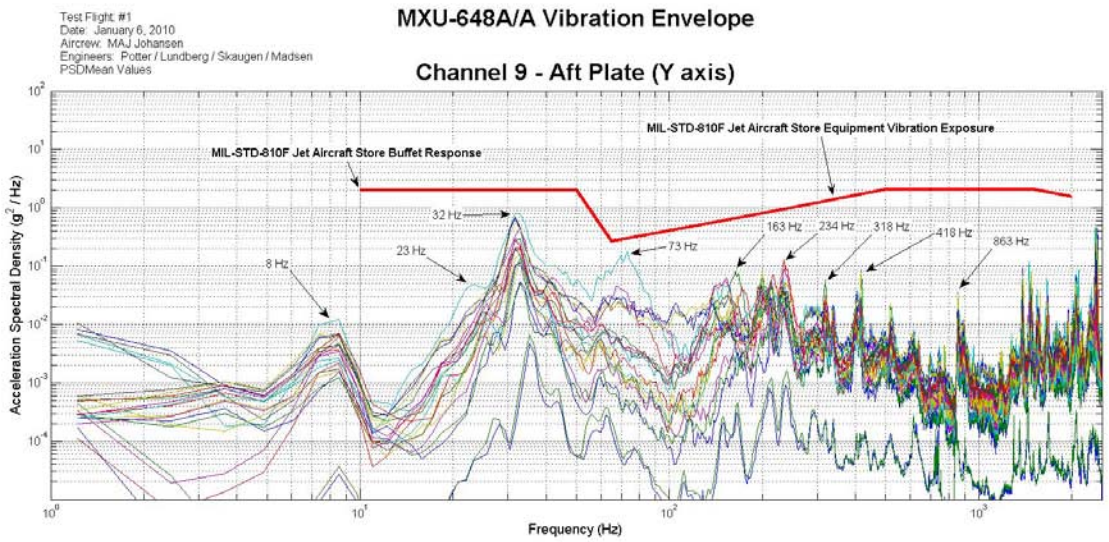

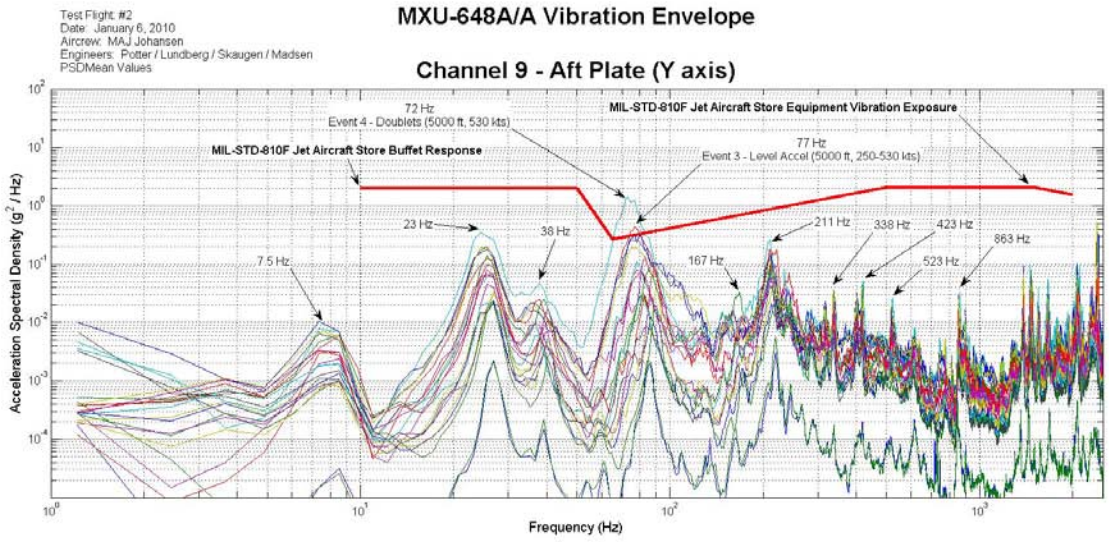

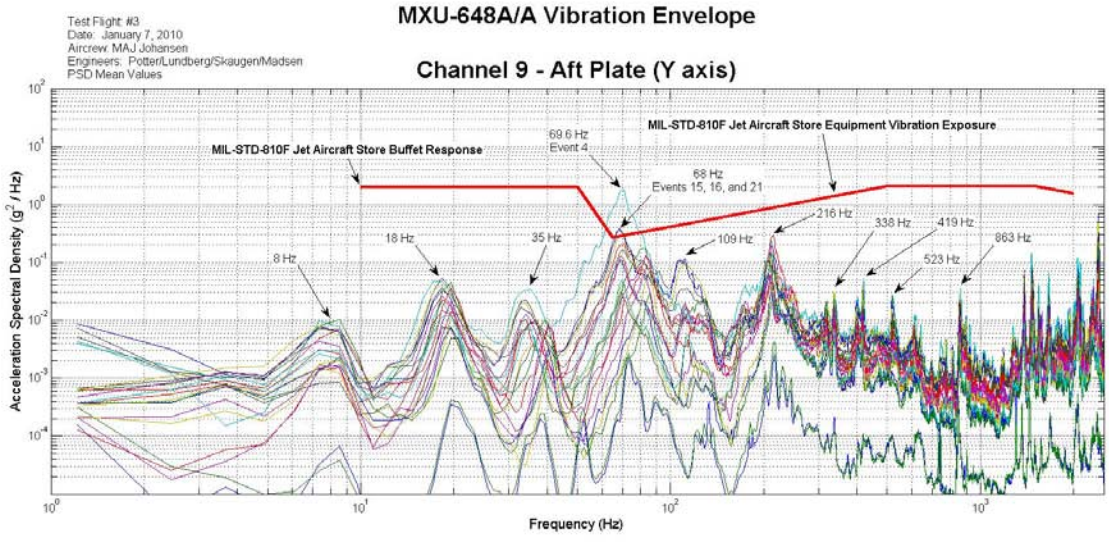

Figure 8.13 Aft Plate Vibration Envelope Plots.

Table 8.3 Vibration Frequencies of Interest.

Flight #	Location	Axis	Frequency (Hz)	Triggering Event
2	Forward	Y (Lateral)	65-80	3 Axis Doublets (5000 ft, 530 KCAS)
2	Aft	Y (Lateral)	75-80	Level Accel (5000 ft, 250-530 KCAS)
2	Aft	Y (Lateral)	65-85	3 Axis Doublets (5000 ft, 530 KCAS)
3	Forward	Y (Lateral)	60-80	3 Axis Doublets (5000 ft, 530 KCAS)
3	Aft	Y (Lateral)	60-80	3 Axis Doublets (5000 ft, 530 KCAS)
3	Aft	Y (Lateral)	65-70	Stabilized Point (1000 ft, 540 KCAS)
3	Aft	Y (Lateral)	65-70	3 Axis Doublets (5000 ft, 530 KCAS)
3	Aft	Y (Lateral)	65-70	Stabilized Point (200 ft, 540 KCAS)

8.3.3 Z-Axis Accelerations

The largest vibration magnitude in the z-axis was measured to be 6.17 g_{rms} during flight #3 while executing pitch, roll, and yaw doublets at 5000 ft and 530 KCAS (Event 4). The aft plate accelerometer reading was 4.1% higher than the flight #2 vibration level for this event and only 2.9% higher than the flight #1 value as shown in figure 8.10. The largest change in z-axis vibration levels over the three flights occurred during the stabilized point at 200 ft and 540 KCAS (Event 21). The vibration levels of the aft plate accelerometer (5.46 g_{rms}) were 31.9% higher than the values measured on flight #1, but only 1.3% higher than the levels measured during flight #2. It should be noted that the highest z-axis vibration levels did not always occur during the third flight (with the largest moment of inertia). In fact, flight #1 (smallest moment of inertia) produced the highest vibration levels during 43% of the evaluated test points. Flight #2 recorded 14% of the test points with the highest vibration levels and Flight #3 accounted for the remaining 43%. Also, the change in z-axis g_{rms} vibration levels from the first flight to third flight was less than 10% during 15 of the 22 test events (68%). Detailed plots which compare individual accelerometer vibration levels between flights are presented in Appendix C, figures C-14 to C-16. Table 8.4 provides a comparison of the z-axis vibration levels for each accelerometer over all three flights. The values in the table represent the percentage change in vibration level compared to the maximum value measured over the three flights.

Table 8.4 Comparison of Z-Axis vibration magnitudes (g_{rms})

Event #	Maneuver	Airspeed/ Altitude (KCAS/ft)	Forward Plate Z-axis			Strong back Z-axis			Aft Plate Z-axis		
			Flight 1	Flight 2	Flight 3	Flight 1	Flight 2	Flight 3	Flight 1	Flight 2	Flight 3
1	Steady Heading Sideslip	250/5000	-7.6%	Max	-1.0%	-6.3%	-3.5%	Max	-10.0%	Max	-3.5%
2	3-Axis Doublets	250/5000	-3.5%	-3.8%	Max	-1.2%	-1.2%	Max	-3.8%	-3.1%	Max
3	Level Acceleration	250-530/5000	-8.3%	Max	-14.8%	-17.9%	Max	-9.7%	-15.4%	Max	-12.7%
4	3-Axis Doublets	530/5000	Max	-3.6%	-3.1%	-7.7%	-5.4%	Max	-2.9%	-4.1%	Max
5/6	Wind Up/Down Turn	530/5000	Max	-9.6%	-5.8%	Max	-21.9%	-17.8%	Max	-20.2%	-14.2%
7	Stabilized Point	450/1000	-0.8%	Max	-2.7%	Max	-3.5%	-1.8%	Max	-1.2%	-1.2%
8	3-Axis Doublets	450/1000	Max	-2.3%	-6.0%	Max	-6.7%	-10.8%	Max	-8.3%	-11.5%
9	3g Steady Turn	450/1000	-1.6%	Max	Max	Max	-1.2%	-2.7%	Max	-1.2%	-3.3%
10	4g Steady Turn	450/1000	-1.3%	-1.7%	Max	Max	-5.5%	-4.2%	Max	-1.8%	-1.8%
11	Stabilized Point	500/1000	Max	-2.0%	-1.6%	-1.3%	-1.9%	Max	Max	-4.5%	-3.7%
12	3-Axis Doublets	500/1000	-0.9%	-4.4%	Max	-1.3%	Max	-1.9%	Max	-0.3%	-1.8%
13	3g Steady Turn	500/1000	-8.8%	-3.4%	Max	-2.1%	-4.3%	Max	-7.6%	-1.5%	Max
14	4g Steady Turn	500/1000	Max	-5.2%	-2.6%	Max	-15.8%	-7.9%	Max	-8.5%	-1.4%
15	Stabilized Point	540/1000	-6.5%	Max	-2.8%	-4.0%	Max	-0.4%	-0.9%	-4.2%	Max
16	3-Axis Doublets	540/1000	-4.1%	-2.0%	Max	-3.1%	-1.8%	Max	-1.6%	Max	-4.5%
17	3g Steady Turn	540/1000	-1.0%	-0.5%	Max	Max	-3.3%	-2.4%	-2.4%	-5.3%	Max
18	4g Steady Turn	540/1000	-3.0%	-2.0%	Max	Max	-2.5%	-2.5%	-2.7%	-1.1%	Max
19	Stabilized Point	450/200	Max	-0.4%	-1.5%	Max	-9.1%	-4.1%	Max	-6.8%	-3.0%
20	Stabilized Point	500/200	-4.1%	-0.6%	Max	Max	-4.8%	-1.2%	Max	-6.5%	-3.6%
21	Stabilized Point	540/200	-4.3%	-3.8%	Max	-30.6%	-2.1%	Max	-31.9%	-1.3%	Max
24	Low Angle Dive	~470/ ~15000	Max	-48.6%	-13.7%	-11.8%	-37.1%	Max	-2.3%	-30.3%	Max
25	Observation Maneuver	500/500	-11.1%	-48.4%	Max	-14.8%	-52.9%	Max	-20.3%	-57.0%	Max

The MXU-648A/A Vibration Envelope plots for the forward plate z-axis accelerometer recorded during each flight are presented in figure 8.14 and the aft plate z-axis accelerometer are presented in figure 8.15. Larger plots are provided in Appendix C, figures C-23 to C-28. The analysis has shown that while the measured vibration levels of both the forward and aft plates in the z-axis (vertical) appear to increase as the moment of inertia was increased, the vibration levels over the measured frequency range are within the guidance specified in MIL-STD-810F during all three flights. The dominant vibration frequency peaks are highlighted on each plot and appear to remain relatively constant over all three flights.

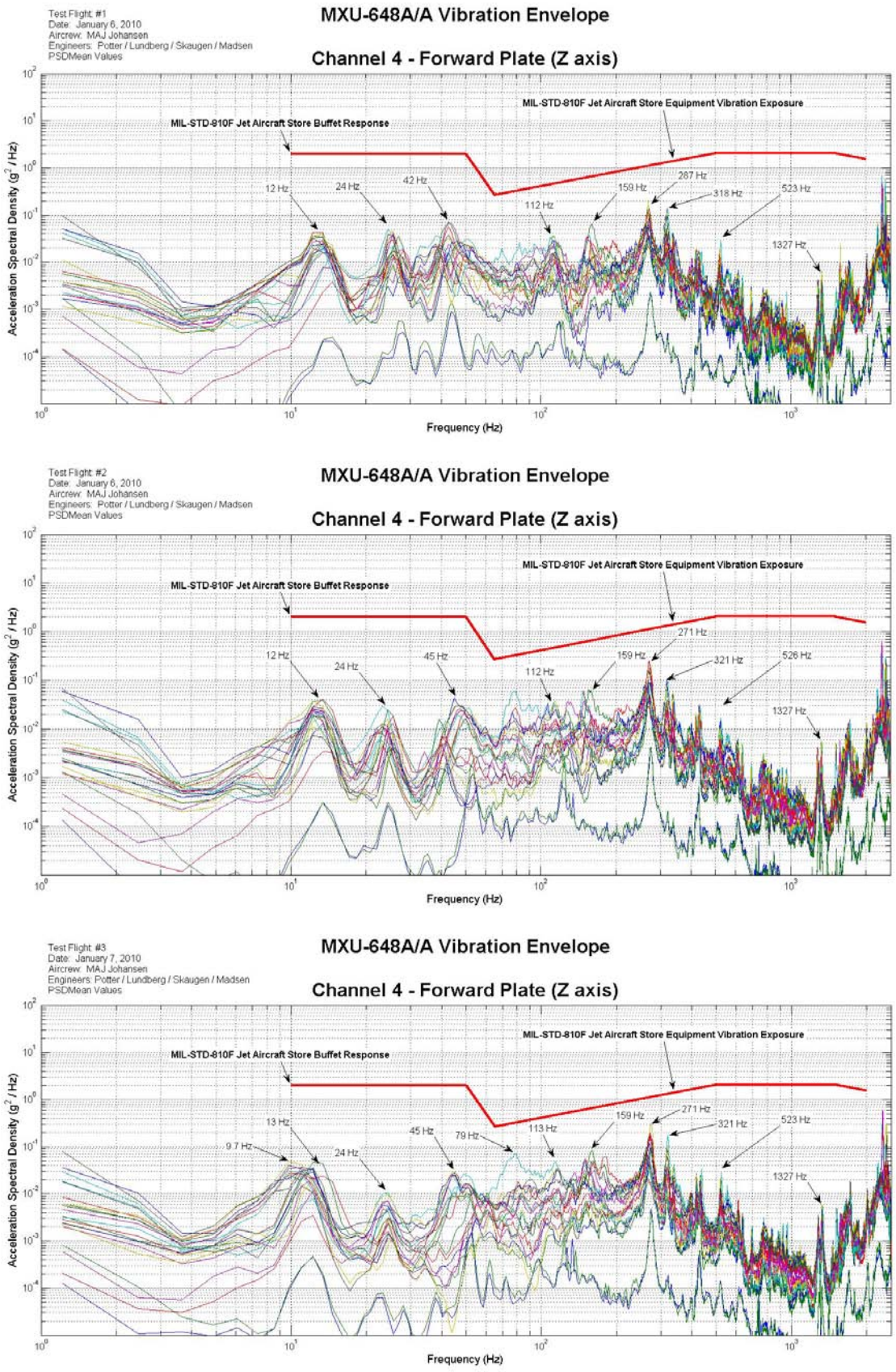

Figure 8.14 Forward Plate Vibration Envelope Plots

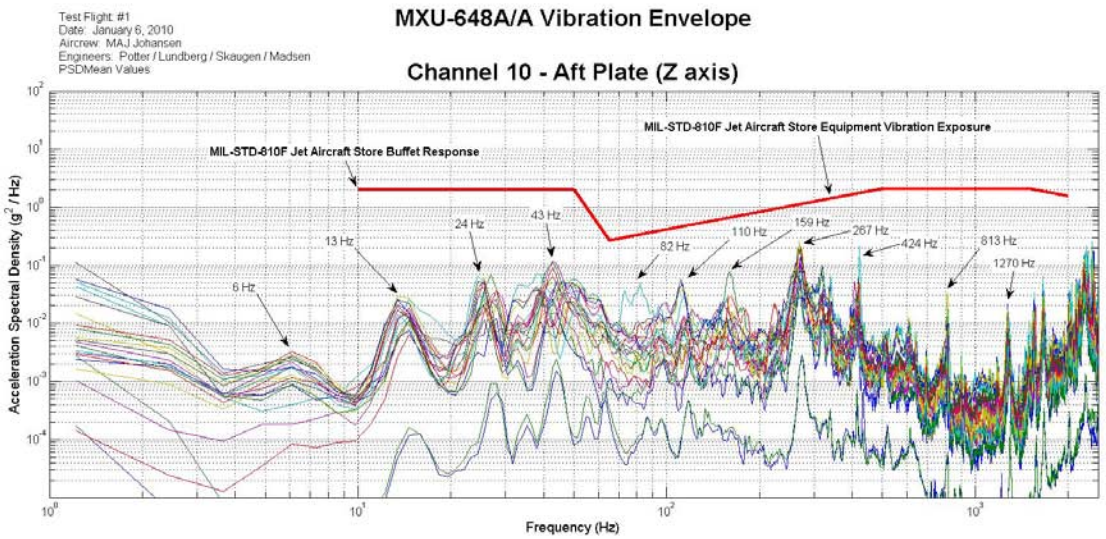

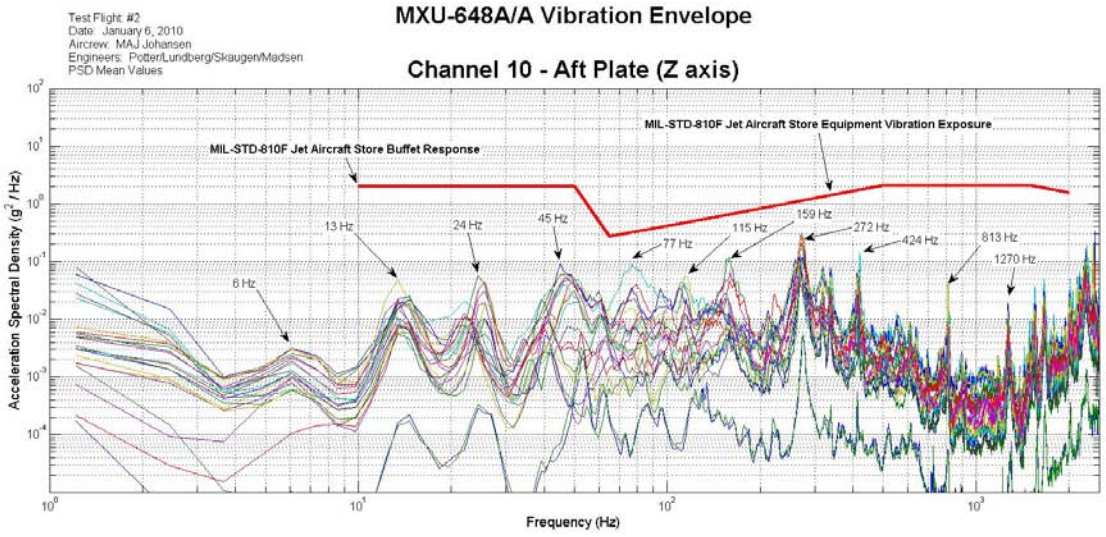

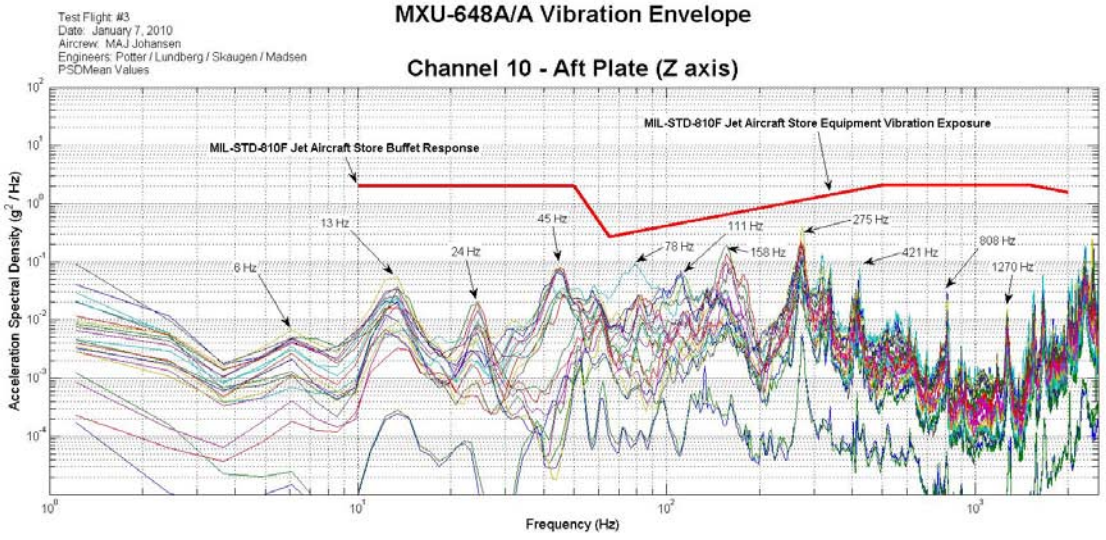

Figure 8.15 Aft Plate Vibration Envelope Plots

8.4 Low Frequency Pod Dynamics

The response of the MXU-648A/A to low frequency excitation (~1 Hz) was evaluated during each flight using the control stick or rudder pedal doublet technique. Individual pitch, roll, and yaw doublet maneuvers were executed at two different altitudes (1000 ft pressure altitude and 200 ft above ground level) and three separate airspeeds (450, 500, and 540 KCAS). Additional 3-axis doublets were executed before and after the level acceleration test event at 5000 ft pressure altitude (250 and 530 KCAS). The high frequency content (> 10Hz) was filtered from the raw accelerometer data and time history plots of acceleration were produced to evaluate the damping characteristics.

The damping ratio, ζ, is a dimensionless measure commonly used to describe how oscillations decay after a disturbance. A critically damped system ($\zeta = 1.0$) exhibits no oscillations and will return to the equilibrium conditions in the quickest time following a disturbance. A system with no damping ($\zeta = 0.0$) will continue to oscillate and will never return to the equilibrium conditions. A more detailed description of damping ratio is provided in the United States Naval Test Pilot School Flight Test Manual 103 [3]. For the purposes of this test, a critically damped system is desired, however, minor pod oscillations ($\zeta > 0.5$) may be permissible and would not impact future NFU research missions.

The MXU-648A/A exhibited a well damped response (damping ratio, $\zeta > 0.7$) in both the vertical (z) and lateral (y) axes when subjected to pitch and roll doublet excitation at all tested airspeeds and altitudes over all three flights. Typical pitch and roll doublet responses are presented in figure 8.16. The yaw doublets produced one overshoot (damping ratio, $\zeta \approx 0.6$) in the lateral axis at 5000 ft Hp and 530 KCAS during the first flight. As the pod moment of inertia was increased on the second and third flights, the damping ratio was reduced to approximately 0.5 (2 overshoots) in response to yaw doublets at the same flight conditions. The lateral response was well damped at all other flight conditions during all three flights.

Flight #1
5,000 ft
530 KIAS
MOI: 20 slug·ft²

Pilot comments:
"Didn't see any oscillations"

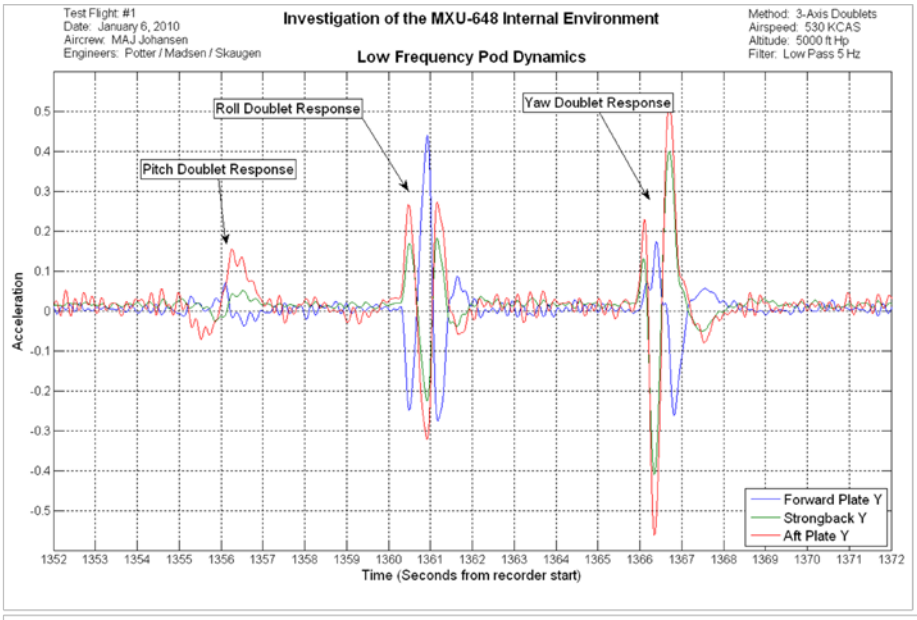

Flight #3
5,000 ft
530 KIAS
MOI: 49 slug·ft²

Pilot comments:
"Deadbeat"

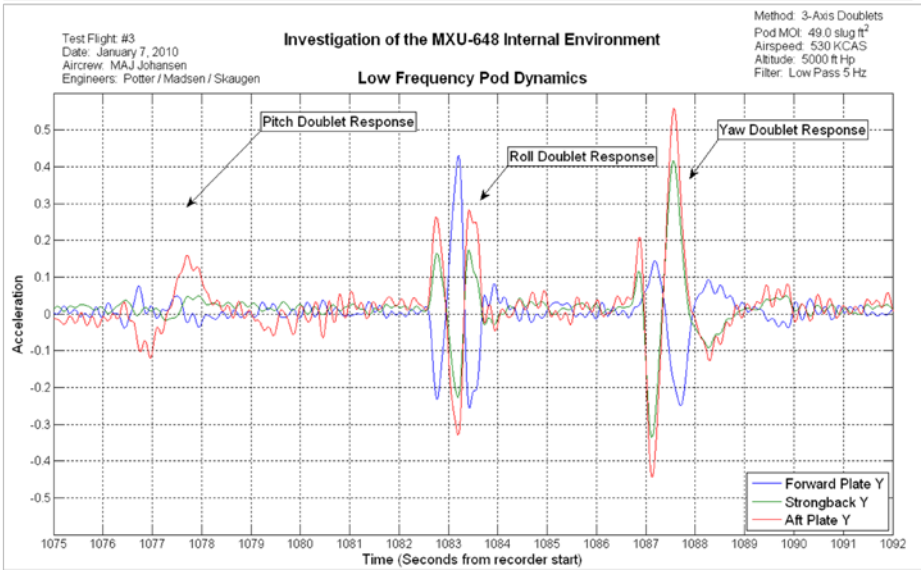

Figure 8.16 MXU-648A/A lateral axis (y) response to 3-Axis Doublets.

8.5 Pilot Comments

Throughout each flight, the test pilot provided qualitative comments on aircraft motion and the perceived vibration levels from the cockpit reference point. The pilot also noted apparent wing oscillations during several test points by direct observation of the wings, the forward end of the MXU-648A/A, and CATM-120 wing tip missiles. Tables B-1 to B-3 summarize the relevant comments that were noted on the HUD tapes. Throughout all three flights, the pilot did not notice any objectionable oscillations or cockpit vibration levels.

9 Conclusions

Within the scope of this test, sufficient data was gathered to document the internal environment of the baseline MXU-648A/A over three consecutive flights, including temperature, pressure, and vibration. Extensive data on three local skin temperatures and inside air temperature and pressure were recorded and was provided to the design teams for review and incorporation into the NFU design process. In terms of vibration and pod dynamic motion, the moment of inertia about the yaw axis was successively increased from 27.1 $kg \cdot m^2$ (20.0 $slug \cdot ft^2$) on the first flight to 40.4 $kg \cdot m^2$ (29.0 $slug \cdot ft^2$) on the second flight and finally to 66.4 $kg \cdot m^2$ (49.0 $slug \cdot ft^2$) on the third flight. The maximum moment of inertia tested on the third flight represented a 398% increase over the empty MXU-648A/A yawing moment of inertia of 16.7 $kg \cdot m^2$ (12.3 $slug \cdot ft^2$). While subtle changes were observed in vibration levels and frequency ranges during each successive flight, no significant concerns or trends were identified. Pilot observations confirm these conclusions.

10 Recommendations

It is recommended that the NFU design teams review the data, observations, and results contained in this report for incorporation into the development and design process.

The forward and aft plate x-axis accelerometers should be relocated during subsequent test flights to avoid the “drum effect”.

The NFU design teams should consider planning additional flight tests to repeat these test points with the structurally modified MXU-648A/A with representative mass distribution and again with the final aerodynamic shape for each NFU pod.

References

1. TO 1F-16AM-1, Flight Manual, USAF/EPAF Series F-16A/B Mid-Life Update, Block 10 and 15 Aircraft, 15 July 2007.
2. National Instruments CompactRIO 9012/9014 Operating Instructions and Specifications, May 2008. http://www.ni.com/pdf/manuals/374126d.pdf
3. United States Naval Test Pilot School Flight Test Manual No. 103 – Fixed Wing Stability and Control, Theory and Flight Test Techniques, January 1997.
4. FLO/S/LU/PF 06-2009 Test Plan, Investigation of the MXU-648 Travel Pod Environment, Norwegian Defense Systems Management Division, Aeronautical Systems Section, 14 May 2009.
5. Weight, Center of Gravity, and Moment of Inertia Test Report for the Cargo/Travel (MXU) Pod, Assembly P/N 402136, 04-0038, Revision NC, 20 May 2004.
6. Stoica, P., and R.L. Moses, *Introduction to Spectral Analysis*, Prentice-Hall, 1997, pp. 24-26.
7. Welch, P.D, "The Use of Fast Fourier Transform for the Estimation of Power Spectra: A Method Based on Time Averaging Over Short, Modified Periodograms," *IEEE Trans. Audio Electroacoustics, Vol. AU-15 (June 1967)*, pp.70-73.
8. MIL-STD-810F, Department of Defense Test Method Standards for Environmental Engineering Considerations and Laboratory Tests, January 1, 2000.

Appendix A Test and Test Conditions Matrix

Test Point	Test Maneuver	Altitude	Airspeed/ AOA/Mach	n_z (g)	Comments	Purpose
1	Steady Heading Sideslip (SHSS)	5,000 ft HP	250 KCAS	1	¼ & ½ pedal **Airspeed Limit: 200 KCAS** Tolerances Airspeed: +/- 5 KCAS Altitude: +/- 100 ft Hp	Collect vibration data.
2	3- Axis Doublets	5,000 ft Hp	250 KCAS	1	**Airspeed Limit: 200 KCAS** Tolerances Airspeed: +/- 5 KCAS Altitude: +/- 100 ft Hp	Excite pod dynamics. Collect vibration data.
3	Level Accel	5,000 ft Hp	250 – 530 KCAS	1	Set 1013 (Use RAD ALT in HUD) **Airspeed Limit: 550 KCAS** Tolerances Altitude: +/- 100 ft Hp	Collect vibration/pressure data over wide range of speed
4	3- Axis Doublets	5,000 ft Hp	530 KCAS	1	**Airspeed Limit: 550 KCAS** Tolerances Airspeed: +/- 5 KCAS Altitude: +/- 100 ft Hp	Excite pod dynamics. Collect vibration data.
5	Wind-Up Turn	5,000 ft Hp	530 KCAS	4.8	**Airspeed Limit: 550 KCAS** **n_z Limit: 5 g (symmetric)** Tolerances Airspeed: +/- 5 KCAS n_z: +/- 0.1g Altitude: +/- 1000 ft Hp	Determine n_z effects and buffet levels.
6	Wind-Down Turn	5,000 ft Hp	530 - 250 KCAS	3	**n_z Limit: 5 g (symmetric)** **AOA Limit: 16°** Tolerances Airspeed: +/- 5 KCAS n_z: +/- 0.1g Altitude: +/- 1000 ft Hp	Collect vibration data over wide range of AoA.
7	Stabilized Point	1,000 ft AGL	450 KCAS	1	Stabilize for ~2 minutes Tolerances Airspeed: +/- 5 KCAS Altitude: +/- 100 ft Hp	NFU Mission Profile
8	3- Axis Doublets	1,000 ft AGL	450 KCAS	1	Tolerances Airspeed: +/- 5 KCAS Altitude: +/- 100 ft Hp	Excite pod dynamics
9	Steady Turn	1,000 ft AGL	450 KCAS	3	**n_z Limit: 5 g(symmetric)** Tolerances n_z: +/- 0.1g Airspeed: +/- 5 KCAS Altitude: +/- 100 ft Hp	Determine n_z effects and buffet levels.
10	Steady Turn	1,000 ft AGL	450 KCAS	4	**n_z Limit: 5 g(symmetric)** Tolerances n_z: +/- 0.1g Airspeed: +/- 5 KCAS Altitude: +/- 100 ft Hp	Determine n_z effects and buffet levels.
11	Stabilized Point	1,000 ft AGL	500 KCAS	1	Stabilize for ~2 minutes Tolerances Airspeed: +/- 5 KCAS Altitude: +/- 100 ft Hp	NFU Mission Profile
12	3- Axis Doublets	1,000 ft AGL	500 KCAS	1	Tolerances Airspeed: +/- 5 KCAS Altitude: +/- 100 ft Hp	Excite pod dynamics
13	Steady Turn	1,000 ft AGL	500 KCAS	3	**n_z Limit: 5 g(symmetric)** Tolerances n_z: +/- 0.1g Airspeed: +/- 5 KCAS Altitude: +/- 100 ft Hp	Determine n_z effects and buffet levels.

Test Point	Test Maneuver	Altitude	Airspeed/ AOA/Mach	n_z (g)	Comments	Purpose
14	Steady Turn	1,000 ft AGL	500 KCAS	4	**n_z Limit: 5 g(symmetric)** Tolerances n_z: +/- 0.1g Airspeed: +/- 5 KCAS Altitude: +/- 100 ft Hp	Determine n_z effects and buffet levels.
15	Stabilized Point	1,000 ft AGL	540 KCAS	1	**Airspeed Limit: 550 KCAS** Stabilize for ~2 minutes Tolerances Airspeed: +/- 5 KCAS Altitude: +/- 100 ft Hp	NFU Mission Profile
16	3- Axis Doublets	1,000 ft AGL	540 KCAS	1	**Airspeed Limit: 550 KCAS** Tolerances Airspeed: +/- 5 KCAS Altitude: +/- 100 ft Hp	Excite pod dynamics
17	Steady Turn	1,000 ft AGL	540 KCAS	3	**Airspeed Limit: 550 KCAS** **n_z Limit: 5 g(symmetric)** Tolerances n_z: +/- 0.1g Airspeed: +/- 5 KCAS Altitude: +/- 100 ft Hp	Determine n_z effects and buffet levels.
18	Steady Turn	1,000 ft AGL	540 KCAS	4	**Airspeed Limit: 550 KCAS** **n_z Limit: 5 g(symmetric)** Tolerances n_z: +/- 0.1g Airspeed: +/- 5 KCAS Altitude: +/- 100 ft Hp	Determine n_z effects and buffet levels.
19	Stabilized Point	200 ft AGL	450 KCAS	1	Stabilize for ~2 minutes Tolerances Airspeed: +/- 5 KCAS Altitude: +/- 50 ft Hp	NFU Mission Profile
20	Stabilized Point	200 ft AGL	500 KCAS	1	Stabilize for ~2 minutes Tolerances Airspeed: +/- 5 KCAS Altitude: +/- 50 ft Hp	NFU Mission Profile
21	Stabilized Point	200 ft AGL	540 KCAS	1	**Airspeed Limit: 550 KCAS** Stabilize for ~2 minutes Tolerances Airspeed: +/- 5 KCAS Altitude: +/- 100 ft Hp	NFU Mission Profile
22	Climb to 36000 ft Hp	200 ft AGL – 36000 ft	0.84 M	1	Best climb speed	Typical NFU Ferry Profile
23	Stabilized Point	36,000 ft Hp	0.84M	1	Best Range or Endurance Speed Stabilize for >5 minutes Tolerances Mach: +/- 0.01M Altitude: +/- 100 ft Hp	"Cold Soak" pod. Document worst case cruise conditions. Temperature of Standard Atmosphere is lowest and becomes constant above this altitude (-56 C).
24	Low Angle Dive Profiles	<15,000 ft AGL	350 - 520 KCAS	As Req'd	Z diagram IAW SOP Dive Angles: 5° - 20° **Min Altitude: 3,000 ft AGL** **Speed Limit: 550 KCAS** **Mach Limit: 0.95M** **n_z Limit: 5/-1 g (sym)** **3/0 g (asym)**	NFU Mission Profile
25	Observation Maneuvers	500 ft AGL	420 - 540 KCAS	As Req'd	**Speed Limit: 550 KCAS** **Mach Limit: 0.95M** nz Limit: 5/-1 g (sym) 3/0 g (asym)	NFU Mission Profile

Appendix B Flight Test Event Logs

Table B.1 Flight #1 Event Summary.

Flight #1
Date: January 6, 2010 Base: Bodø MAS
Aircrew: MAJ Kent-Harold Johansen Test Aircraft: F-16A (S/N 665, side # 107)

Test Point	Maneuver	HUD Time (Start/Stop)	Altitude (ft Hp)	Airspeed/ Mach	Nz	OAT (°C)	Comments
1	SHSS	09:13:35/ 09:13:48	5000	250	1	-15	½ Left Rudder
1	SHSS	09:14:08/ 09:14:15	5000	250	1	-15	Full Left Rudder
1	SHSS	09:14:28/ 09:14:52	4970	255	1	-15	½ Right Rudder
1	SHSS	09:15:00/ 09:15:10	4970	248	1	-15	Full Right Rudder
2	Pitch doublet	09:15:40/ 09:15:50	5000	260	1	-15	Deadbeat
2	Pitch doublet	09:16:08/ 09:16:15	5050	250	1	-15	Deadbeat
2	Roll doublet	09:16:20/ 09:16:30	5060	250	1	-15	Deadbeat
2	Yaw doublet	09:16:40/ 09:16:50	5020	255	1	-15	L/R, 1 overshoot
2	Yaw doublet	09:16:55/ 09:17:10	5000	250	1	-15	L/R, 1 overshoot
3	Level Accel	09:18:00/ 09:19:15	5000	250-530	1	-15	A/C wants to roll right, 1 dot of left roll trim needed
4	Pitch doublet	09:19:15/ 09:19:20	5000	530	1	-15	A/C sensitive, but deadbeat response
4	Roll doublet	09:19:20/ 09:19:25	5000	530	1	-15	L/R, no overshoot, but sensitive
4	Yaw doublet	09:19:26/ 09:19:31	5000	530	1	-15	L/R, no overshoot
5/6	Wind Up Turn/ Wind Down Turn	09:19:57/ 09:20:36	5070	530	4.8	-15	Practice point. Use WUT/WDT at 09:50:40 No vibrations noticed Reached 17 AOA at 250 KCAS
5/6	Wind Up Turn/ Wind Down Turn	09:22:30/ 09:23:20	5000	535	4.8	-15	Test Point OK. Use WUT/WDT at 09:50:40
7	Stabilized Point	09:24:40/ 09:26:40	1010	450	1	-9	Little turbulence with little wing tip oscillations
8	Pitch doublet	09:26:40/ 09:26:43	1000	450	1	-9	Deadbeat response
8	Roll doublet	09:26:44/ 09:26:47	1000	450	1	-9	L/R, Deadbeat response
8	Yaw doublet	09:26:47/ 09:26:53	1000	450	1	-9	L/R, Deadbeat response
9	Steady Turn	09:28:00/ 09:28:10	1000	450	3	-9	Maneuver starts at 09:26:52

Test Point	Maneuver	HUD Time (Start/Stop)	Altitude (ft Hp)	Airspeed/ Mach	Nz	OAT (°C)	Comments
10	Steady Turn	09:28:30/ 09:28:47	1000	450	4	-9	MIL Power, no vibrations noticed during turns
11	Stabilized Point	09:30:30/ 09:32:29	1000	500	1	-9	Airspeed indication jumping frequently
12	Pitch doublet	09:32:35/ 09:32:40	1000	500	1	-9	Deadbeat response
12	Roll doublet	09:32:41/ 09:32:45	1000	500	1	-9	R/L, Deadbeat response
12	Yaw doublet	09:32:46/ 09:32:50	1000	500	1	-9	R/L, Deadbeat response
13	Steady Turn	09:33:20/ 09:33:40	1000	500	3	-9	Maneuver starts at 09:32:59
14	Steady Turn	09:34:15/ 09:34:21	1000	500	4	-9	Maneuver starts at 09:33:50
15	Stabilized Point	09:35:30/ 09:37:40	1000	540	1	-9	Fuel Qty: 7900 lb @ 09:35:00
16	Pitch doublet	09:37:43/ 09:37:47	1000	540	1	-9	Deadbeat response
16	Roll doublet	09:37:49/ 09:37:52	1000	540	1	-9	R/L, Deadbeat response
16	Yaw doublet	09:37:54/ 09:37:58	1000	540	1	-9	R/L, Deadbeat response
17	Steady Turn	09:38:00/ 09:38:30	1000	540	3	-9	
18	Steady Turn	09:38:30/ 09:39:00	1000	540	4	-9	
19	Stabilized Point	09:40:50/ 09:42:50	200	450	1	-11	
20	Stabilized Point	09:43:54/ 09:45:54	200	500	1	-11	Very turbulent, Pod steady on wind, both wing tips oscillating
21	Stabilized Point	09:46:54/ 09:48:54	200	540	1	-11	Yaw trim centered, 1 dot left roll trim Fuel Qty: 6000 lb @ 09:47:38 Winds: 18008 @ 09:48:15
5/6	Wind Up Turn/ Wind Down Turn	09:50:40/ 09:51:47	5000	535	5.0	-15	Use for best data
25	Observation Mnv	09:53:55/ 09:54:50	500	420-540	~4	-10	Fuel Qty: 5100 lb @ 09:52:30 Very easy to over g
24	Low Angle Dives	09:56:50/ 09:59:30	15000-350	470	1	-	6-7 deg dive profile, lighthouse target See temperature profile
22	Climb to 36000 ft	10:00:00/ 10:04:00	3000-36000	0.9	1	-	Useful to document temperature change See temperature profile
23	Stabilized Point	10:04:26/ 10:09:29	36000	280/0.84	1	-61	Cold Soak

Table B.2 Flight #2 Event Summary.

Flight #2
Date: January 6, 2010 Base: Bodø MAS
Aircrew: MAJ Kent-Harold JohansenTest Aircraft: F-16A (S/N 665, side # 107)

Test Point	Maneuver	HUD Time (Start/Stop)	Altitude (ft Hp)	Airspeed/ Mach	Nz	OAT (°C)	Comments
1	SHSS	12:29:30/ 12:29:35	5000	250	1	-15	¼ Left Rudder
1	SHSS	12:29:35/ 12:29:50	5000	250	1	-15	½ Left Rudder
1	SHSS	12:29:55/ 12:30:05	4970	252	1	-15	¼ Right Rudder
1	SHSS	12:30:05/ 12:30:24	4970	252	1	-15	½ Right Rudder
2	Pitch doublet	12:30:30/ 12:30:36	5000	250	1	-15	Deadbeat
2	Roll doublet	12:30:45/ 12:30:52	5060	250	1	-15	Deadbeat
2	Yaw doublet	12:30:55/ 12:31:03	5020	250	1	-15	L/R, 2 overshoots
3	Level Accel	12:31:30/ 12:33:10	5000	250-530	1	-15	
4	Pitch doublet	12:33:35/ 12:33:42	5000	530	1	-15	
4	Roll doublet	12:33:43/ 12:33:46	5000	530	1	-15	
4	Yaw doublet	12:33:47/ 12:33:53	5000	530	1	-15	
5/6	Wind Up Turn/ Wind Down Turn	12:34:00/ 12:34:55	5000	530	4.8	-15	WUT 12:34:00 – 12:34:30 WDT 12:34:30 – 12:34:55
7	Stabilized Point	12:37:25/ 12:39:30	1000	450	1	-9	Little turbulence with some wing tip oscillations, pod steady. Winds: 16012 @ 12:38:15
8	Pitch doublet	12:39:30/ 12:39:39	1000	450	1	-9	Deadbeat response
8	Roll doublet	12:39:40/ 12:39:45	1000	450	1	-9	R/L, Deadbeat response
8	Yaw doublet	12:39:48/ 12:39:52	1000	450	1	-9	L/R, Deadbeat response
9	Steady Turn	12:40:00/ 12:40:45	1000	450	3	-9	
10	Steady Turn	12:40:45/ 12:41:29	1000	450	4	-9	Best data 12:41:10 – 12:41:29
11	Stabilized Point	12:42:30/ 12:44:30	1000	500	1	-9	
12	Pitch doublet	12:44:30/ 12:44:39	1000	500	1	-9	Deadbeat response
12	Roll doublet	12:44:40/ 12:44:43	1000	500	1	-9	R/L, Deadbeat response
12	Yaw doublet	12:44:44/ 12:44:48	1000	500	1	-9	L/R, Deadbeat response
13	Steady Turn	12:44:50/ 12:45:37	1000	500	3	-9	

Test Point	Maneuver	HUD Time (Start/Stop)	Altitude (ft Hp)	Airspeed/ Mach	Nz	OAT (°C)	Comments
14	Steady Turn	12:45:37/ 12:46:15	1000	500	4	-9	
15	Stabilized Point	12:47:20/ 12:49:20	1000	540	1	-9	
16	Pitch doublet	12:49:18/ 12:49:22	1000	540	1	-9	Deadbeat response
16	Roll doublet	12:49:22/ 12:49:24	1000	540	1	-9	R/L, Deadbeat response
16	Yaw doublet	12:49:25/ 12:49:29	1000	540	1	-9	R/L, Deadbeat response
17	Steady Turn	12:49:31/ 12:50:01	1000	540	3	-9	
18	Steady Turn	12:50:01/ 12:50:35	1000	540	4	-9	
19	Stabilized Point	12:52:24/ 12:54:24	200	450	1	-11	
20	Stabilized Point	12:56:24/ 12:58:24	200	500	1	-11	Very turbulent, Pod steady on wind, both wing tips oscillating
21	Stabilized Point	13:00:00/ 13:02:00	200	540	1	-11	Yaw trim centered, 1 dot left roll trim
24	Low Angle Dives	13:04:50/ 13:02:00	15000-210	370-470	1	-	6-7 deg dive profile, lighthouse target See temperature profile
25	Observation Mnv	13:07:30/ 13:08:25	420	420-540	~4	-10	Fuel Qty: 5100 lb @ 09:52:30 Very easy to over g

Table B.3 Flight #3 Event Summary.

Flight #3
Date: January 7, 2010 Base: Bodø MAS
Aircrew: MAJ Kent-Harold JohansenTest Aircraft: F-16A (S/N 665, side # 107)

Test Point	Maneuver	Time Ref (Start/Stop)	Altitude (ft Hp)	Airspeed/ Mach	Nz	OAT (°C)	Comments
1	SHSS	08:52:10/ 08:52:20	5000	250	1	-10	¼ Left Rudder
1	SHSS	08:52:30/ 08:52:46	5000	250	1	-10	½ Left Rudder
1	SHSS	08:53:08/ 08:53:18	4970	251	1	-10	¼ Right Rudder
1	SHSS	08:53:30/ 08:53:48	4970	251	1	-10	½ Right Rudder
2	Pitch doublet	08:54:30/ 08:54:37	5000	250	1	-10	Deadbeat
2	Roll doublet	08:54:45/ 08:54:52	5060	250	1	-10	Deadbeat, sluggish response
2	Yaw doublet	08:55:00/ 08:55:15	4980	250	1	-10	L/R, 1 overshoot
2	Yaw doublet	08:55:19/ 08:55:30	4950	252	1	-10	R/L, 1 overshoot
3	Level Accel	08:55:50/ 08:57:30	5000	250-530	1	-10	Starts to feel A/C cycling/oscillating at 430 KCAS Pod is steady
4	Pitch doublet	08:57:30/ 08:57:36	5000	530	1	-10	Deadbeat
4	Roll doublet	08:57:38/ 08:57:42	5000	530	1	-10	Deadbeat
4	Yaw doublet	08:57:42/ 08:57:50	5000	530	1	-10	Deadbeat
5/6	Wind Up Turn/ Wind Down Turn	08:58:00/ 08:59:00	5000	530	4.8	-10	WUT 08:58:00 – 08:58:30 WDT 08:58:30 – 08:59:00
7	Stabilized Point	09:00:40/ 09:02:40	1000	450	1	-7	
8	Pitch doublet	09:02:55/ 09:03:02	1000	450	1	-7	Deadbeat response
8	Roll doublet	09:03:02/ 09:03:07	1000	450	1	-7	R/L, Deadbeat response
8	Yaw doublet	09:03:10/ 09:03:15	1000	450	1	-7	L/R, Deadbeat response
9	Steady Turn	09:03:15/ 09:04:24	1000	450	3	-7	
10	Steady Turn	09:04:25/ 09:05:15	1000	450	4	-7	
11	Stabilized Point	09:06:25/ 09:08:25	1000	500	1	-7	Little turbulence (better than yesterday). Slower yaw freq than yesterday, not objectionable. Pod steady.
12	Pitch doublet	09:08:45/ 09:08:55	1000	500	1	-7	Deadbeat response

Test Point	Maneuver	Time Ref (Start/Stop)	Altitude (ft Hp)	Airspeed/ Mach	Nz	OAT (°C)	Comments
12	Roll doublet	09:08:55/ 09:09:05	1000	500	1	-7	L/R, Deadbeat response
12	Yaw doublet	09:09:05/ 09:09:11	1000	500	1	-7	L/R, Deadbeat response Sensed some oscillation
12	Yaw doublet	09:09:15/ 09:09:22	1000	500	1	-7	R/L, Deadbeat response Notice some resonance from pod.
13	Steady Turn	09:09:43/ 09:10:30	1000	500	3	-7	
14	Steady Turn	09:10:30/ 09:11:12	1000	500	4	-7	Can feel some lateral movement, lower freq than yesterday, can't tell if it is turbulence or pod. Winds 19526.
15	Stabilized Point	09:13:40/ 09:15:40	1000	540	1	-7	
16	Pitch doublet	09:15:45/ 09:15:52	1000	540	1	-7	Deadbeat response
16	Roll doublet	09:15:52/ 09:15:56	1000	540	1	-7	R/L, Deadbeat response
16	Yaw doublet	09:15:56/ 09:16:05	1000	540	1	-7	L/R then R/L, Deadbeat response
17	Steady Turn	09:16:20/ 09:17:02	1000	540	3	-7	
18	Steady Turn	09:17:02/ 09:17:40	1000	540	4	-7	
19	Stabilized Point	09:19:35/ 09:21:35	200	450	1	-6	
20	Stabilized Point	09:23:14/ 09:25:14	200	500	1	-6	
21	Stabilized Point	09:27:00/ 09:29:00	200	540	1	-6	
24	Low Angle Dives	09:33:00/ 09::00	8000-320	390-530	1	-18 to -6	6-7 deg dive profile, lighthouse target See temperature profile
25	Observation Mnv	09:35:30/ 09:36:25	500	420-540	~4	-6	Fuel Flow 12,000 lb/hr at 540 KCAS Fuel Qty: 4,500 lb at 09:37:24

Appendix C Additional Figures

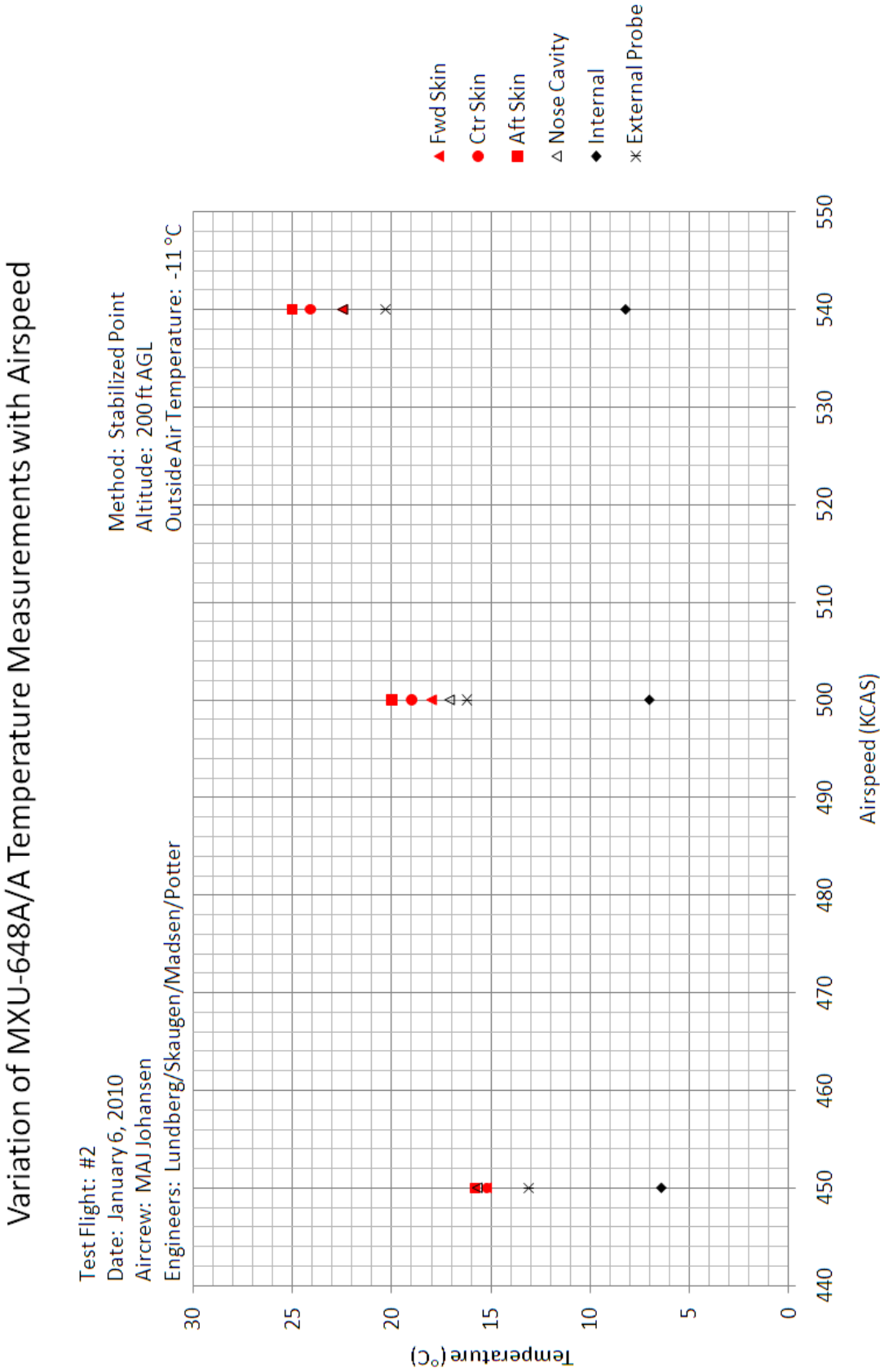

Figure C.1 Variation of Temperature with Airspeed (Flight #2, 200 ft AGL).

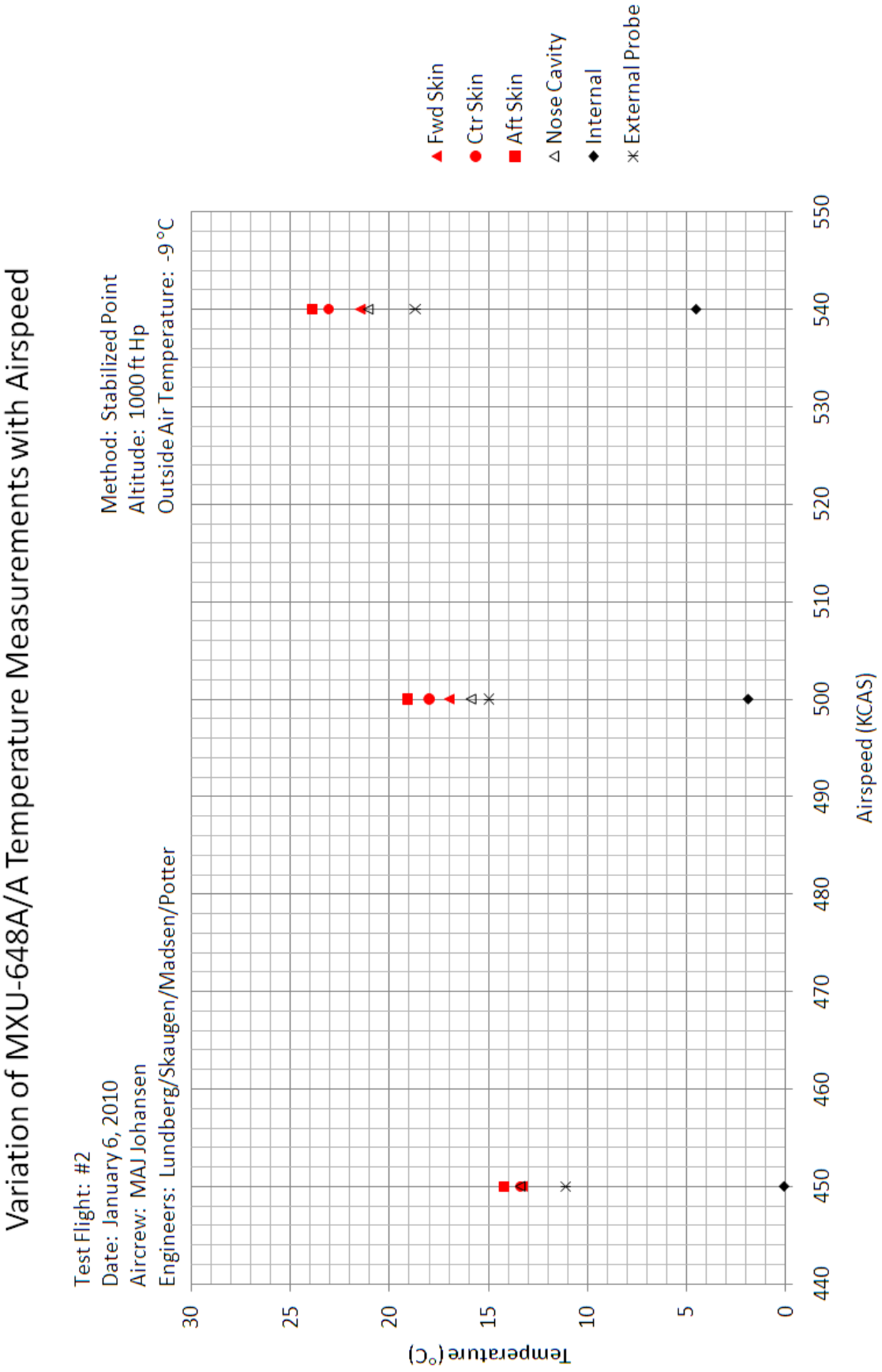

Figure C.2 Variation of Temperature with Airspeed (Flight #2, 1000 ft Hp).

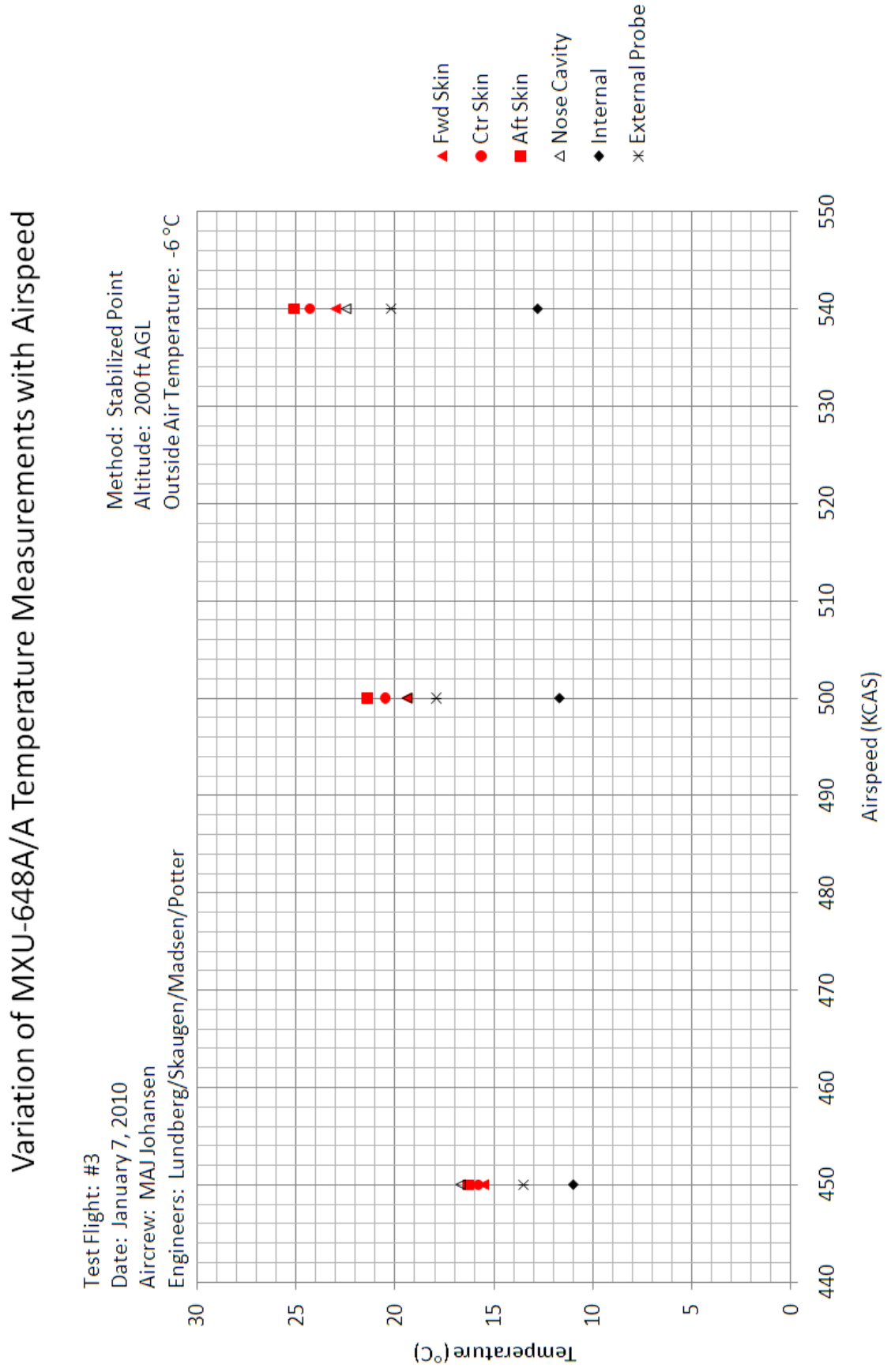

Figure C.3 Variation of Temperature with Airspeed (Flight #3, 200 ft AGL).

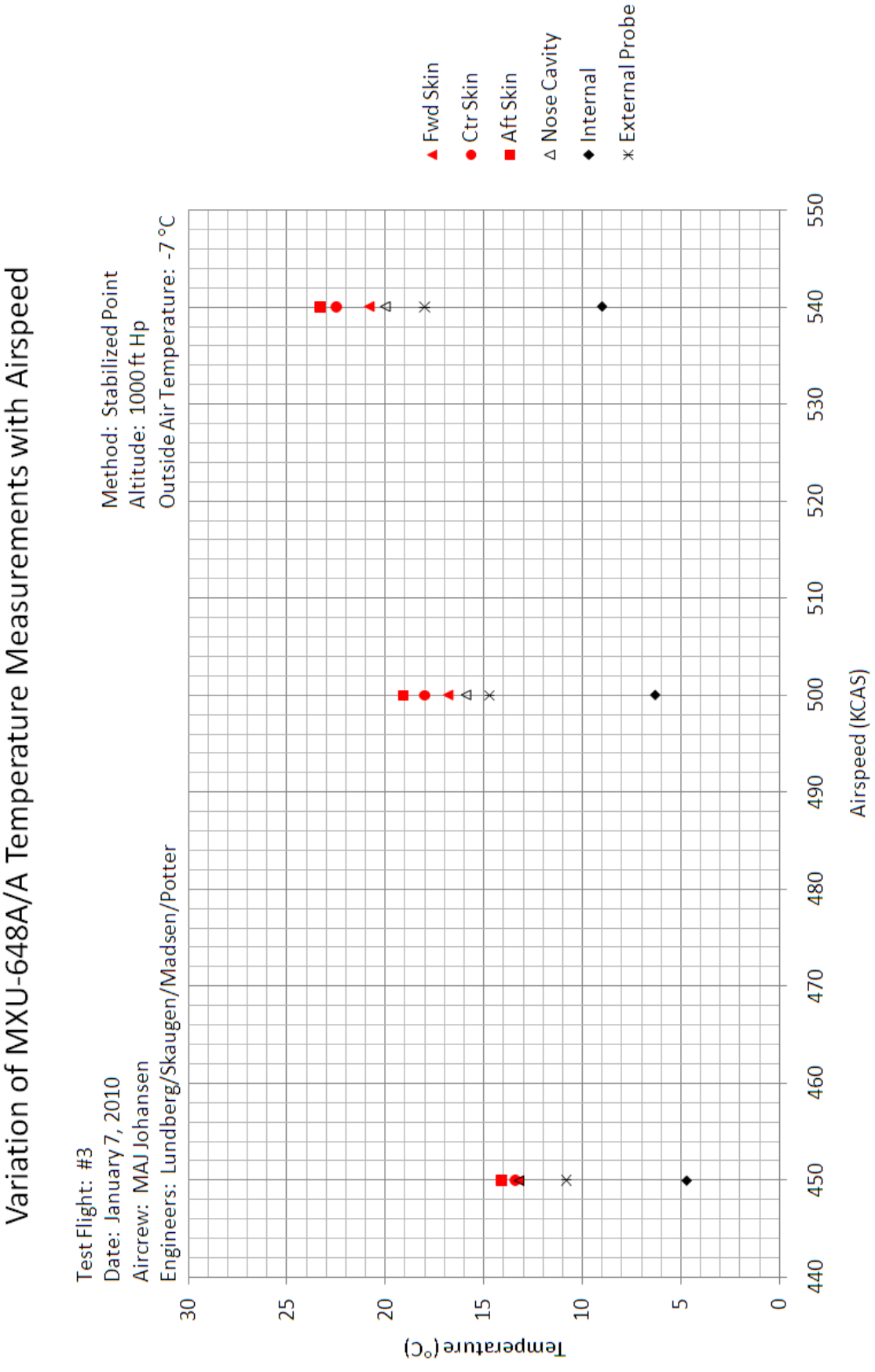

Figure C.4 Variation of Temperature with Airspeed (Flight #3, 1000 ft Hp).

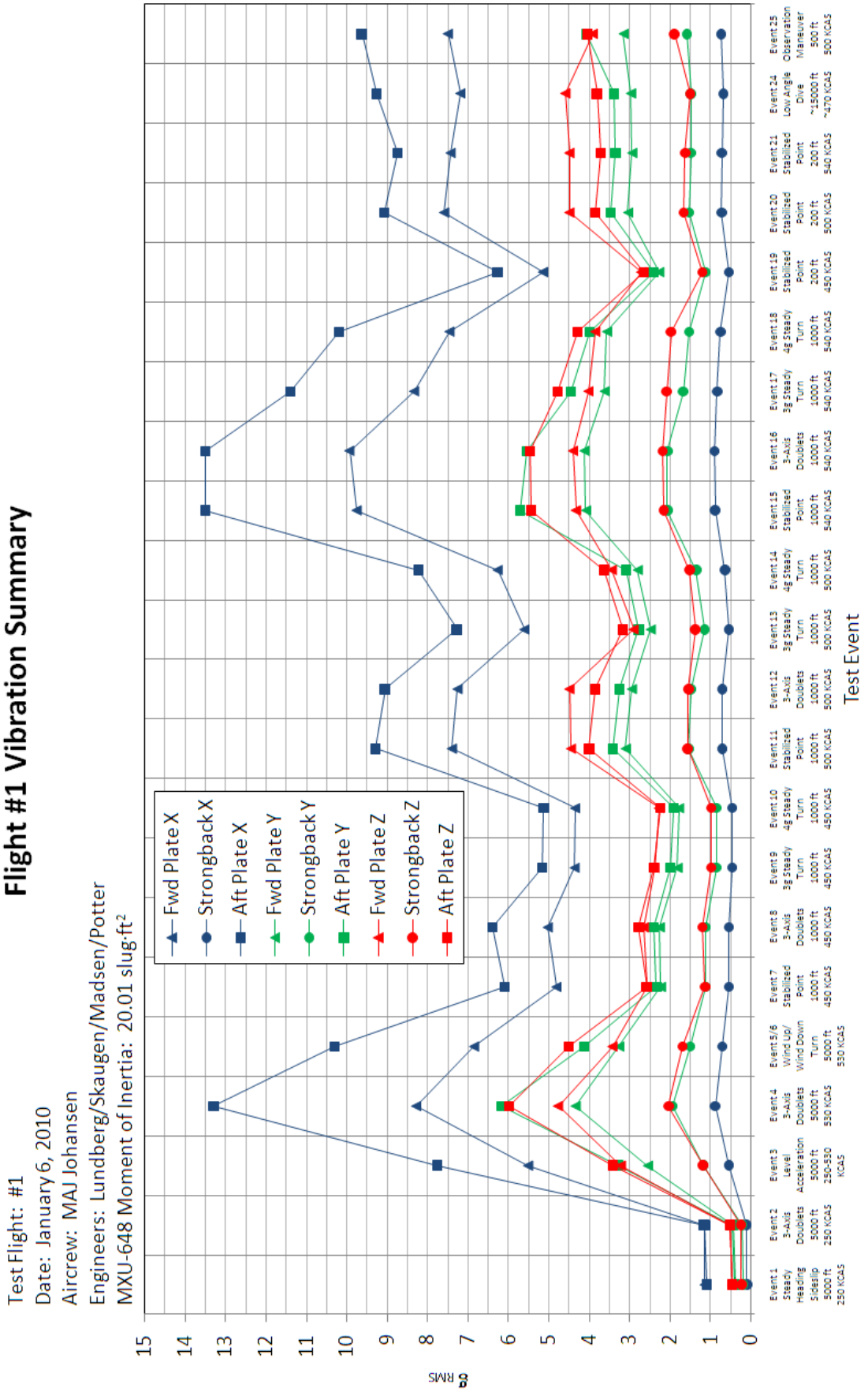

Figure C.5 Flight #1 Vibration Summary.

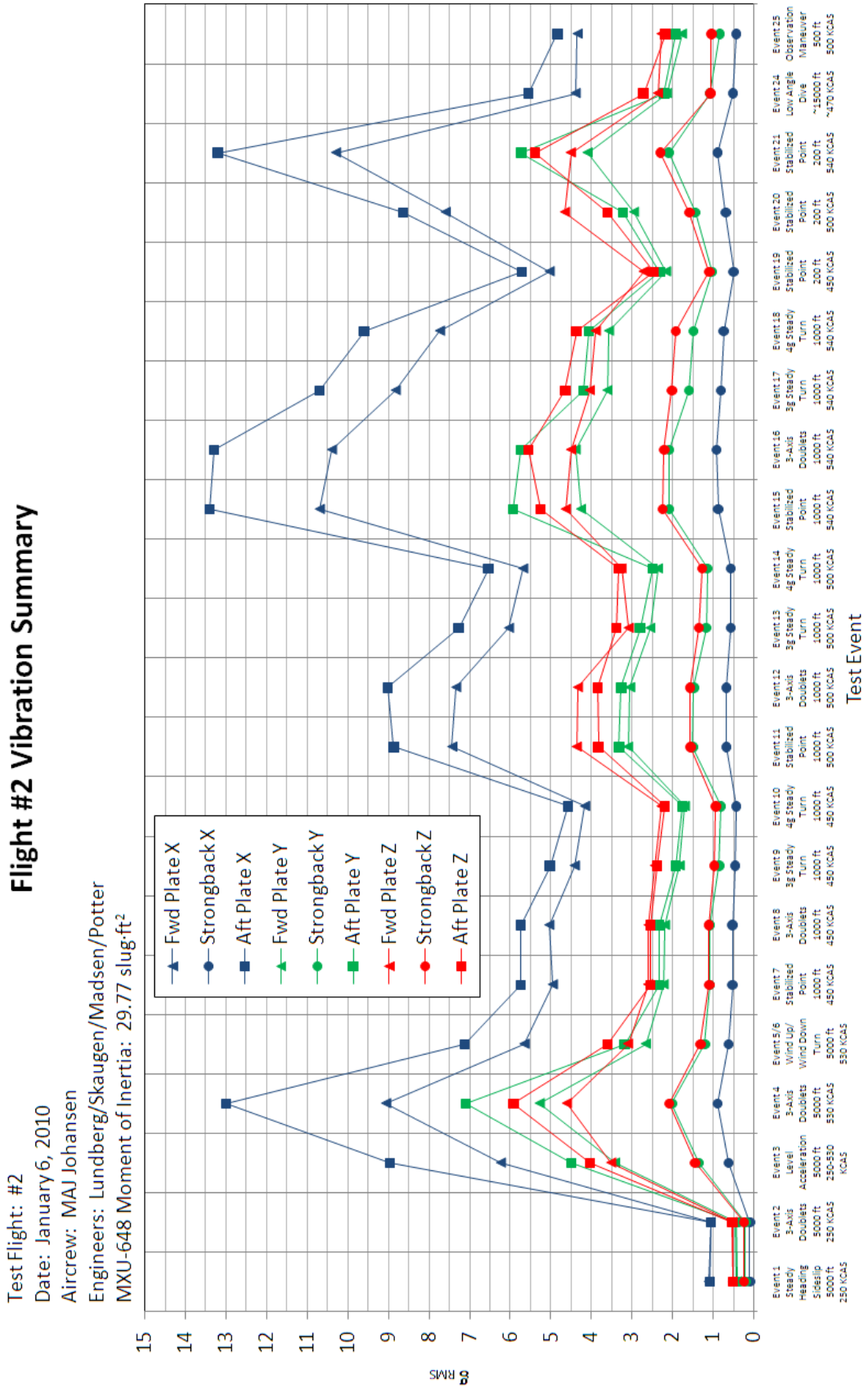

Figure C.6 Flight #2 Vibration Summary.

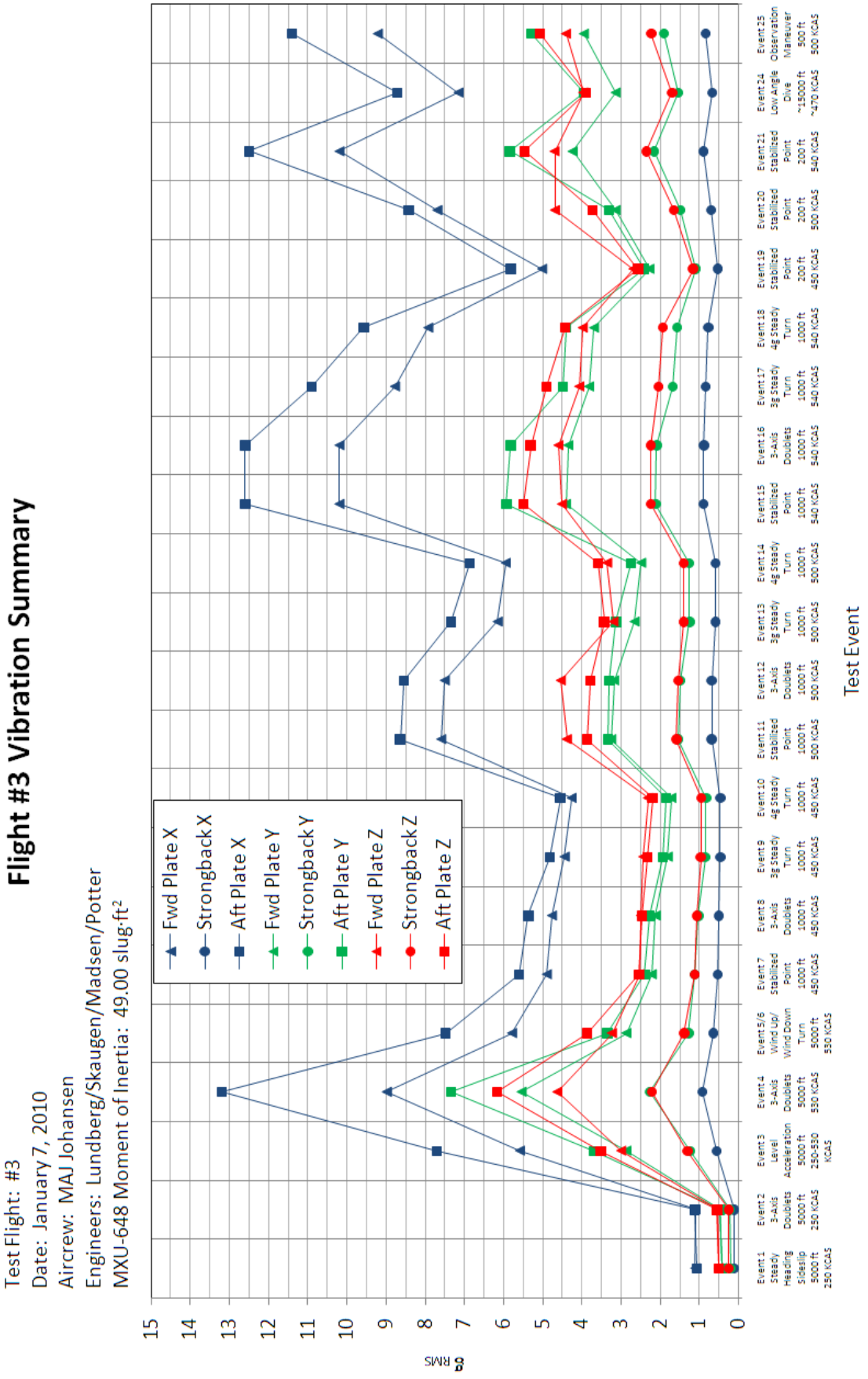

Figure C.7 Flight #3 Vibration Summary.

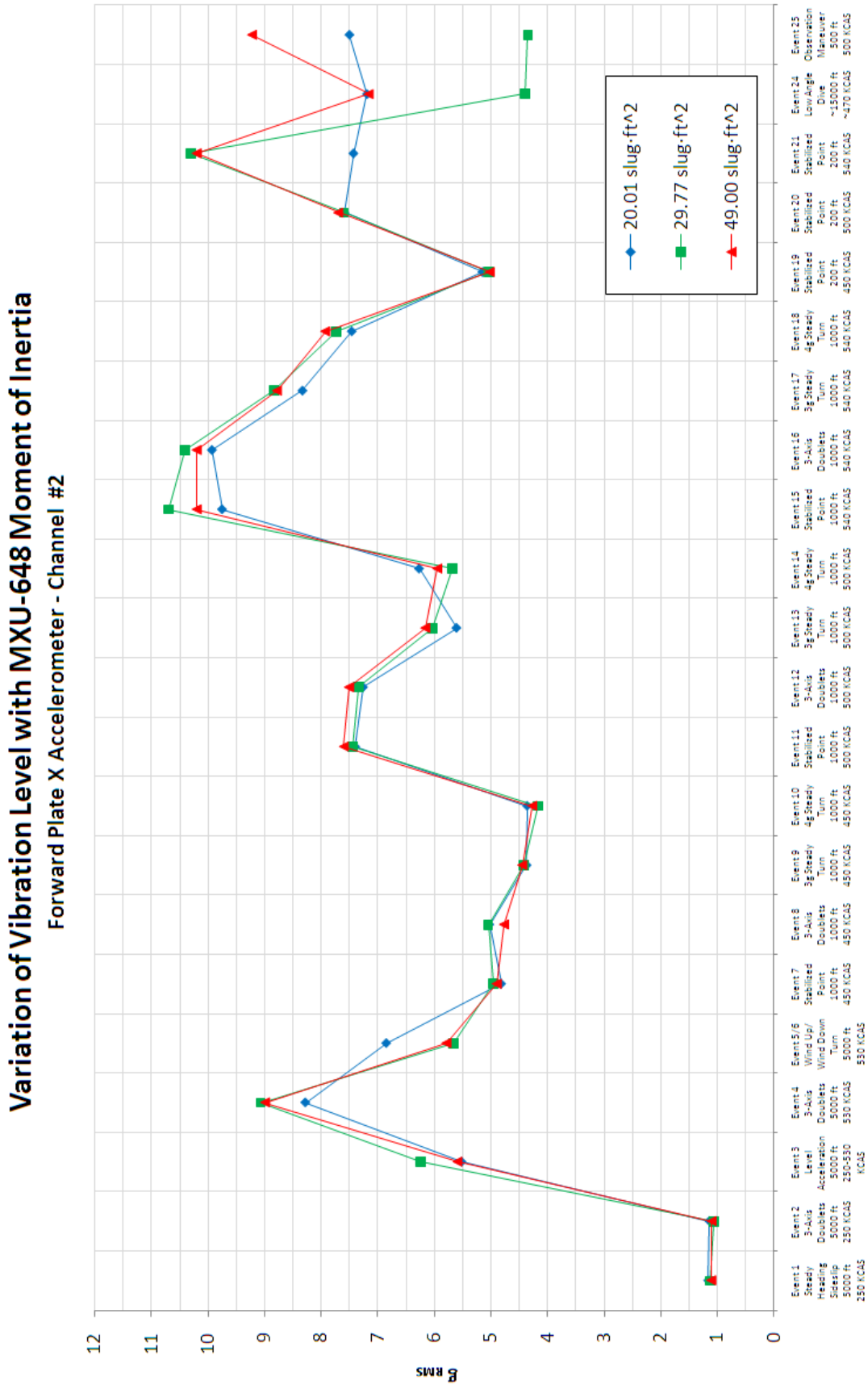

Figure C.8 Variation of Vibration Level with Moment of Inertia (Forward X-axis).

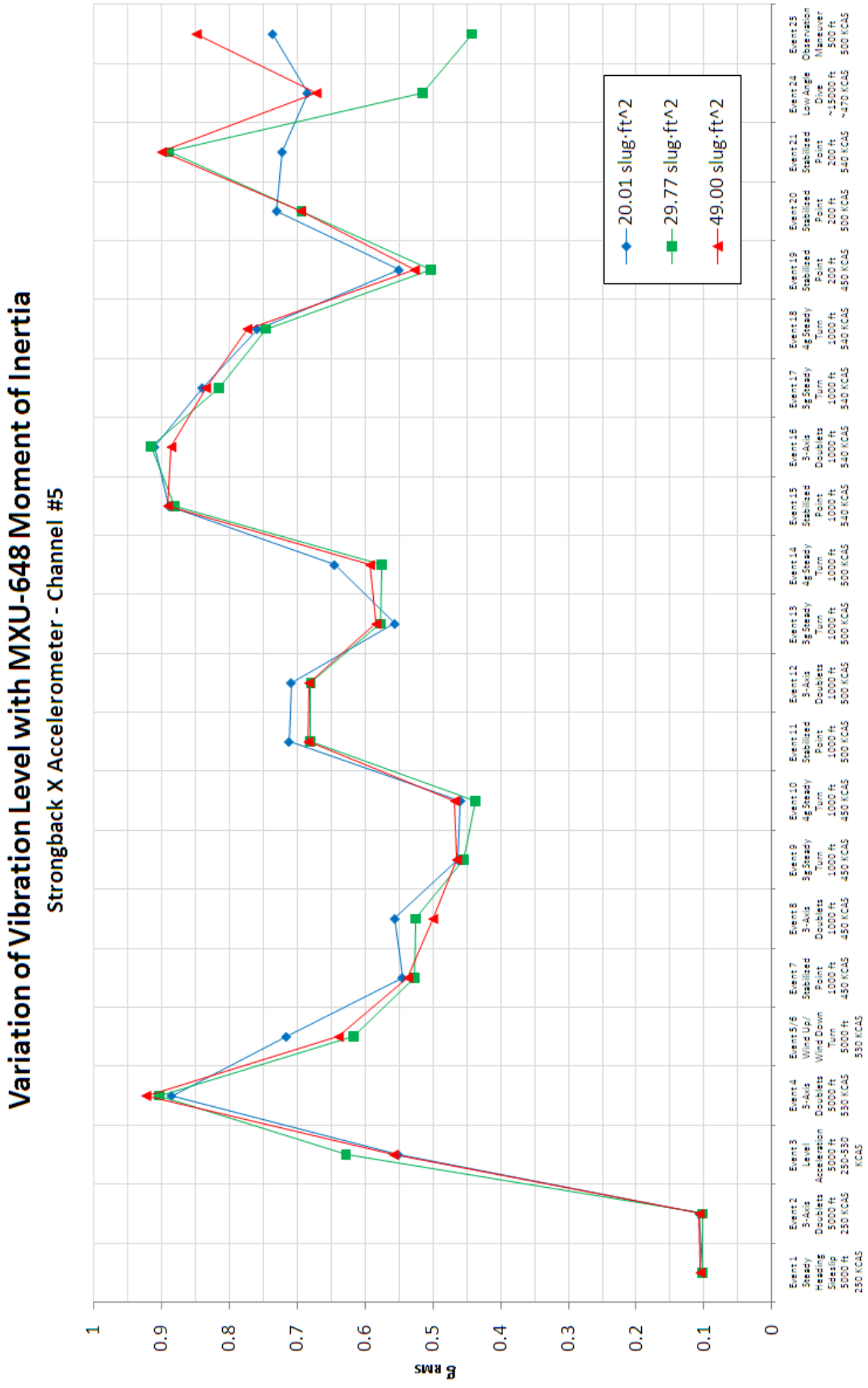

Figure C.9 Variation of Vibration Level with Moment of Inertia (Strongback X-axis).

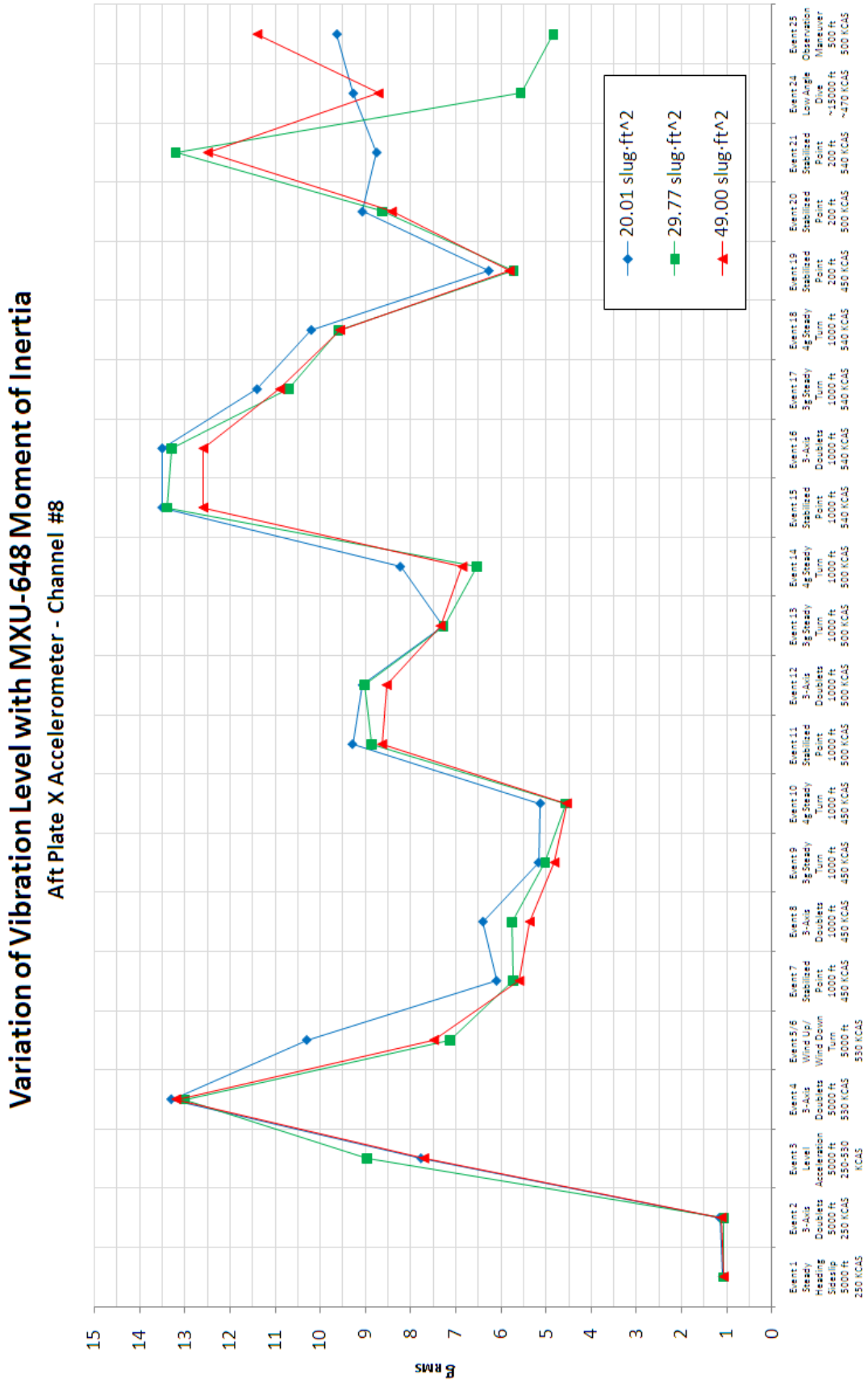

Figure C.10 Variation of Vibration Level with Moment of Inertia (Aft X-axis).

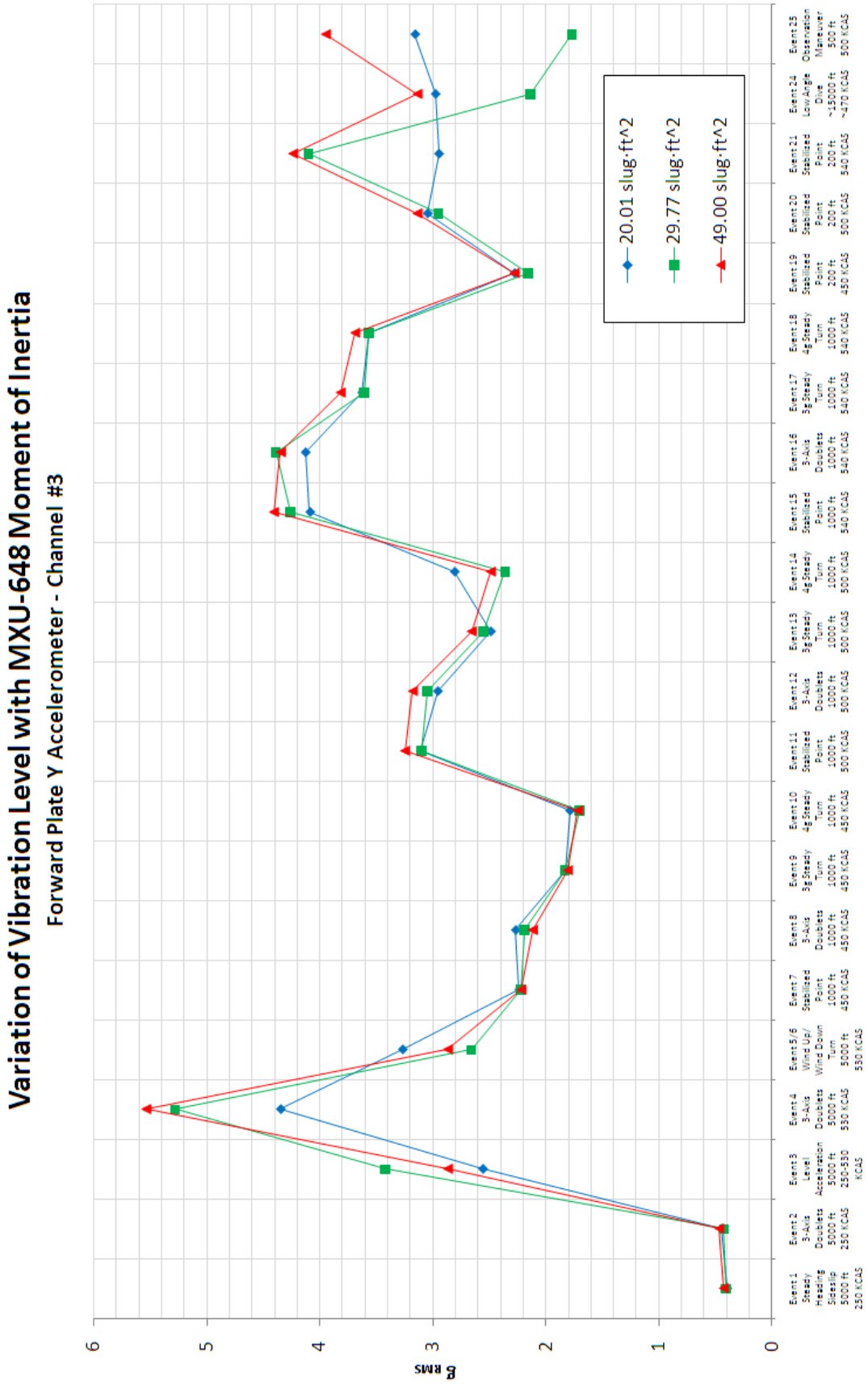

Figure C.11 Variation of Vibration Level with Moment of Inertia (Forward Y-axis).

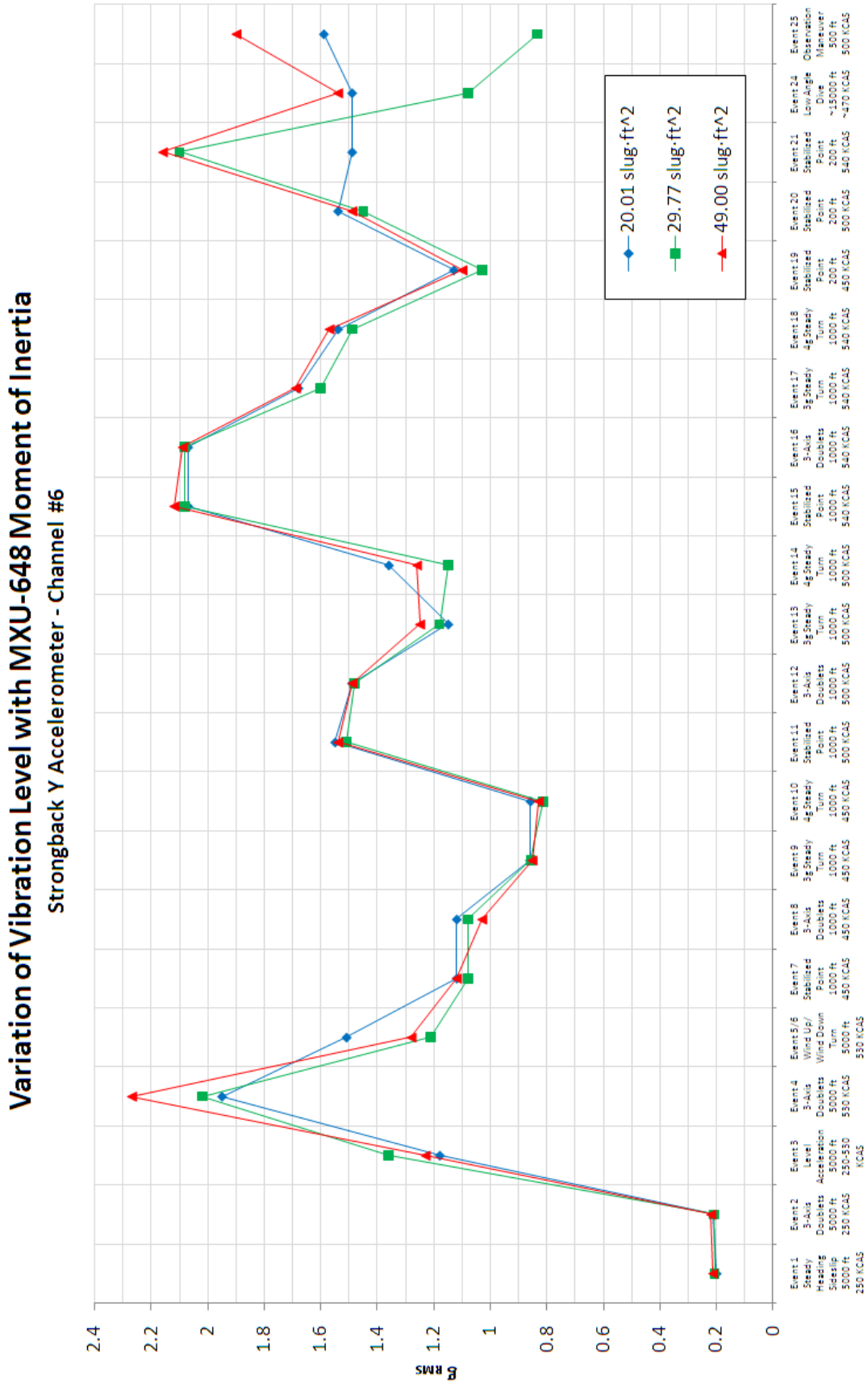

Figure C.12 Variation of Vibration Level with Moment of Inertia (Strongback Y-axis).

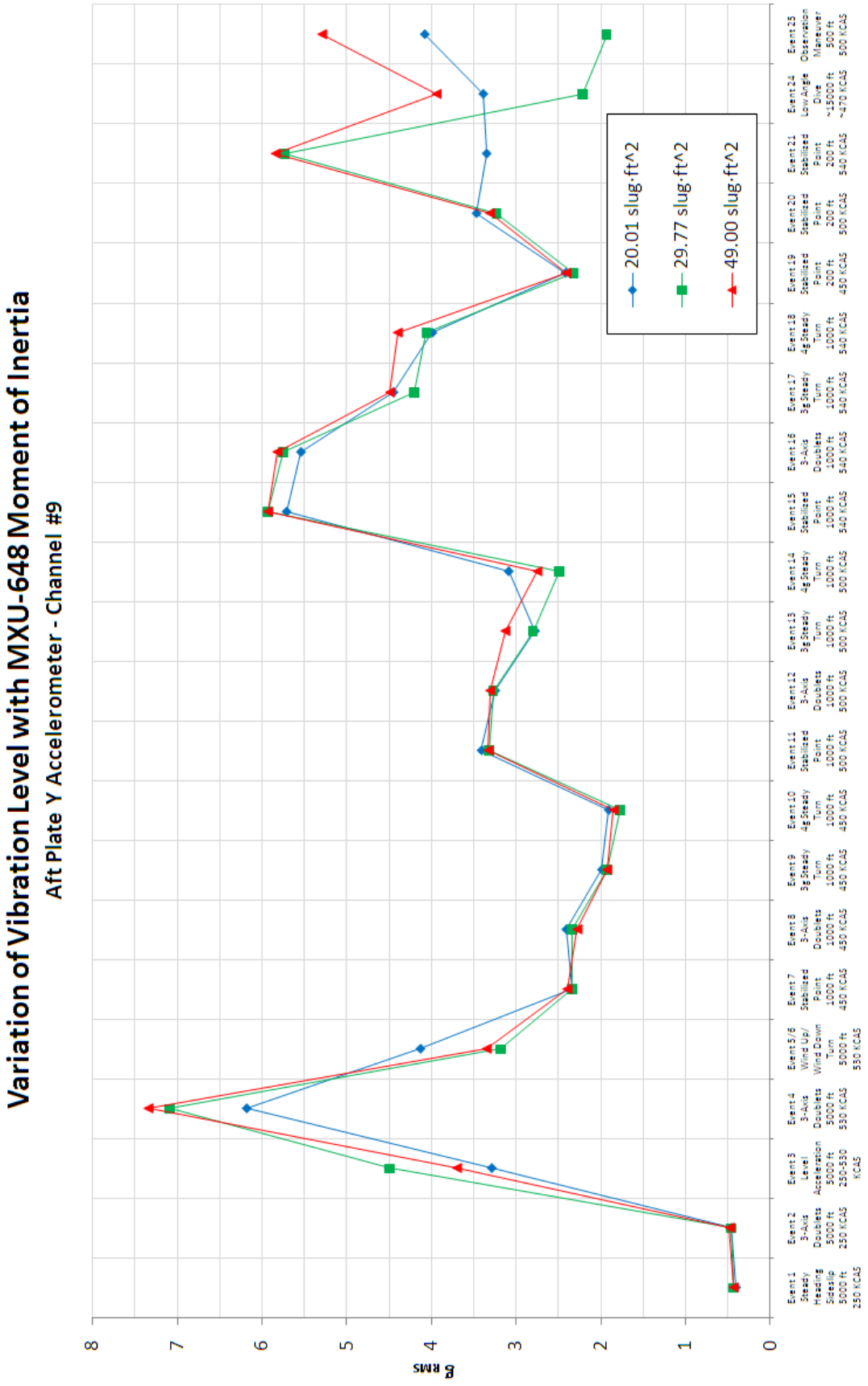

Figure C.13 Variation of Vibration Level with Moment of Inertia (Aft Y-axis).

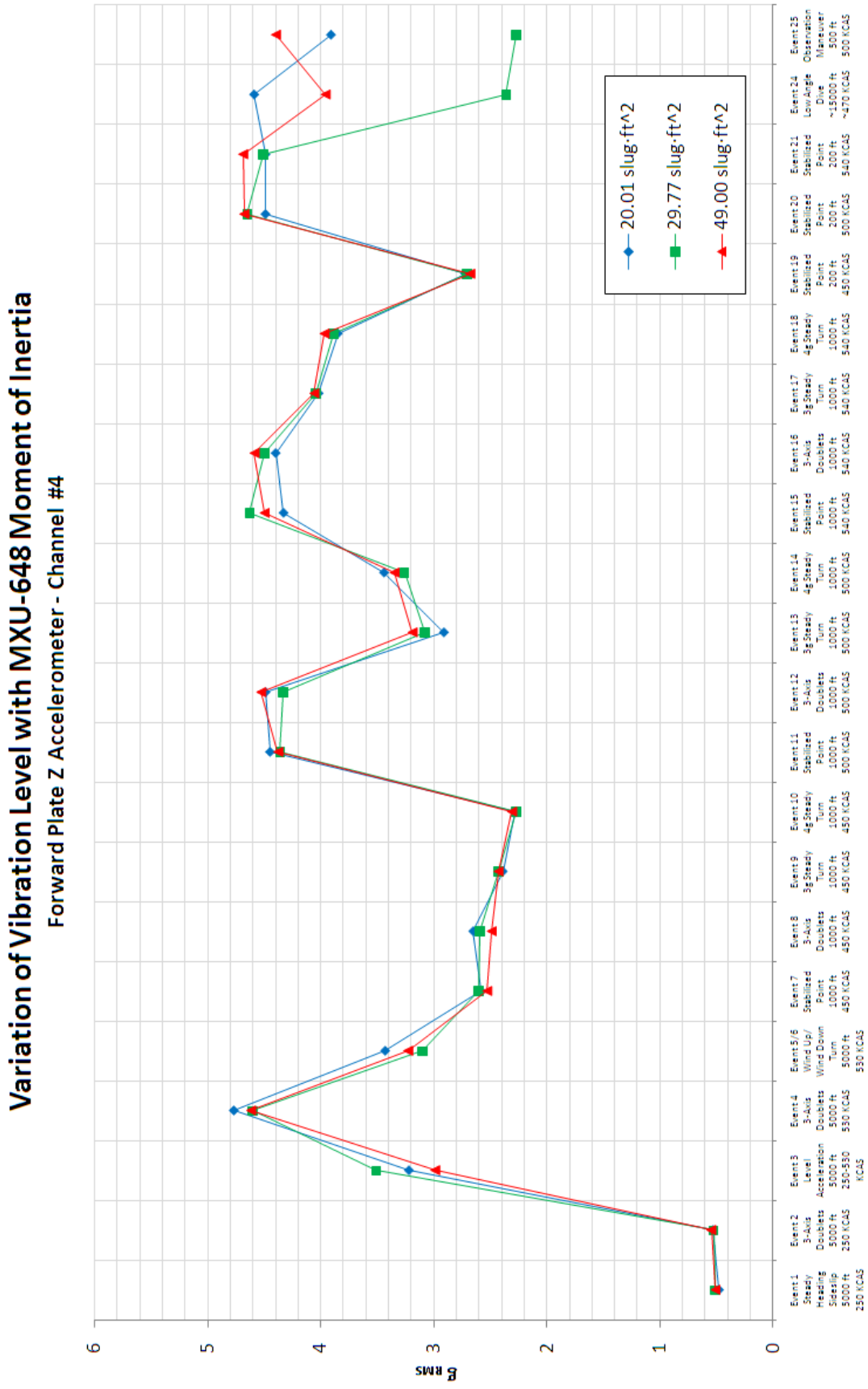

Figure C.14 Variation of Vibration Level with Moment of Inertia (Forward Z-axis).

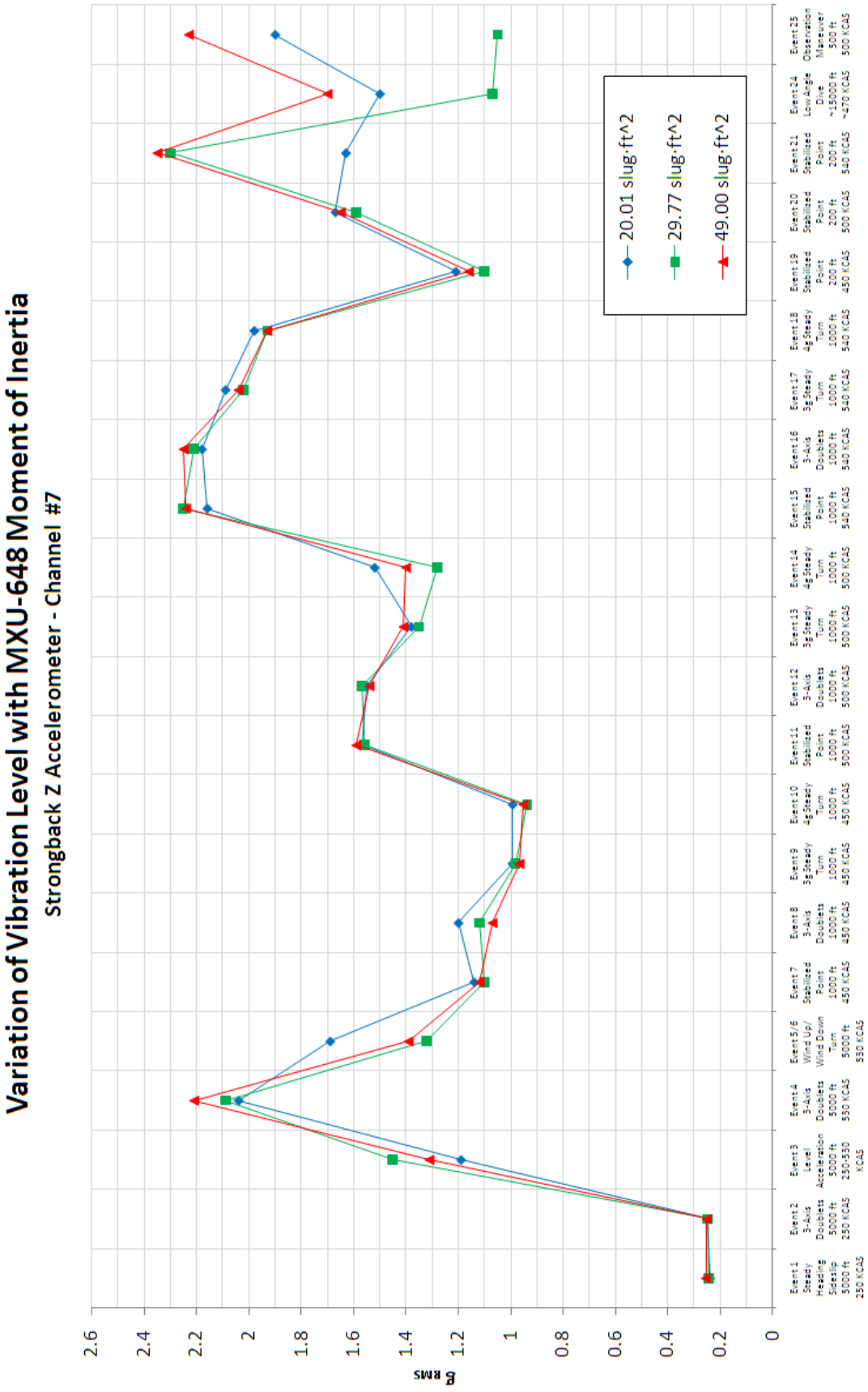

Figure C.15 Variation of Vibration Level with Moment of Inertia (Strongback Z-axis).

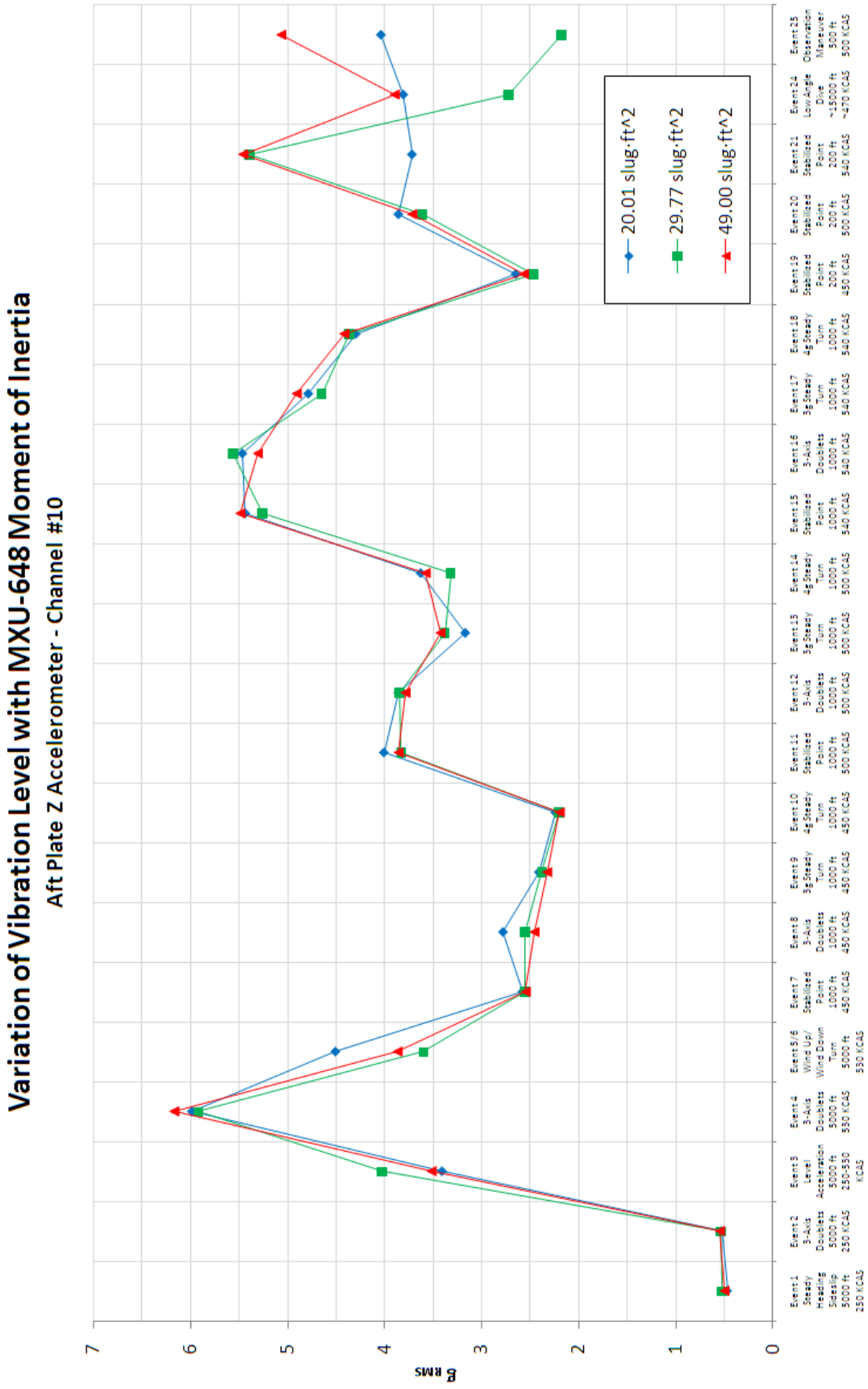

Figure C.16 Variation of Vibration Level with Moment of Inertia (Aft Z-axis).

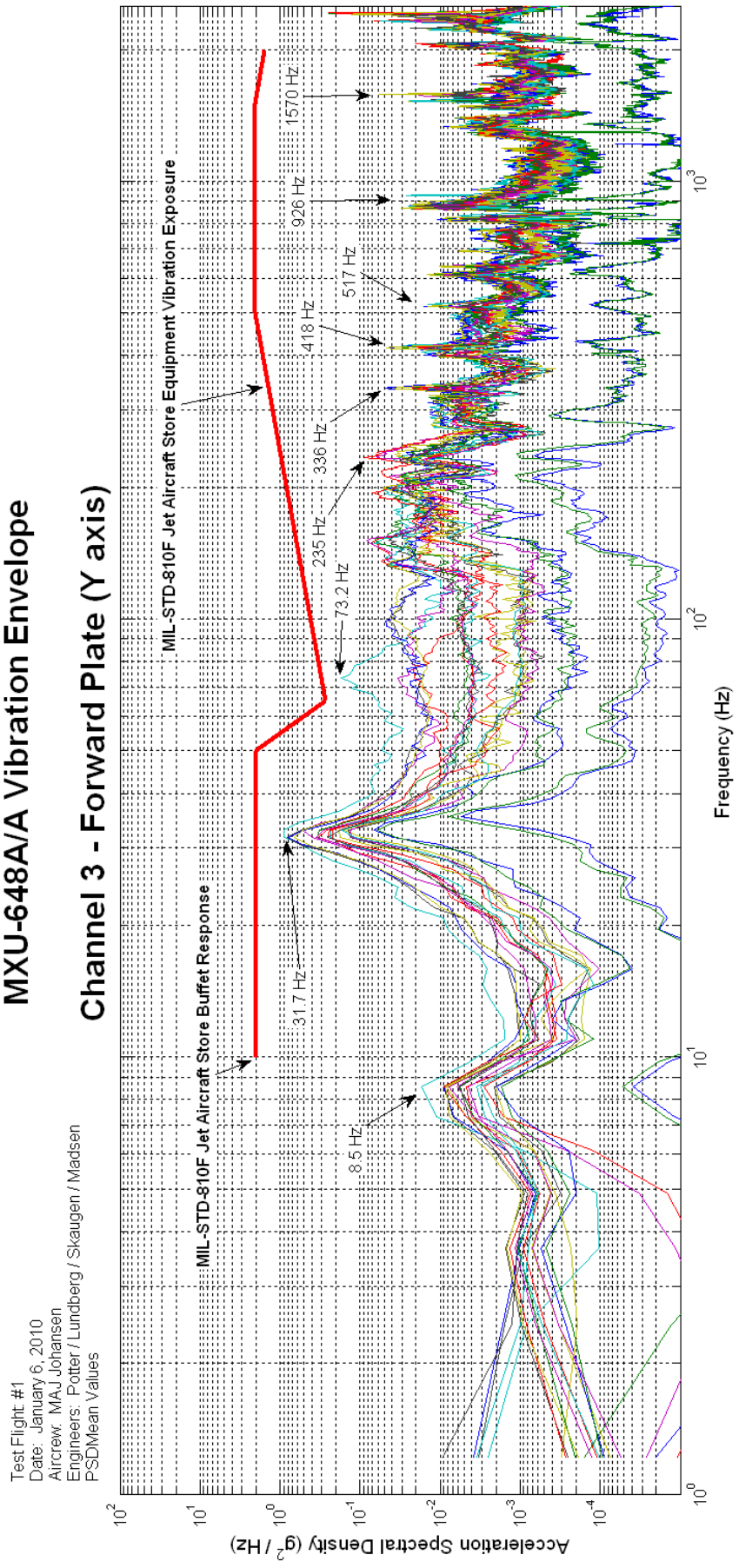

Figure C.17 Flight #1 Vibration Envelope (Forward Plate Y-axis).

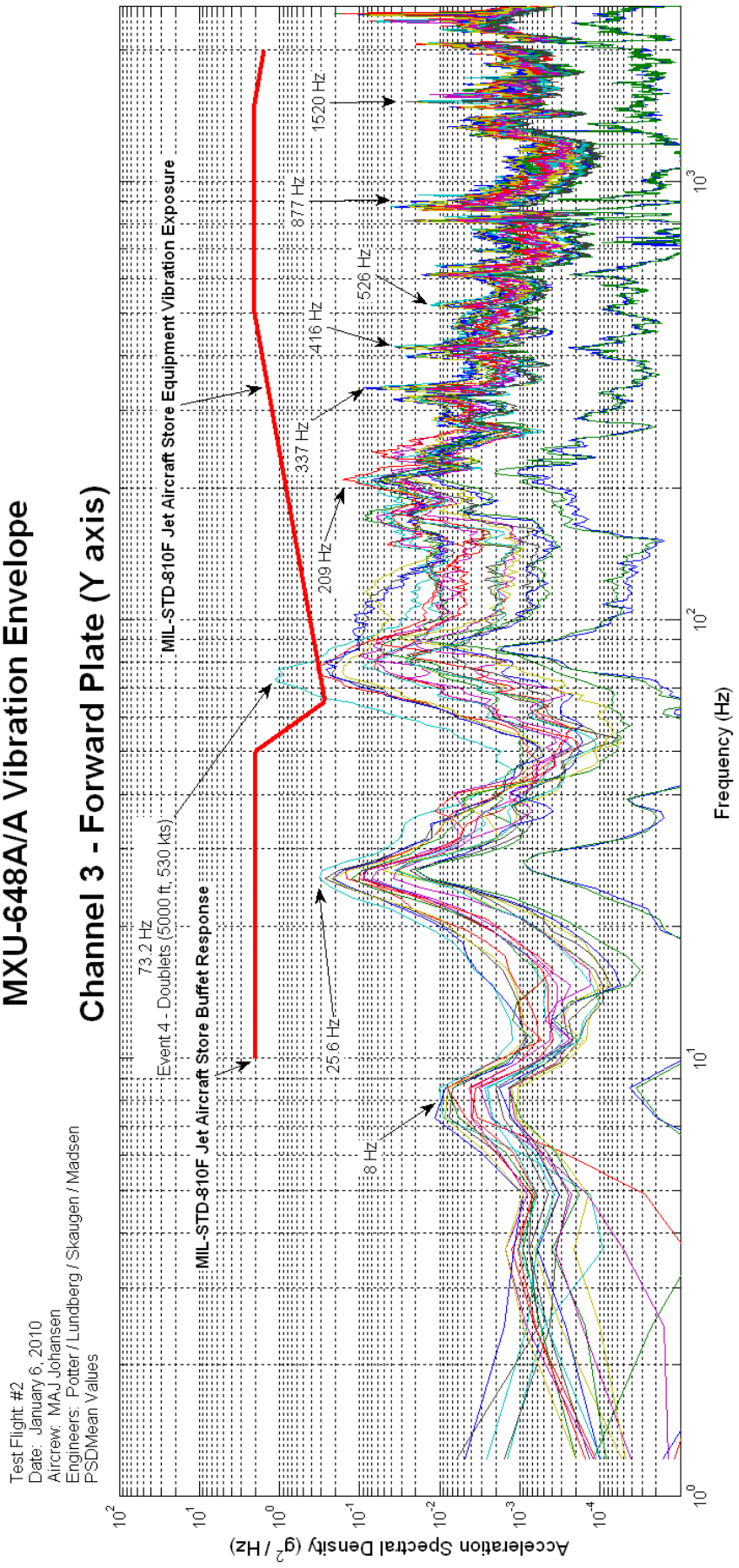

Figure C.18 Flight #2 Vibration Envelope (Forward Plate Y-axis).

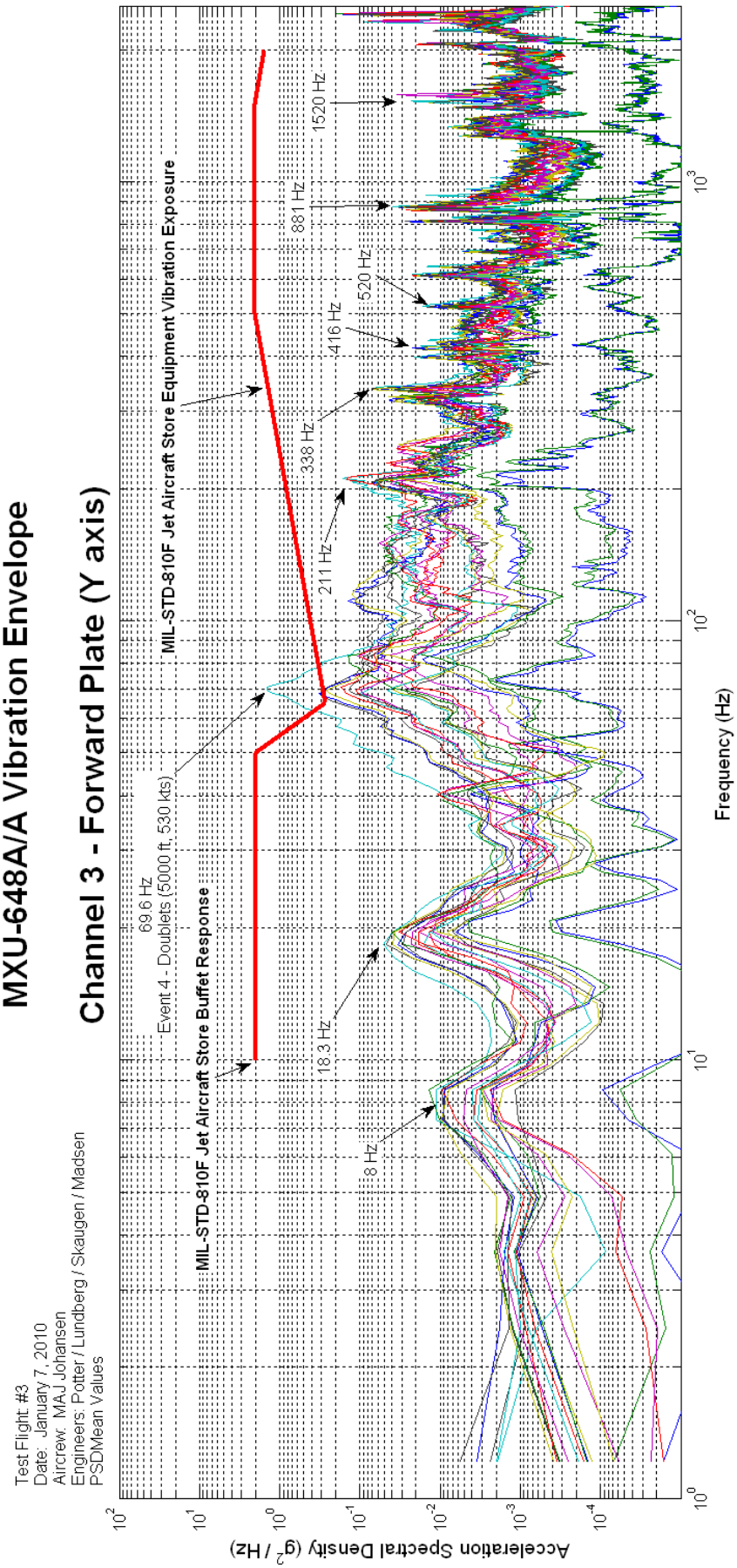

Figure C.19 Flight #3 Vibration Envelope (Forward Plate Y-axis).

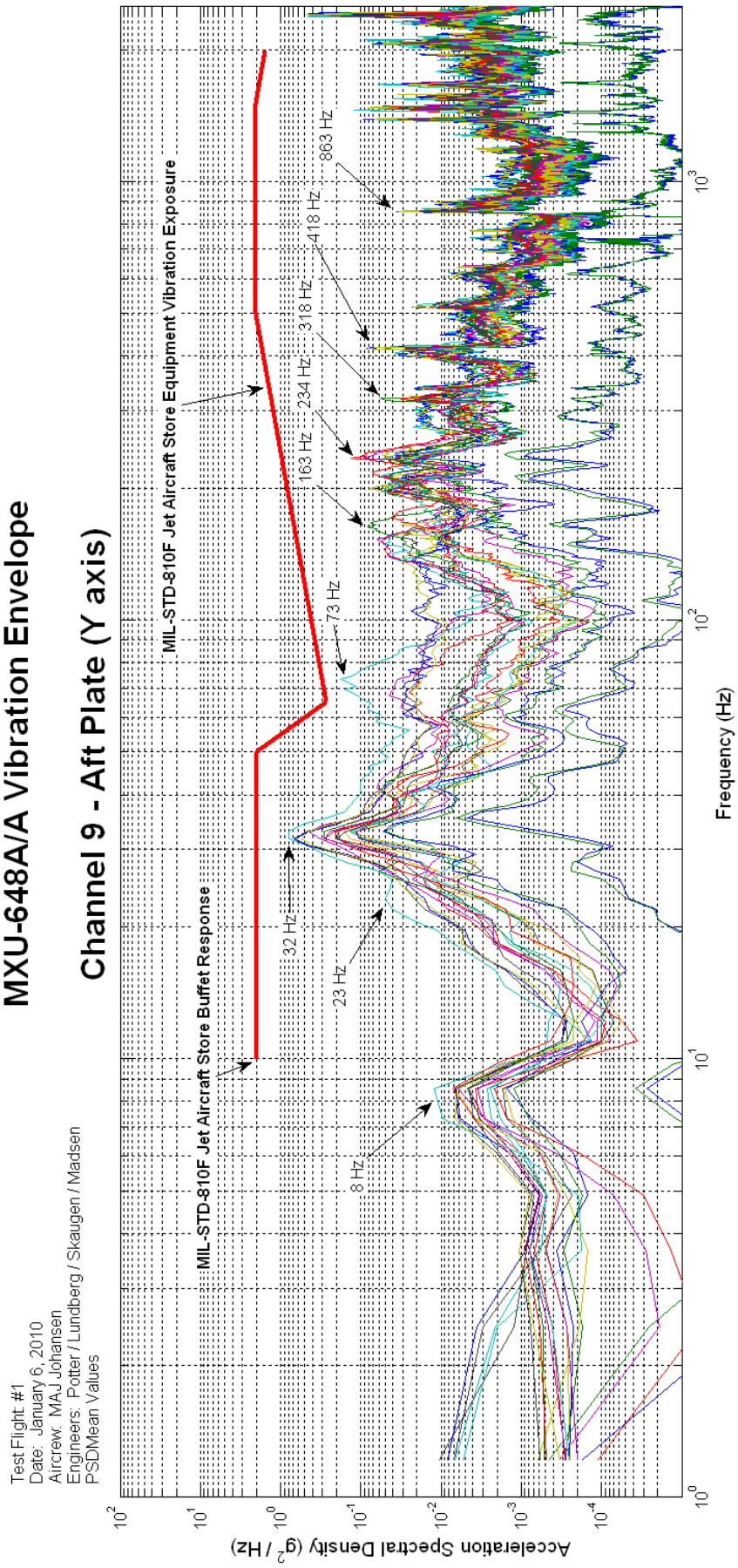

Figure C.20 Flight #1 Vibration Envelope (Aft Plate Y-axis).

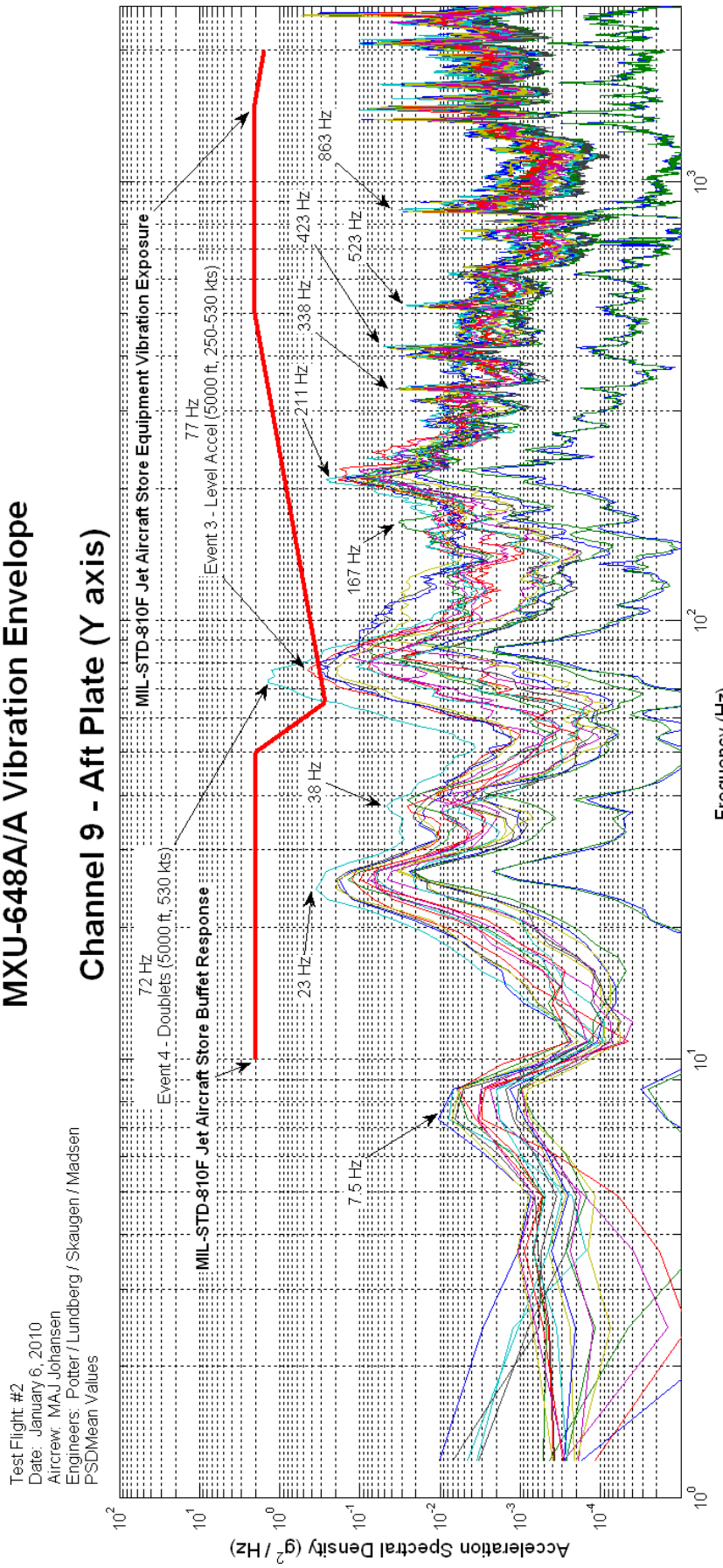

Figure C.21 Flight 2 Vibration Envelope (Aft Plate Y-axis).

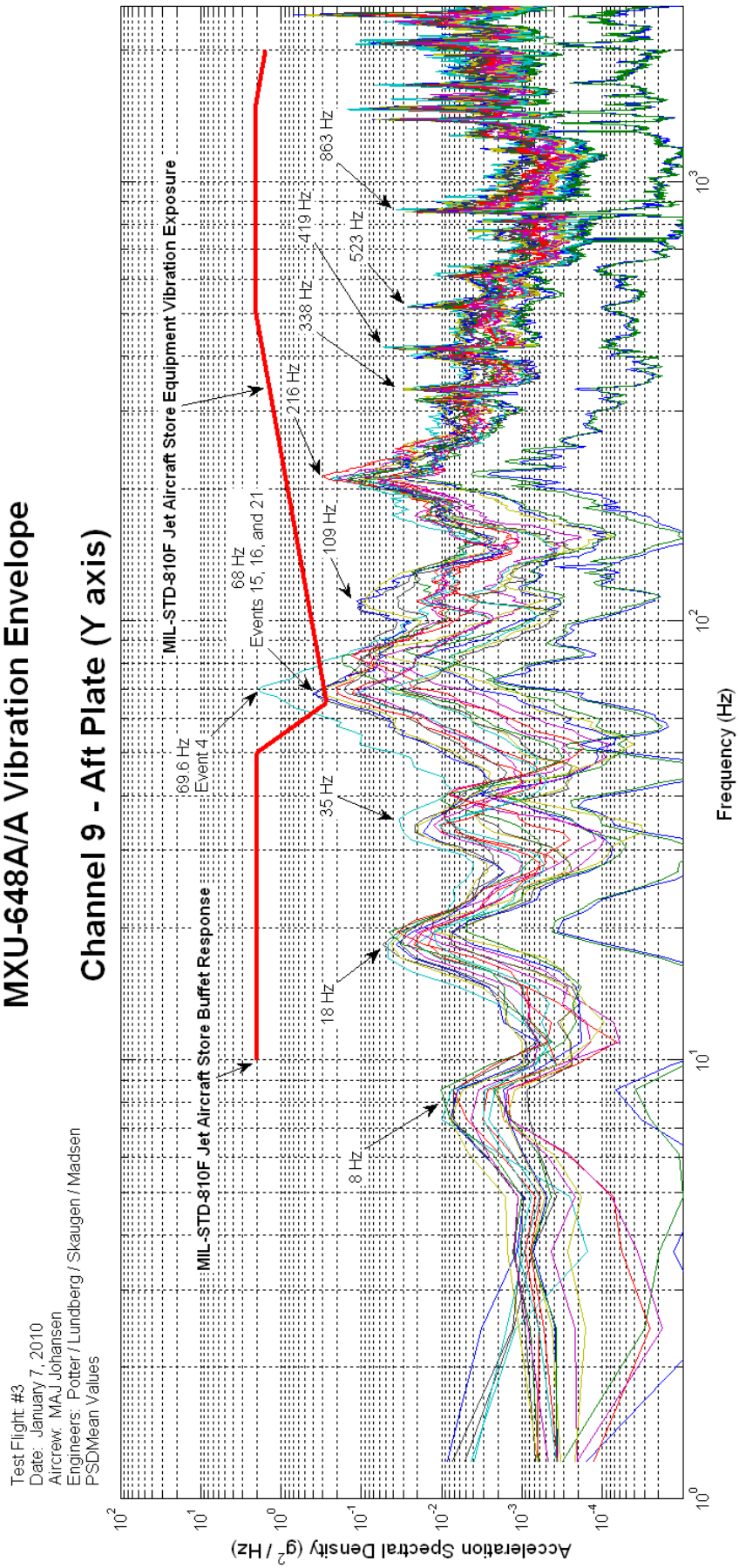

Figure C.22 Flight #3 Vibration Envelope (Aft Plate Y-axis).

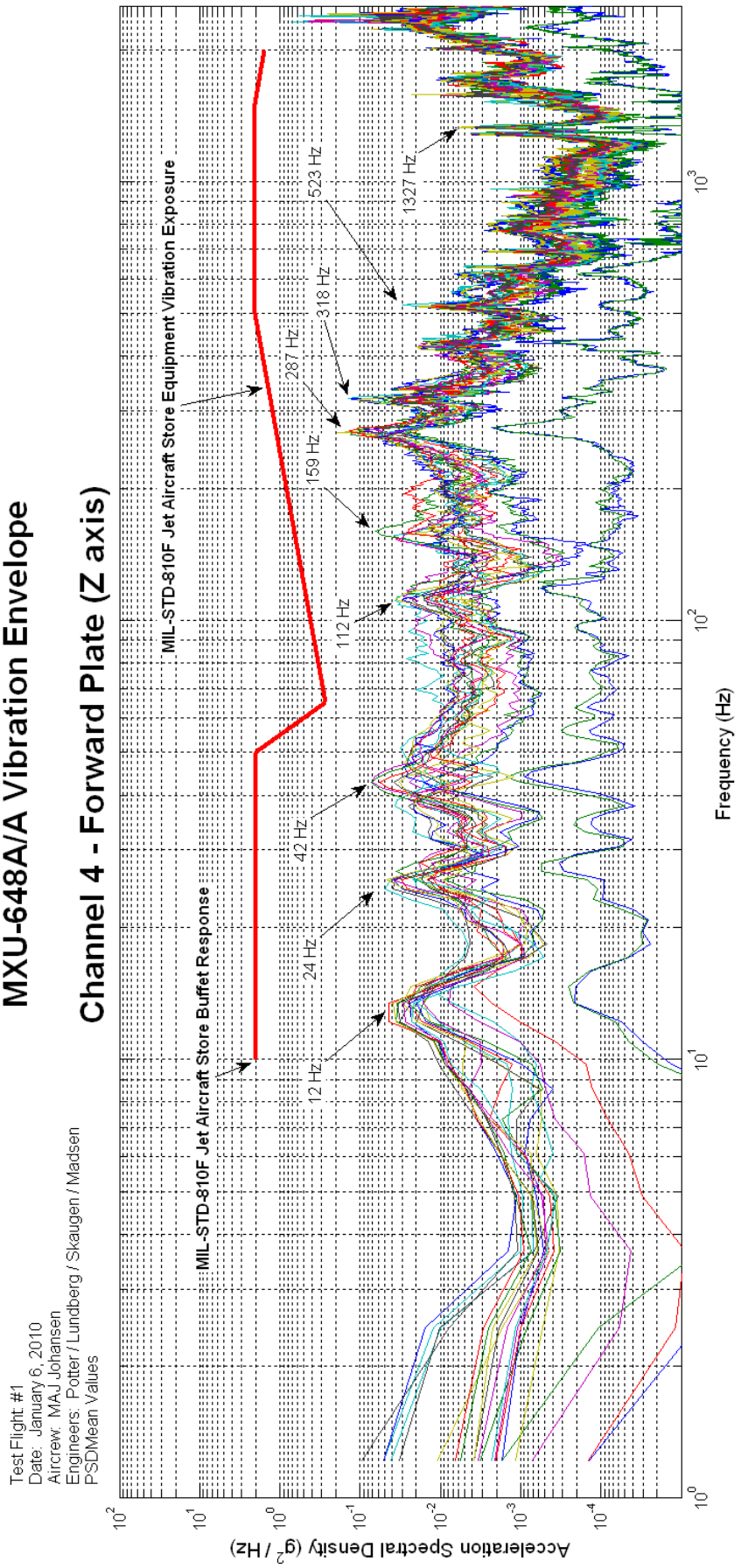

Figure C.23 Flight #1 Vibration Envelope (Forward Plate Z-axis).

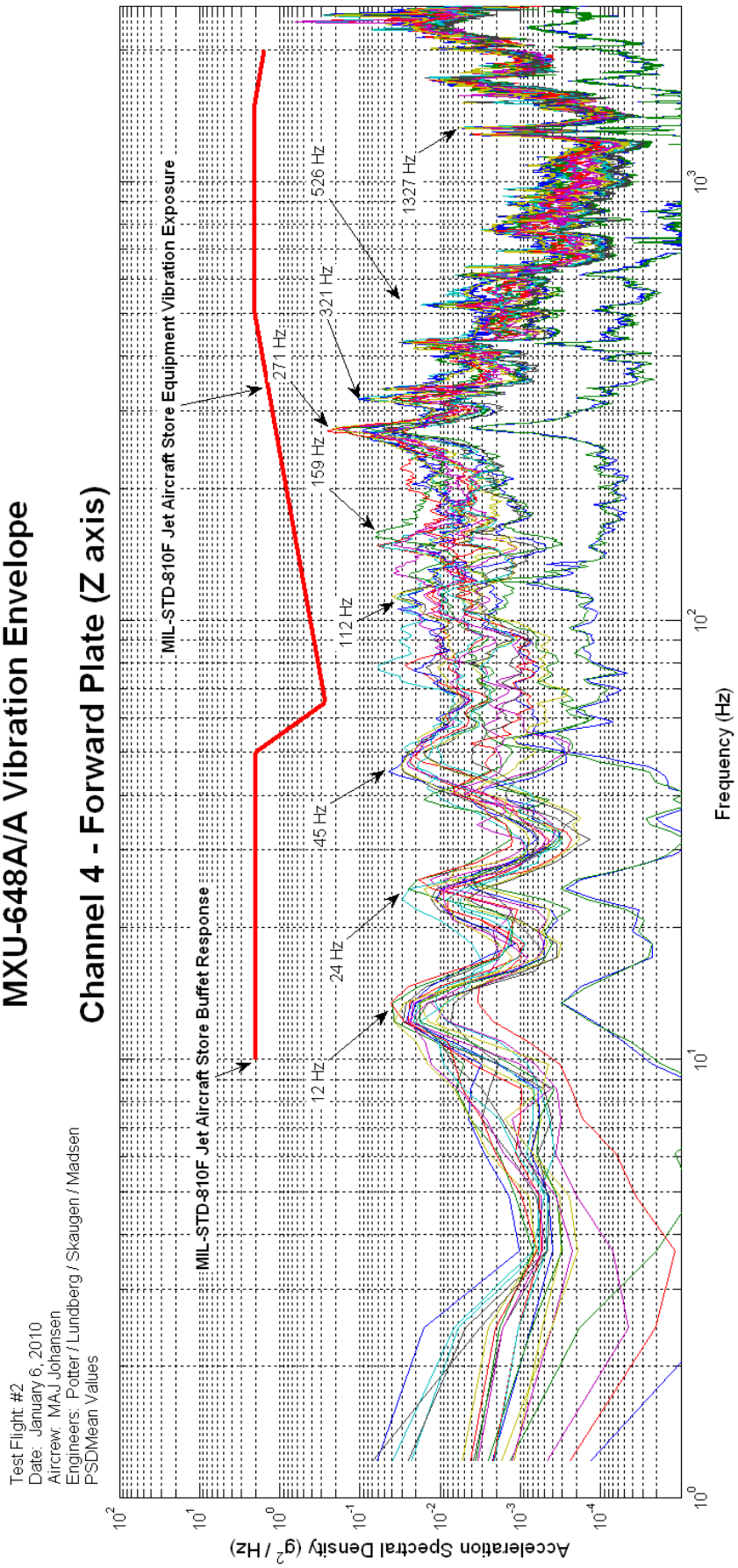

Figure C.24 Flight #2 Vibration Envelope (Forward Plate Z-axis).

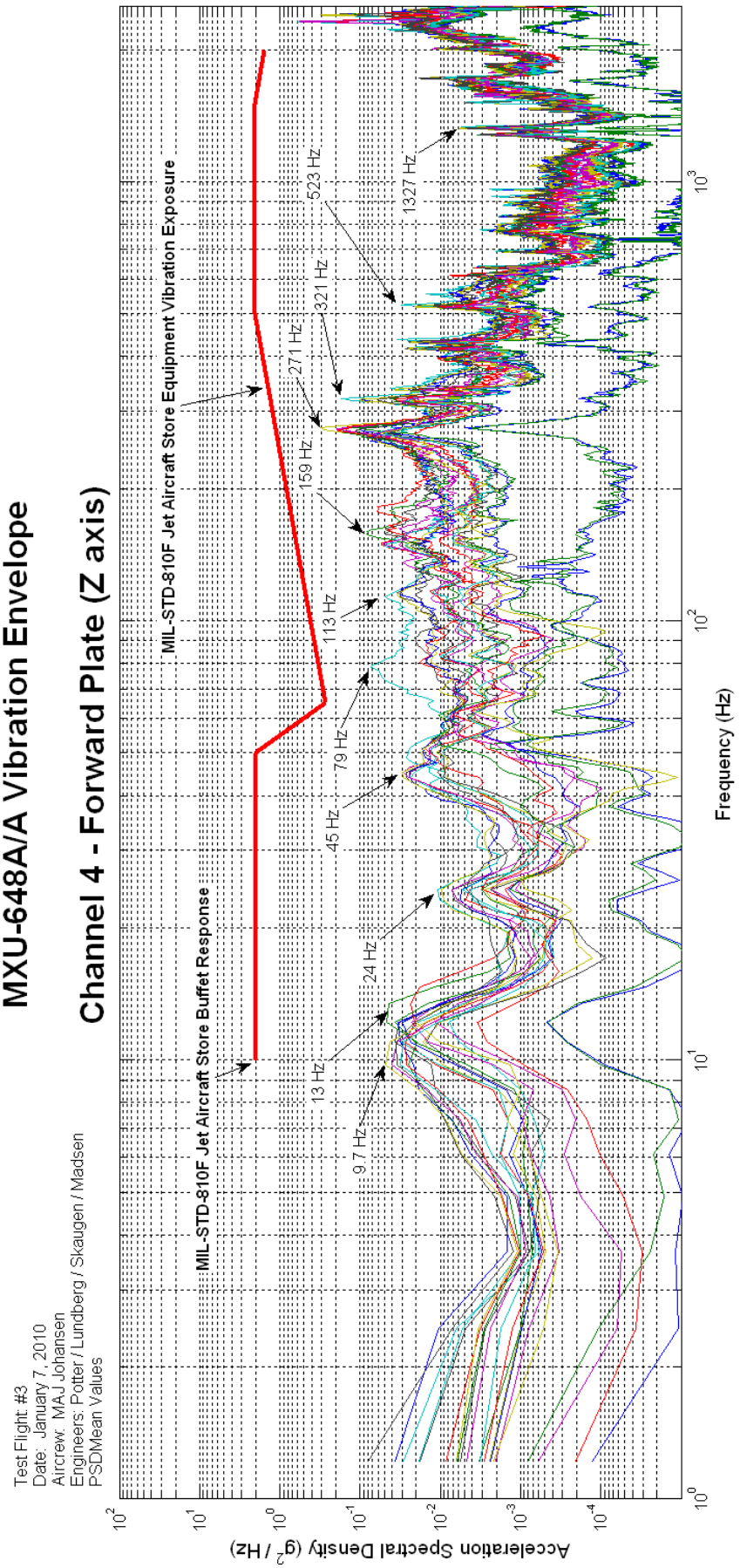

Figure C.25 Flight 31 Vibration Envelope (Forward Plate Z-axis).

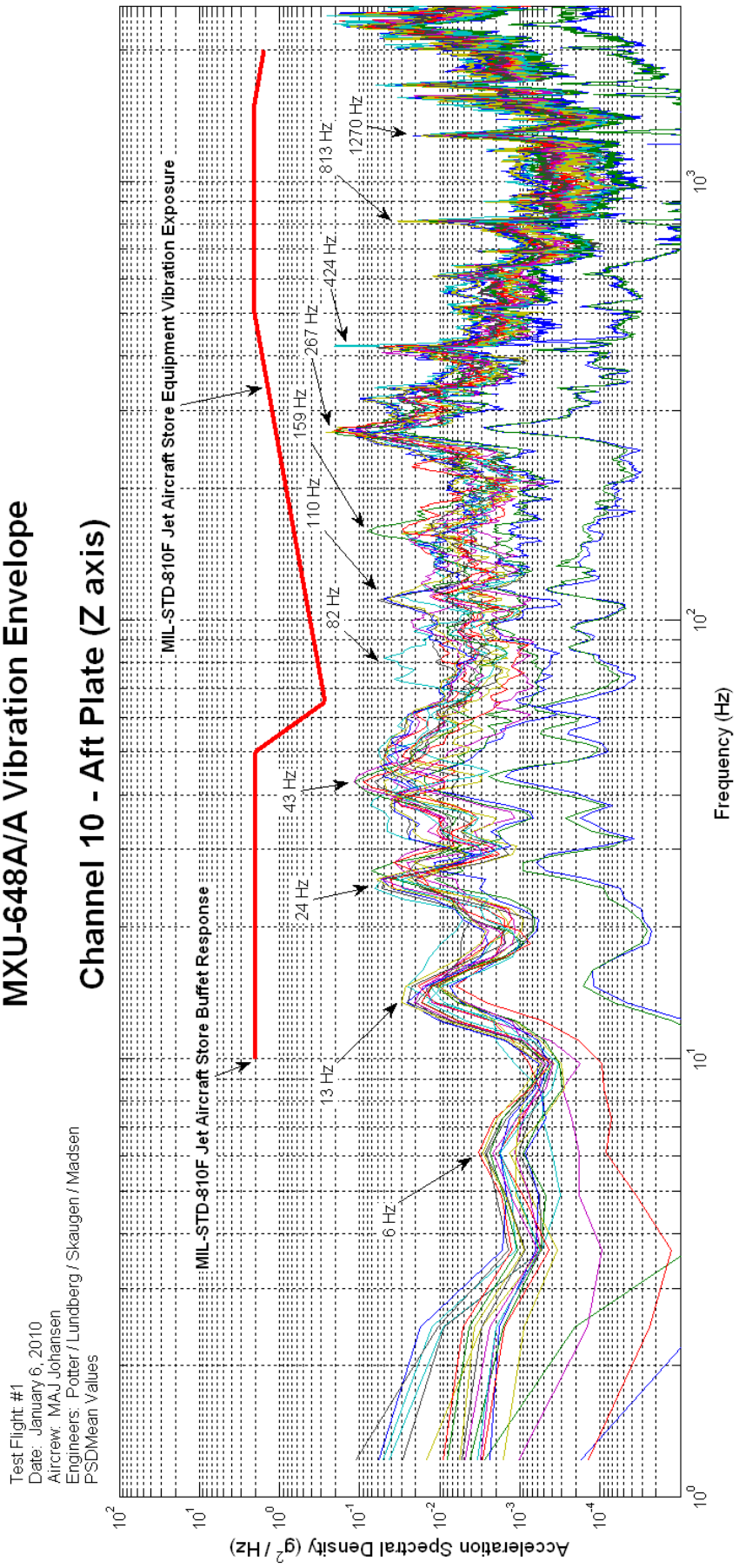

Figure C.26 Flight #1 Vibration Envelope (Aft Plate Z-axis).

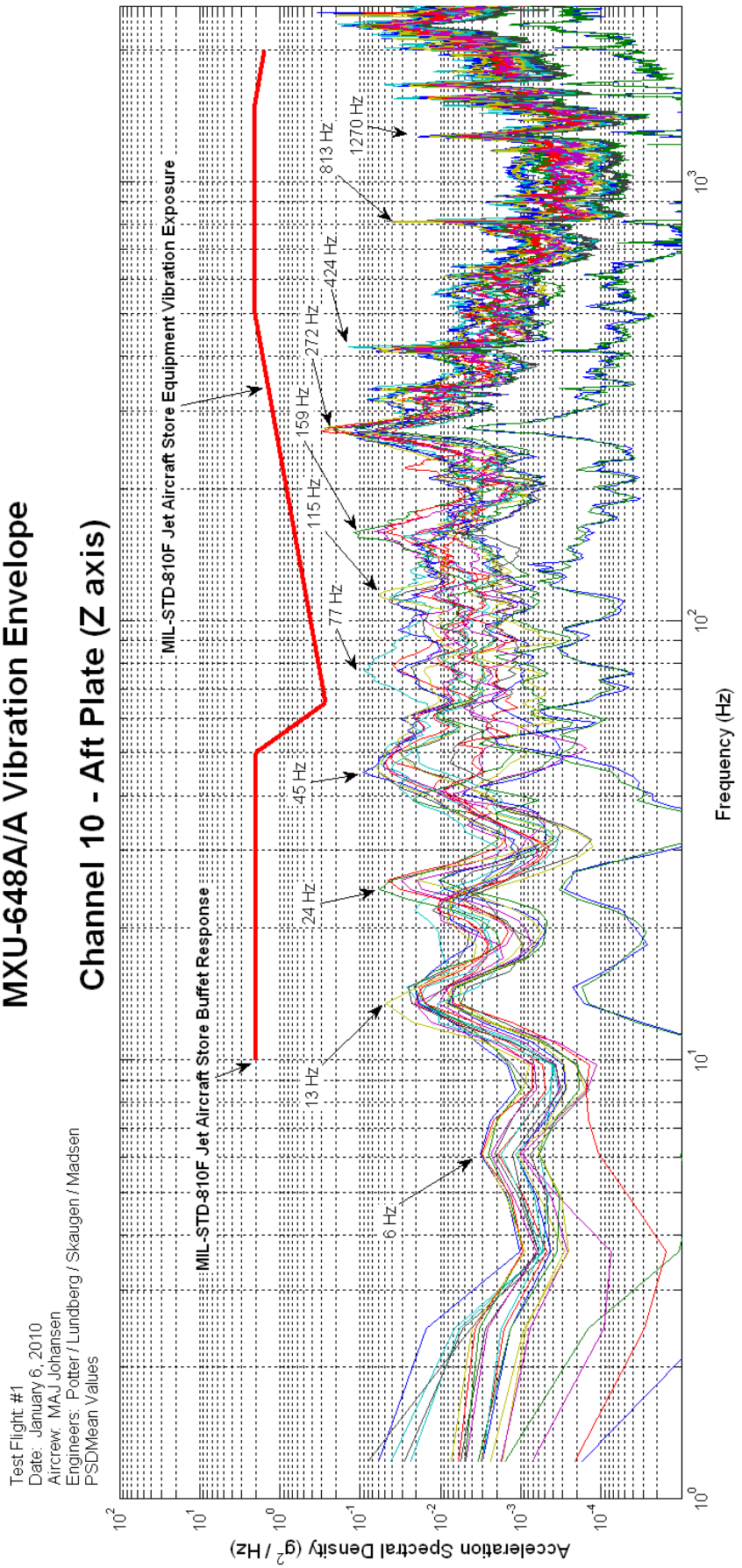

Figure C.27 Flight #2 Vibration Envelope (Aft Plate Z-axis).

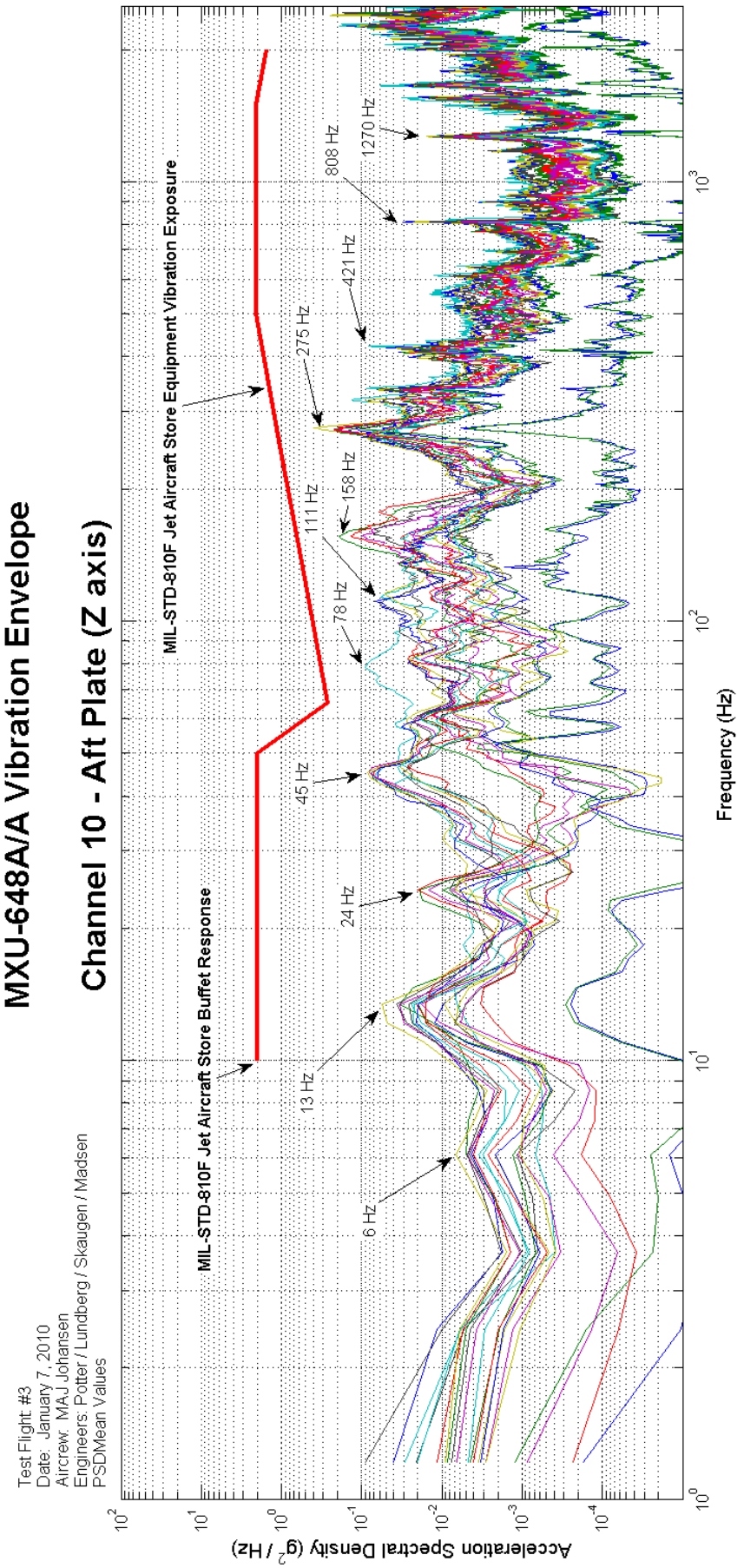

Figure C.28 Flight #3 Vibration Envelope (Aft Plate Z-axis).